Distribution Agreement

In presenting this thesis or dissertation as a partial fulfillment of the requirements for an advanced degree from Emory University, I hereby grant to Emory University and its agents the non-exclusive license to archive, make accessible, and display my thesis or dissertation in whole or in part in all forms of media, now or hereafter known, including display on the world wide web. I understand that I may select some access restrictions as part of the online submission of this thesis or dissertation. I retain all ownership rights to the copyright of the thesis or dissertation. I also retain the right to use in future works (such as articles or books) all or part of this thesis or dissertation.

Signature:

_____ _____

Jeanne E. McKeon Date

Ubiquitin C-terminal hydrolase L1 regulation and dysfunction in neurodegenerative disease pathogenesis

By

Jeanne E. McKeon
Doctor of Philosophy

Graduate Division of Biological and Biomedical Science
Neuroscience

Lih-Shen Chin, Ph.D.
Advisor

Lian Li, Ph.D.
Advisor

Victor Faundez, M.D., PhD.
Committee Member

Gary W. Miller, Ph.D.
Committee Member

Yoland Smith, Ph.D.
Committee Member

Accepted:

Lisa A. Tedesco, Ph.D.
Dean of the James T. Laney School of Graduate Studies

Date

Ubiquitin C-terminal hydrolase L1 regulation and dysfunction in neurodegenerative disease pathogenesis

By

Jeanne E. McKeon

B.A., Smith College, 2006

Advisors: Lih-Shen Chin, Ph.D
Lian Li, Ph.D

An abstract of
A dissertation submitted to the Faculty of the
James T. Laney School of Graduate Studies of Emory University
In partial fulfillment of the requirements for the degree of
Doctor of Philosophy

Graduate Division of Biological and Biomedical Science
Neuroscience

2014

Abstract

Ubiquitin C-terminal hydrolase L1 regulation and dysfunction in neurodegenerative disease pathogenesis

By Jeanne E. McKeon

Mutations in the gene encoding ubiquitin C-terminal hydrolase L1 (UCH-L1) are linked to familial Parkinson disease (PD) and neurodegeneration with optic atrophy in humans as well as gracile axonal dystrophy in mice. UCH-L1 is observed in Lewy body deposits and soluble UCH-L1 protein is reduced in sporadic PD brain. However, mechanisms regulating the UCH-L1 level and the role UCH-L1 loss-of-function plays in neurodegenerative disease pathogenesis remain unknown. In my dissertation work, I investigated the association between UCH-L1 and parkin, an E3 ubiquitin protein ligase commonly mutated in autosomal recessive PD. I found evidence *in vitro* and *in vivo* showing that parkin regulates the lysosomal degradation of UCH-L1 via polyubiquitination. Next, to examine the effect of UCH-L1 loss-of-function on the maintenance and structure of peripheral nerves, I assessed axonal distributions in the L4 dorsal root, L4 ventral root, and sciatic nerve of UCH-L1 deficient mice. I also assessed sensory and motor nerve conduction from these animals. My data support an age-dependent distal-to-proximal mode of primary axonal degeneration in the peripheral nervous system of UCH-L1 deficient mice. Together the work described in this dissertation reveals a novel mechanism regulating UCH-L1 protein level with relevance to PD pathogenesis, and demonstrates, for the first time, functional deficits in peripheral nerves corresponding with axonal degeneration and phenotype severity resulting from UCH-L1 loss-of-function.

Ubiquitin C-terminal hydrolase L1 regulation and dysfunction in neurodegenerative disease pathogenesis

By

Jeanne E. McKeon

B.A., Smith College, 2006

Advisors: Lih-Shen Chin, Ph.D
Lian Li, Ph.D

A dissertation submitted to the Faculty of the
James T. Laney School of Graduate Studies of Emory University
In partial fulfillment of the requirements for the degree of
Doctor of Philosophy

Graduate Division of Biological and Biomedical Science
Neuroscience

2014

Acknowledgements

I must first thank my advisors Drs. Lian Li and Lih-Shen Chin for their support and guidance during my graduate career. I must also thank my committee members for their help and thoughtful discussions over the years: Dr. Gary Miller, Dr. Yoland Smith, and Dr. Victor Faundez. I am grateful to the Director of Graduate Studies for the Neuroscience Program, Dr. Malu Tansey, for advice and moral support this past year. I have benefited greatly from interactions with several wonderful labmates and consider my time learning from them a crucial element to my training. I would not have survived without them, most especially Sammy Lee, Di Sha, Jennifer Hurst-Kennedy, Patrick Reynolds, Cheryl Yung, Cris Lee, and Dana Fallaize. I am also very grateful to Dr. Jonathan Glass and Seneshaw Asress for their time, advice, patience, and assistance in carrying out many of the experiments described in Chapter 3. Finally, I must thank my family and friends for their help in preserving my sanity and morale while producing this monstrosity.

Table of Contents

List of Figures

List of Tables

Chapter 1: Introduction and Background

Opening Comments

Neurodegenerative disorders, including Parkinson disease (PD), Alzheimer disease (AD), amyotrophic lateral sclerosis (ALS), and Charcot-Marie-Tooth (CMT) disease affect the central and/or peripheral nervous systems and are broadly characterized by progressive region-specific neuronal cell death and degeneration. The biggest risk factor for all neurodegenerative disorders is aging making these diseases a rising concern due to increased life expectancies among the general population. The economic and societal impacts of neurodegenerative diseases are substantial, as are the physical and emotional toll for both patients and their caregivers (Young, 2009, Dorsey et al., 2013). Current treatments for neurodegenerative diseases are palliative but ultimately unable to halt disease. Thus, it is critical to understand underlying disease mechanisms in order to facilitate development of targeted and effective therapeutics.

Ubiquitin carboxyl-terminal hydrolase L1 (UCH-L1) is a neuronal deubiquitinating enzyme that plays a critical role in the regulation of monomeric ubiquitin levels (Osaka et al., 2003). Autosomal dominant UCH-L1 mutation has been identified in a familial PD kindred (Leroy et al., 1998) and more recently, an autosomal recessive loss-of-function mutation has been identified as causative of neurodegeneration with optic atrophy (NDGOA), a disorder characterized by childhood-onset blindness, muscle spasticity, somatosensory ataxia, as well as cortical, cerebellar, and optic nerve atrophy (Bilguvar et al., 2013). UCH-L1 is found in Lewy bodies (Lowe et al., 1990), the proteinaceous inclusions typical of postmortem PD brain, and we have also shown that the level of soluble UCH-L1 protein is reduced in PD brain compared to age-matched controls (Choi et al., 2004). Moreover, loss-of-function mutations in UCH-L1 cause gracile axonal dystrophy in mice, a progressive neurodegenerative disorder characterized by

somatosensory ataxia, hindlimb paralysis, and premature death (Yamazaki et al., 1988, Saigoh et al., 1999, Walters et al., 2008, Chen et al., 2010). Together these studies link UCH-L1 abnormalities to PD and peripheral neuropathy disease etiology, but the role UCH-L1 dysregulation plays in disease pathogenesis remains unknown. In addition, aberrant upregulation of UCH-L1 has been reported in several cancers (Tezel et al., 2000, Chen et al., 2002, Mastoraki et al., 2009, Hurst-Kennedy et al., 2012), further underscoring the importance in gaining insight into mechanisms regulating UCH-L1 protein level.

In the first part of my thesis work, I examined biochemical mechanisms regulating UCH-L1 protein level and found that parkin, an E3 ubiquitin protein ligase commonly mutated in autosomal recessive PD, mediates ubiquitination and UCH-L1 degradation via the autophagy-lysosomal pathway. My findings described in Chapter 2 are the first demonstrating UCH-L1 as a substrate of parkin-mediated ubiquitination and to define a novel link between these disease-associated proteins. For the second part of my dissertation research, I examined the effect of UCH-L1 loss-of-function on peripheral nerve maintenance and transmission. In Chapter 3, I describe my findings of axonal degeneration in the sciatic nerve of aged symptomatic animals as well as reduced sensory nerve and compound muscle action potentials. However, sciatic nerve degeneration and electrophysiological alterations were not found in young presymptomatic animals, supporting an age-dependent mode of degeneration. I also provide evidence to suggest that a population of large caliber axons is reduced in the dorsal and ventral roots of aged UCH-L1 null mice which may be indicative of axonal atrophy. However, in symptomatic mice, the nerve conduction velocities in sensory and motor nerves, action potential onset latencies, and structural appearance of the nodes of Ranvier were not altered. Together, these data demonstrate distal-to-proximal

degeneration in the PNS of UCH-L1 deficient mice and support a role for UCH-L1 in peripheral axonal maintenance and in the initiation, but not propagation, of action potentials in sensory and motor nerves. In the final chapter of my thesis, I discuss the significance and implications of my findings within the broader context of neurodegenerative disease and propose future studies toward gaining a better understanding of the role UCH-L1 plays in nervous system health and disease.

1.1 The ubiquitin system and regulation of protein turnover

Ubiquitination machinery and ubiquitin signaling

Ubiquitin-dependent signaling is required for myriad cellular functions, and disruptions in this system are associated with human disease, including neurodegenerative disorders and cancer (Hussain et al., 2009, Kowalski and Juo, 2012, Satija et al., 2013, McKinnon and Tabrizi, 2014). The ubiquitin system is a complex and tightly regulated pathway that participates in diverse cellular signaling events through the addition or removal of ubiquitin moieties to target proteins. Protein ubiquitination is a post-translational modification that requires the coordinated and sequential action of three proteins – E1-activating, E2-conjugating, and E3-ligating enzymes (Fig. 1.1) (Pickart and Eddins, 2004, Pickart and Fushman, 2004, van Tijn et al., 2008). The E1-activating enzyme catalyzes formation of a thioester bond at the C-terminus of a ubiquitin molecule in an ATP-dependent manner. In the subsequent reactions, the activated ubiquitin is transferred from the E1 to an E2-conjugating enzyme which then recruits an E3-ligating enzyme for the final conjugation of ubiquitin to the substrate. The E3-ligases are the most diverse and largest class (>500) of the ubiquitination machinery

and provide specificity to the ubiquitination cascade through selective interaction with substrates (Metzger et al., 2012).

The ubiquitination reaction proceeds through fusion of the ubiquitin C-terminal glycine with a substrate lysine (K) residue via isopeptide bond or nontraditionally at internal cysteine residues or the substrate's N-terminus. Substrates can be monoubiquitinated or further modified by the joining of additional ubiquitin moieties at one of ubiquitin's seven internal lysine residues to form a polyubiquitin chain joined by isopeptide bonds (Pickart and Eddins, 2004, Pickart and Fushman, 2004, van Tijn et al., 2008). The nature of the ubiquitin linkage mediates substrate fate, with many cellular processes mediated through linkage-specific ubiquitin signaling (Fig. 1.1). K48-linked polyubiquitin chains with 4 or more ubiquitins serve as the canonical signal for substrate degradation by proteasomes, whereas the addition of K63-ubiquitin chains has been implicated in several cellular events, including DNA repair, endocytic trafficking, and autophagic degradation (Olzmann et al., 2007, Olzmann and Chin, 2008, Chen and Sun, 2009). K11-polyubiquitination has also been shown to target proteins for proteasomal degradation, whereas outcomes governed by other polyubiquitin linked chains (K6, K27, K29, K33) are not well understood (Sadowski et al., 2012). Monoubiquitination, on the other hand, has been shown to mediate non-proteasomal processes including receptor endocytosis, DNA repair, and gene transcription (Sigismund et al., 2004, Chen and Sun, 2009).

Deubiquitinating enzymes (DUBs)

Ubiquitin moieties can be removed from target proteins to regulate ubiquitin dependent signaling events; the removal of monomeric or polymeric ubiquitin from target

proteins can block their degradation or alter protein function or localization. Removal of ubiquitin moieties from target proteins is achieved through a class of proteases collectively known as deubiquitinating enzymes (DUBs). DUBs are critical for ubiquitin processing, ubiquitin recycling, polyubiquitin chain cleavage, and ubiquitin chain editing (Fig.1.2) (Reyes-Turcu et al., 2009, Eletr and Wilkinson, 2014). There are approximately 90 DUBs encoded by the human genome (Love et al., 2007, Eletr and Wilkinson, 2014). Like the E3 ubiquitin ligases, DUB enzymes participate in the regulation of multiple cellular pathways, and DUB dysfunction and genetic mutations have been implicated in several human cancers (Hussain et al., 2009) as well as in neurological diseases including spinocerebellar ataxia and PD (Singhal et al., 2008, Kowalski and Juo, 2012).

In mammals, ubiquitin is encoded by four genes as either a linear chain of tandem repeats or as a ribosomal fusion protein and processing by DUBs is required to generate ubiquitin monomers (Wiborg et al., 1985, Baker and Board, 1987). DUBs also cleave polyubiquitin from protein targets and further process freed ubiquitin chains to generate monomeric ubiquitin (Wilkinson et al., 1995, Piotrowski et al., 1997). Additionally, DUBs regenerate monomers from C-terminally modified ubiquitin molecules which are produced by nucleophilic attack of amides or esters with ubiquitin thiol ester intermediates during the ubiquitination cascade (Pickart and Rose, 1985).

DUB Families

There are five families of DUBs which are classified by their ubiquitin protease domain homology: the ubiquitin specific proteases (USPs), the ubiquitin C-terminal hydrolases (UCHs), the Machado-Josephin domain (MJD) containing family, the ovarian tumor suppressor proteases (OTUs), and the JAB1/MPN/Mov34 metalloenzyme domain

(JAMM) containing family (Komander et al., 2009, Reyes-Turcu et al., 2009). The first four DUB families are all cysteine/thiol proteases, while the JAMM family members are zinc metalloproteases.

The USPs make up the largest family of DUBs with approximately 50 proteins encoded by the human genome. The USPs can cleave polyubiquitin chains from substrate proteins and also process polyubiquitin chains from either end or internally along a polyubiquitin chain. Many of these enzymes demonstrate a preference for either K48- or K63-linked chains. The USP catalytic domain ranges in size from 295 – 850 amino acids, and contains six conserved motifs interspersed with five non-catalytic domain insertions that separate the catalytic core domains (Ye et al., 2009). The overall structure resembles a right hand, including the thumb, fingers, and palm (Hu et al., 2002). The non-catalytic domain insertions include ubiquitin associated domains (UBAs), ubiquitin interacting motifs (UIMs), and B-box domains which are thought to serve a regulatory function by affecting USP activity or substrate binding and/or cellular localization (Ye et al., 2009). Mutations and aberrant expression levels of USP enzymes have been implicated in tumorigenesis (Sacco et al., 2010), and additionally, mutation of Usp14 causes ataxia and synaptic deficits in mice (Wilson et al., 2002).

The human genome encodes four UCH enzymes: UCH-L1, UCH-L3, UCH37, and BRCA1-associated protein-1 (BAP1) (Barrett and Rawlings, 2001). The UCH enzymes contain a catalytic domain comprised of approximately 230 amino acids which facilitates cleavage of C-terminally modified ubiquitin molecules to regenerate the ubiquitin monomer (Eletr and Wilkinson, 2014). The UCH enzymes are unique to other DUBs because the active site is occluded by a crossover loop, the length of which dictates specificity as substrates must tunnel under the loop for productive catalysis.

Active site accessibility of UCH-L1 and UCH-L3, for example, appears to be limited to monomeric ubiquitin containing small C-terminal ubiquitin adducts, such as thioesters and amides (Boudreaux et al., 2010). UCH-L1 and UCH-L3 are highly homologous, but UCH-L1 is primarily expressed in neurons whereas UCH-L3 is ubiquitously expressed and can also cleave C-terminally modified molecules of the ubiquitin-like protein Nedd8 (Larsen et al., 1998, Wada et al., 1998). Whereas UCH-L1 and UCH-L3 cannot cleave diubiquitin or polyubiquitin (Larsen et al., 1998, Boudreaux et al., 2010), the longer crossover loops in UCH37 and BAP1 facilitate active site accessibility to larger molecules, including di-ubiquitin and polyubiquitin chains (Lam et al., 1997, Zhou et al., 2012). As described in the opening comments, UCH-L1 abnormalities have been linked to neurological disease and tumorigenesis. UCH-L3 and UCH37 are also upregulated in some human cancers, while BAP1 has been identified as a putative tumor suppressor (Fang et al., 2010).

The human genome encodes four MJD domain proteins which contain a 180 amino acid catalytic domain: ataxin-3, ataxin-3L, josephin-1, and josephin-2. Josephin-1 and josephin-2 do not contain additional functional domains, but ataxin-3 and ataxin-3L contain ubiquitin interaction motifs (UIMs) and a polyglutamine expansion in the C-terminus. The MJD enzymes demonstrate a preference for long K63-polyubiquitin chains, but they can also cleave K48-polybiquitin chains and peptide adducts of ubiquitin (Weeks et al., 2011). Autosomal dominant mutations in ataxin-3 that result in polyglutamine expansion at the C-terminus cause spinocerebellar ataxia (also called Machado-Joseph disease), a rare disorder characterized by spasticity, gait impairment, muscle atrophy, as well as pain and numbness in the limbs (Paulson et al., 1997, Durr and Brice, 2000).

The human genome encodes fifteen 180 amino acid containing OTU DUBs divided into three classes (OTUs, otubains, and the A20-like OTUs) (Komander et al., 2009). These enzymes which process ubiquitinated substrates and polyubiquitin chains have been implicated in the regulation of cellular signaling cascades, including NF-κB signaling, interferon signaling, and DNA repair (Wertz et al., 2004, Kayagaki et al., 2007, Nakada et al., 2010). Finally, eight zinc-dependent JAMM metalloproteases are encoded by the human genome. JAMMs cleave polyubiquitin from substrates and also disassemble chains. (Yao and Cohen, 2002, Komander et al., 2009). This family includes AMSH (associated molecule with SH3 domain of STAM), an important regulator of endocytic sorting (McCullough et al., 2004, Sierra et al., 2010).

Role of ubiquitin signaling in the regulation of protein degradation in mammalian cells

In mammalian cells, protein degradation occurs via two major pathways – the ubiquitin proteasome system (UPS) and the autophagy-lysosomal pathways; both of these processes are regulated through ubiquitin system signaling. The UPS is primarily responsible for the proteasomal degradation of short-lived cysolic and nuclear proteins as well as damaged or unfolded/misfolded proteins resident to the cytosol or dislocated from the endoplasmic reticulum (Bernasconi and Molinari, 2011, Amm et al., 2014, McKinnon and Tabrizi, 2014). The autophagy-lysosomal degradation systems are responsible for the degradation and recycling of long-lived cytosolic proteins, protein complexes, protein aggregates, and whole organelles (Cuervo, 2004, Barrachina et al., 2006, Mizushima et al., 2008, Eskelinen and Saftig, 2009).

Accumulation of misfolded and damaged proteins into aggregates is a common feature in many neurodegenerative diseases, including PD, AD, and ALS (Douglas and Dillin, 2010). Inclusion bodies in disease tissue and aggresomes in cellular disease models typically contain numerous ubiquitinated proteins, and these structures are thought to form as protein quality control systems and the UPS become overwhelmed (Chin et al., 2010, McKinnon and Tabrizi, 2014). The 26S proteasome consists of the 20S barrel-shaped catalytic core and two 19S regulatory capping subunits at either end of the barrel (Kish-Trier and Hill, 2013). Ubiquitinated substrates, typically those modified with K48-linked polyubiquitin chains, are recognized by ubiquitin binding domains within the regulatory caps, followed by deubiquitination and unfolding before threading through the catalytic core for degradation (Amm et al., 2014). Three DUBs are associated with the proteasome – the JAMM containing POH1 which couples substrate deubiquitination to core entry, and UCH37 and USP14 which process the released polyubiquitin chains into monomers (Yao and Cohen, 2002, Komander et al., 2009). The structure of the proteasome places steric limitations on proteasome substrates such that protein complexes, protein aggregates, and whole organelles cannot be accommodated by the proteolytic core.

These large cellular structures as well as long-lived cytosolic proteins are degraded by the autophagy-lysosomal degradation system, which is subdivided into three distinct pathways: microautophagy, chaperone mediated autophagy (CMA), and macroautophagy (Cuervo, 2004, Barrachina et al., 2006, Mizushima et al., 2008, Eskelinen and Saftig, 2009). These pathways are critical to the regulation of various cellular processes, including survival and energy production under short-term starvation, innate and adaptive immunity, programed cell death, and protection from intracellular pathogens (Eskelinen and Saftig, 2009, Boya et al., 2013). Autophagy-lysosome system

dysfunction has been reported in multiple cancers, neurodegenerative diseases, and lysosomal storage disorders (Eskelinen and Saftig, 2009).

Microautophagy, which has predominantly been studied in yeast, is a nonselective lysosomal degradation system that involves the direct engulfment of cytoplasmic contents by the lysosomal membrane for their subsequent degradation (Mijaljica et al., 2011, Li et al., 2012). Chaperone mediated autophagy (CMA) is a selective autophagy pathway responsible for the degradation of soluble proteins containing a lysosomal targeting motif (KFERQ or other biochemically related pentapeptide). Substrates are recognized by the chaperone molecule Hsc70 (heat shock cognate protein of 70 kDa) and then transferred to the lysosomal membrane as a complex where the lysosomal receptor LAMP-2A facilitates translocation of the target protein into the lumen for degradation (Cuervo, 2004, Kiffin et al., 2004, Kaushik and Cuervo, 2006). The PD-associated proteins α-synuclein and LRRK2 (leucine rich repeat kinase 2) are degraded by CMA. α-Synuclein mutations and gene multiplication are associated with familial PD (Polymeropoulos et al., 1997, Kruger et al., 1998, Singleton et al., 2003, Chartier-Harlin et al., 2004), and aggregated α–synuclein is the major component of Lewy bodies observed in PD patient brain (Spillantini et al., 1997, Baba et al., 1998). Reduced CMA activity and blockade of CMA through aberrantly tight binding of mutant α-synuclein and LRRK2 with LAMP-2A have been implicated in disease pathogenesis (Cuervo et al., 2004, Orenstein et al., 2013, Cuervo and Wong, 2014). Additionally, the PD-linked mutant UCH-L1 protein also interacts strongly with CMA machinery and has been shown to inhibit α-synuclein degradation (Kabuta et al., 2008a, Kabuta and Wada, 2008), although UCH-L1 has not itself been identified as a CMA substrate.

Macroautophagy is an evolutionarily conserved bulk recycling and degradation pathway that involves the engulfment of cytoplasmic content or whole organelles into autophagosome vesicles which are then targeted to the lysosome for degradation of their contents (Eskelinen and Saftig, 2009, Boya et al., 2013). Cargo-selective forms of autophagy including mitophagy (mitochondrial autophagy) and aggrephagy (aggresome autophagy) have recently been described, challenging the traditional view of macroautophagy as a nonselective process. Macroautophagy is initiated by formation of a double layer isolation membrane (phagophore) around cargo intended for degradation. The isolation membrane then elongates around the cargo until the inner and outer bilayers fuse to form the autophagosome vesicle. The autophagosome then fuses directly with a lysosome to form the autolysosome where cargo degradation occurs, although sometimes autophagosomes fuse with late endosomes prior to autolysosome formation (Ravikumar et al., 2010, Nixon, 2013). Macroautophagy is regulated by the mammalian target of rapamycin (mTOR) and Class III phosphatidylinositol-3-OH kinase (PI(3)K) signaling pathways (Tanida et al., 2004, Kim et al., 2011, Nixon, 2013).

Regulation of cargo selection and targeting to the macroautophagy pathway is not well understood, but recent evidence has a revealed a critical role for dual ubiquitin-binding and microtubule-associated protein 1 light chain 3 (LC3) interacting adaptor proteins, such as p62/SQSTM1 and NBR1 (neighbor of BRCA 1) which are thought to serve as autophagy receptors (Pankiv et al., 2007, Kirkin et al., 2009a, Lamark et al., 2009). These proteins contain a ubiquitin associated (UBA) domain and LC3-interacting region (LIR) which mediates simultaneous binding of ubiquitinated cargoes (typically K63-linked) and LC3 on autophagosomes, facilitating targeting of the cargo to the autolysosome where the cargo and adaptor proteins are both degraded.

1.2 Disrupted ubiquitin signaling in neurological diseases

Disruption of ubiquitin signaling and subsequent altered protein quality control and degradation is implicated in the pathogenesis of many human diseases, including cancer and neurodegenerative disease (Hussain et al., 2009, Kowalski and Juo, 2012, Satija et al., 2013, McKinnon and Tabrizi, 2014). With particular relevance to my thesis work, ubiquitin system dysfunction has been implicated in Parkinson disease and sensory and motor neuropathies and ataxia, as discussed below.

Parkinson disease

Parkinson disease (PD) is the most common neurodegenerative movement disorder (Savitt et al., 2006, Dorsey et al., 2007), affecting 1-3% of the population over age 65. Clinically, PD is characterized by motor deficits including bradykinesia, resting tremor, and postural instability (Fahn, 2003, Hamani and Lozano, 2003). Non-motor deficits are also commonly seen in PD patients, and include gastrointenstinal discomfort and dysfunction, cognitive decline, depression, and sleep disruption (Bernal-Pacheco et al., 2012). Pathologically, PD is characterized by the presence of Lewy bodies and the progressive loss of dopaminergic neurons in the substantia nigra pars compacta (SNpc). Lewy bodies are thought to develop from disruptions in protein quality control and degradation pathways (Fahn, 2003) including dysfunction in ubiquitin signaling in both UPS and autophagy pathways (Matsuda and Tanaka, 2010). Lewy body deposits have also been observed in non-nigral brain regions, including the locus coeruleus and cerebral cortex which may underlie many of the non-motor features of the disease (Wolters, 2009).

PD is widely recognized as a multifaceted and multisystem disorder with both genetic and environmental components that interact to trigger disease onset and influence progression. Mutations in several genes (summarized in Table 1) have been linked to familial PD and account for approximately 5-10% of PD cases (Farrer, 2006, Sun et al., 2007, Lesage and Brice, 2009, Shulman et al., 2011). Importantly, genetic studies have identified mutations in proteins involved in the ubiquitin signaling pathway, namely UCH-L1 (Leroy et al., 1998) and parkin (Kitada et al., 1998), in familial PD patients suggesting that disruption of ubiquitin signaling contributes to PD pathogenesis. My thesis work demonstrates that parkin-mediated ubiquitination regulates UCH-L1 degradation and that disruption of this process may contribute to PD pathogenesis. However, the majority (90-95%) of PD cases are of unknown etiology, although increasing age has been identified as the most prominent disease risk factor. Several epidemiological studies have also identified oxidative stress and environmental toxicant exposure, in particular exposure to pesticides and heavy metals which increase levels of reactive oxygen species (ROS), as major disease risk factors (Semchuk et al., 1991, 1992, Le Couteur et al., 1999, Priyadarshi et al., 2000, Kanthasamy et al., 2005, Hatcher et al., 2008). Oxidative stress is elevated in post mortem PD patient brain and PD-linked proteins including UCH-L1 and DJ-1 are oxidatively modified by ROS (Butterfield, 2004, Choi et al., 2004, Choi et al., 2005, Choi et al., 2006) which may pathologically alter their structure or function and contribute to disease.

The standard treatment strategies for PD target the dopaminergic system of the basal ganglia and can reduce some symptoms, but cannot halt disease progression. Typically, PD patients are treated with the dopamine precursor levodopa (L-Dopa) to increase dopamine levels within the nigrostriatial circuitry. However, L-Dopa treatment loses efficacy over time and is associated with unwanted side effects including motor

fluctuations and dyskinesias (Lewitt, 2008, Hickey and Stacy, 2011). Advanced stage patients with reduced response to pharmacotherapy concomitant with disabling motor fluctuations and/or dyskinesias are candidates for deep brain stimulation (DBS) surgery. This procedure involves placement of a stimulating electrode in the internal segment of the globus pallidus or the subthalamic nucleus to modulate activity within the basal ganglia thalamocortical circuitry and can improve some motor symptoms (Okun, 2012, Miocinovic et al., 2013). Elucidating mechanisms underlying PD pathogenesis will facilitate the development of more effective pharmacotherapeutics and provide additional treatment options prior to invasive DBS brain surgery.

Peripheral sensory and motor neuropathies

Peripheral neuropathy is a general term that refers to a family of acquired and hereditary disorders that affect peripheral nerves and cause disabling sensory and motor impairment. The overall prevalence of peripheral neuropathy among the general population is around 2.4% and increases to almost 8% for individuals over age 55 (Martyn and Hughes, 1997). Neuropathy patients typically exhibit with a common family of symptoms which worsen over time, and include reduced sensation, tingling, numbness, and pain in distal extremeties, as well as muscle weakness, atrophy, and impaired gait. In some patients, autonomic functions are also effected causing bowel and bladder dysfunction (Azhary et al., 2010). Underscoring the importance of gaining a better understanding of underlying disease mechanisms, there are no current treatments that restore or prevent further nerve damage. Patient care is geared toward easing symptoms and improving quality of life through pain medication, use of orthotics, and physical and occupational therapy (England and Asbury, 2004, Azhary et al., 2010).

Peripheral neuropathies are clinically classified in several general ways: by type (acquired, hereditary); number of nerves affected (one or more); and modality affected (sensory, motor, autonomic). The most common cause of acquired peripheral neuropathy is diabetes mellitus, with other cases resulting from a variety of factors including kidney disease, renal failure, autoimmune disorders, vitamin deficiencies, physical trauma such as nerve compression, and exposure to various drugs and toxins including chemotherapeutics (England and Asbury, 2004, Azhary et al., 2010). Hereditary sensory and motor neuropathies, collectively referred to as Charcot-Marie-Tooth (CMT) disease, encompass a family of peripheral neuropathies caused by mutations in over 40 Schwann cell specific and/or neuronal genes. Autosomal dominant, autosomal recessive, and X-linked modes of inheritance have been reported (Jani-Acsadi et al., 2008, Patzko and Shy, 2011). Clinically and pathologically, most CMT cases are subdivided into those that result from demyelination (CMT1) and cases resulting from axonal degeneration (CMT2). Nerve conduction velocity (NCV) analyses are commonly used to differentiate demyelinating and axonal forms of CMT, as CMT1 patients typically have characteristically slowed NCV (<38 m/s) whereas CMT2 patients have NCV above this cutoff but demonstrate significantly reduced action potential amplitudes (Jani-Acsadi et al., 2008, Patzko and Shy, 2011). Ataxia refers to the loss of balanced and coordinated movement and is commonly observed in peripheral neuropathy patients. Ataxic individuals have difficulty with tasks requiring fine motor control, as well as impairments in standing, walking, and making saccadic eye movements. Typically, ataxia is caused by cerebellar degeneration and atrophy or proprioceptor degeneration in the limbs (Barsottini et al., 2014).

There is evidence of ubiquitin system dysfunction in peripheral neuropathy and ataxia pathogenesis. Ubiquitin positive inclusions have been observed in patient

cerebellum and nerves and in rodent models of neuropathy (Fortun et al., 2005, Dueñas et al., 2006, Iwahashi et al., 2006, Seidel et al., 2010, Seidel et al., 2012, Vital et al., 2014), indicating the likely disruption of ubiquitin-dependent protein degradation mechanisms in disease. Genetic mutation in the ubiquitin protein ligase LRSAM1 (leucine rich repeat and sterile alpha motif 1) has been implicated in autosomal recessive CMT2 (Guernsey et al., 2010). Additionally, mutation in the E3 ligase TRIM2 (tripartite motif containing 2) gene has been identified in a patient with early-onset axonopathy (Ylikallio et al., 2013), and mice deficient in TRIM2 expression demonstrate progressive neurodegeneration and early-onset ataxia (Balastik et al., 2008). Autosomal dominant mutation in the putative E3 ligase RNF170 has been implicated in hereditary sensory ataxia (Valdmanis et al., 2011). As previously mentioned, spinocerebellar ataxia results from autosomal dominant mutations in the DUB enzyme ataxin-3 (Paulson et al., 1997, Durr and Brice, 2000), and spontaneous mutation in Usp14 causes ataxia and synaptic deficits in mice (Wilson et al., 2002). In mice and humans, UCH-L1 loss-of-function mutations cause a neurodegenerative phenotype with symptoms consistent with neuropathy and sensorimotor ataxia (Yamazaki et al., 1988, Saigoh et al., 1999, Walters et al., 2008, Chen et al., 2010, Bilguvar et al., 2013).

1.3 Role of UCH-L1 in neurodegenerative disease pathogenesis

UCH-L1 abnormalities are associated with neurodegenerative disease in humans

UCH-L1 is a DUB predominantly expressed in neurons that accounts for 1-2% of soluble brain protein (Wilkinson et al., 1989). UCH-L1 cleaves small C-terminal thioester and amide adducts of ubiquitin to regenerate the ubiquitin monomer (Larsen et al.,

1998, Case and Stein, 2006, Boudreaux et al., 2010), and plays an important role in regulating monomeric ubiquitin pool homeostasis (Osaka et al., 2003, Kyratzi et al., 2008). Mice deficient in UCH-L1 expression have a significantly reduced monomeric ubiquitin level in brain (Osaka et al., 2003, Walters et al., 2008) and sciatic nerve (Osaka et al., 2003). UCH-L1 also has a reported dimerization-dependent E3 ubiquitin ligase activity *in vitro* (Liu et al., 2002) but the physiological relevance of this activity is presently unclear.

Recently, a novel homozygous loss-of-function mutation in UCH-L1 was identified in three children from a consanguineous first cousin pairing demonstrating progressive neurodegeneration as well as motor and somatosensory abnormalities (Bilguvar et al., 2013). The pathogenic E7A mutation is located within the ubiquitin binding surface of UCH-L1 and significantly reduces the UCH-L1 hydrolase activity by approximately 90% (Bilguvar et al., 2013). The disorder has since been classified in the Online Mendelian Inheritance in Man (OMIM) database as neurodegeneration with optic atrophy, childhood onset (NDGOA) (http://www.omim.org/entry/615491). The patients' clinical features included childhood onset blindness, nystagmus, ataxia, head tremor, and muscle spasticity. Subsequent analyses via magnetic resonance imaging (MRI) revealed atrophy of the optic nerve and optic chiasm as well as diffuse cortical and cerebellar atrophy (Bilguvar et al., 2013). Electrophysiological recordings revealed reduced flash visual-evoked potentials and reduced somatosensory-evoked potentials upon peripheral nerve stimulation. Nerve conduction velocities were within the normal range, but myokymia, or spontaneous contractions, was detected in multiple muscles during EMG analysis. These findings indicate upper motor neuron dysfunction as well as signal transduction deficits between proprioceptors in the periphery and the somatosensory cortex, which is indicative of dysfunction in the dorsal column medial

lemniscus (DCML) pathway. The DCML is a major afferent pathway that carries somatosensory information from the lower extremities to the somatosensory cortex via the spinal cord. In particular, the DCML pathway primarily carries signals for mechanosensation, proprioception, texture, fine touch, and two-point discrimination (Gilman, 2002).

UCH-L1 abnormalities have also been reported in other neurodegenerative diseases. For example, downregulation of UCH-L1 mRNA has been reported in the sciatic nerve from the pmp22 overexpressing CMT1a mouse model (Vigo et al., 2005) and in human sporadic ALS motor cortex (Lederer et al., 2007). UCH-L1 was first implicated in familial PD after identification of the I93M mutation in a family with autosomal dominant PD (Leroy et al., 1998). The I93M mutant UCH-L1 has ~50% reduced deubiquitinating activity (Leroy et al., 1998, Nishikawa et al., 2003) as well as decreased solubility (Setsuie et al., 2007). Moreover, in a transgenic mouse model, overexpression of human I93M mutant UCH-L1 results in dopaminergic cell loss in the substantia nigra, reduced striatal dopamine, and increased susceptibility to the dopaminergic toxin MPTP (1-methyl-4-phenyl-1,2,3,6-tetrahydropyridine) (Setsuie et al., 2007). A potentially neuroprotective S18Y polymorphism of UCH-L1 has been associated with decreased sporadic PD risk in certain cohorts (Satoh and Kuroda, 2001, Elbaz et al., 2003, Maraganore et al., 2004, Carmine Belin et al., 2007), but this link has not been found in all studied populations (Healy et al., 2006, Hutter et al., 2008, Zhang et al., 2008), leaving the protective designation of the S18Y variant controversial. The S18Y form of UCH-L1 may have unique antioxidant properties, as its overexpression has been shown to protect cultured neurons from oxidative insults (Kyratzi et al., 2008, Xilouri et al., 2012).

Postmortem soluble UCH-L1 protein levels are reduced in cortex from sporadic PD and AD patients (Choi et al., 2004) as well as in cortex from patients with dementia with Lewy bodies (Barrachina et al., 2006) compared to age-matched controls. The soluble UCH-L1 level is also reduced in medulla oblongata and substantia nigra tissues derived from PD patients, although this study did not find reduced UCH-L1 expression in cortex (Barrachina et al., 2006). UCH-L1 has also been identified as a component of Lewy bodies (Lowe et al., 1990) and neurofibrillary tangles (Lowe et al., 1990, Choi et al., 2004), a neuropathological hallmark of AD. Thus, UCH-L1 degradation may be disrupted in these diseases and contribute to pathogenesis. Additionally, our lab has previously reported that in postmortem PD and AD cortical tissues, the UCH-L1 protein is altered by oxidative modifications, namely extensive carbonylation and methionine and cysteine oxidation (Choi et al., 2004). Oxidative carbonyl modification of UCH-L1 has also been observed in spinal cord from the SOD1-G93A mouse model of ALS (Poon et al., 2005). Carbonylation decreases UCH-L1 solubility and increases its association with binding partners in a manner similar to the I93M disease mutant protein (Kabuta et al., 2008b). For example, both I93M mutant and carbonyl-modified wild type UCH-L1 demonstrate a reduced association with monomeric ubiquitin and an enhanced interaction with α- and β-tubulins, with evidence that the enhanced tubulin interactions may alter microtubule dynamics (Kabuta et al., 2008b). UCH-L1 also interacts with the CMA components LAMP-2A, Hsc70, and Hsp90 (Kabuta et al., 2008a, Kabuta and Wada, 2008) and these interactions are enhanced by I93M mutation of UCH-L1 (Kabuta et al., 2008a) as well as by alkenal-induced carbonylation (Kabuta and Wada, 2008). Oxidative modification can also alter the deubiquitinating activity of UCH-L1. Reduced hydrolase activity was reported following incubation of recombinant UCH-L1 with 4-HNE (4-hydroxynonenal), a lipid peroxidation byproduct (Nishikawa et al., 2003). Partial

recovery of activity was achieved with addition of the reducing agent, N-acetylcysteine (Nishikawa et al., 2003) suggesting that UCH-L1 activity is subject to redox control. Thus, oxidized and I93M disease-linked mutant UCH-L1 proteins may contribute to PD pathogenesis through both reduced catalytic activity (loss of function) and aberrant protein interaction dynamics (toxic gain of function).

Neurodegeneration observed in UCH-L1 null mice

In 1988, Yamazaki and colleagues described a spontaneously occurring homozygous mutant mouse displaying progressive neurodegeneration, hindlimb muscle wasting, and sensory and motor ataxia (Yamazaki et al., 1988). Histopathological analyses revealed abnormalities in the DCML pathway, particularly dystrophic axons in the gracile nucleus of the medulla and nerve fiber degeneration along the gracile fasicules of the spinal cord (Yamazaki et al., 1988) which contains the nerve fibers connecting dorsal root ganglia (DRGs) and the gracile nucleus. Accordingly, this mouse model was dubbed the gracile axonal dystrophy (*gad*) mutant. Several years after the first report, the *gad* mutation was mapped to the UCH-L1 gene and found to encode a truncated, nonfunctional enzyme due to in-frame deletion of exons 7 and 8 (Saigoh et al., 1999).

Since the *gad* mutant was originally described, a second spontaneous UCH-L1 mutant mouse, the *nm3419* mouse, arose in a separate colony. The *nm3419* allele contains a partial deletion of exon 6 and encodes a truncated form of UCH-L1 that lacks catalytic activity (Walters et al., 2008). The *nm3419* mutant mice display a similar neurological and biochemical phenotype as *gad* mutants, including motor impairment, reduced life span, and reduced monomeric ubiquitin level (Walters et al., 2008). Mice

containing targeted deletion of the UCH-L1 gene are now commercially available and have similar phenotypic profiles as the *gad* and *nm3419* spontaneous mutants. Hereafter, the above mouse models will be referred to generically as UCH-L1 null.

Signs of neurological dysfunction in UCH-L1 null mice first present around day 30 in the form of abnormal hindlimb clasping when animals are suspended by the tail (Yamazaki et al., 1988). The mice progressively develop sensorimotor ataxia, footdrop, hunched posture, and reduced grooming behavior. Although weighing less on average, UCH-L1 null mice gain weight at a similar rate as controls until day 40 when weight gain begins to plateau (Oda et al., 1992). Muscle weakness, atrophy, and paralysis progress rapidly over time, with mice eventually losing functionality of the hindlimbs in advanced stages of disease (Yamazaki et al., 1988, Oda et al., 1992). Survival rates drop dramatically beyond 5-6 months of age (Yamazaki et al., 1988, Chen et al., 2010) and null mice that live beyond this period (requiring nutritional enrichment) eventually also develop forelimb paralysis (Chen et al., 2010).

Within the gracile tract, nerve fiber degeneration and reduced nerve bundle number are evident by 80 days of age (Yamazaki et al., 1988, Mukoyama et al., 1989). In the gracile nucleus, dystrophic axons, spheroids (focally swollen axons), and astrocytic proliferation are also present after day 80 and increase in severity with age. Axonal spheroids are detected first in the gracile nucleus and rostral gracile fasiculi and then increase in number along the gracile tract in a retrograde manner corresponding with disease progression, indicating distal-to-proximal degeneration from synaptic terminals in gracile nucleus toward their DRG cell bodies. Spheroid bodies are also present in spinal cord grey and white matter, and in the peduncles and vermis of cerebellum, indicative of spinocerebellar tract degeneration (Kikuchi et al., 1990). The

spinocerebellar tract is an afferent pathway that relays proprioceptive information from the limbs to the cerebellum (Bosco and Poppele, 2001). Electron microcopy analyses have shown that dystrophic axons in the CNS are characterized by an abnormal accumulation of neurofilaments, mitochondria, dense bodies, and tubulovesicular structures (Mukoyama et al., 1989). Additionally, immunohistochemical studies indicated an increased immunoreactivity for GFAP (glial fibrillary acidic protein), substance P (Yamazaki et al., 1993), ubiquitin-positive puncta (Wu et al., 1995), amyloid precursor protein and β-amyloid (Ichihara et al., 1995), as well as β- and γ-synucleins (Wang et al., 2004) along the gracile tract. Such aberrant accumulation of organelles and proteins in degenerating axons suggests that protein degradation and/or axonal transport may be impaired in these animals. In support of the latter, experiments from cultured neurons revealed that pharmacological inhibition of UCH-L1 activity impaired retrograde trafficking of BDNF signaling endosomes (Poon et al 2013), providing evidence that UCH-L1 loss of function can disrupt cargo transport along axons which may contribute to disease pathogenesis.

Synaptic terminal degeneration is also evident in the PNS of UCH-L1 null animals at muscle spindles and neuromuscular junctions (NMJs) of sensory and motor nerves, respectively. In extensor digitorum longus (EDL) muscles of 20 day old UCH-L1 mice (before onset of symptoms), degeneration is apparent at muscle spindles, the sensory receptor terminals of Ia afferent fibers that signal changes in muscle length. Although some axons appear to regenerate from new nerve fibers until day 60, these too eventually degenerate leaving the majority of muscle spindles in EDL denervated by day 100 (Oda et al., 1992). This sensory terminal loss precedes motor terminal loss, as significant motor endplate degeneration is not observed until day 60. In anterior gracillis (AG) muscle, terminal degeneration of NMJs occurs first at the distally innervated portion

of AG, which is followed by progressive degeneration in the proximally innervated zone beginning around day 80 (Miura et al., 1993). Additionally, within the nerve zone between AG distal and proximal endplates, the quantity of myelinated axons decreased over time, with large diameter axons degenerating first (Miura et al., 1993). Age-dependent motor endplate denervation has also been reported in triangularis sterni (TS) muscles, with evidence of degeneration beginning at day 60 (Chen et al., 2010). The DRG cell bodies have not yet been examined *in situ* in this animal model. However, dissociated DRG cultures derived from adult UCH-L1 null mice are more susceptible to lipid peroxidation-induced cell death, indicating an increased vulnerability of this neuronal population (Nagamine et al., 2010).

Synaptic terminal degeneration occurs largely before involvement of other axonal structures and occurs first at distal sites, supporting a “dying back” or distal-to-proximal mode of axonal degeneration in UCH-L1 null animals. Although axonal degeneration in the gracile tract of the CNS has been described in UCH-L1 null mice, the effect of UCH-L1 loss-of-function in peripheral nerves has not been well characterized, as only terminal loss and peroneal nerve degeneration have been reported in aged UCH-L1 mice (Chen et al., 2010). My studies examined pathological alterations in dorsal roots, ventral roots, and sciatic nerves of UCH-L1 deficient mice, and support a distal-to-proximal mode of axonal degeneration in the PNS, implicating a role for UCH-L1 in general axon maintenance.

Potential role of UCH-L1 in synaptic function

Recent studies have demonstrated electrophysiological and synaptic abnormalities in the CNS and PNS of UCH-L1 null mice, suggesting that UCH-L1 may

play a key role in normal neurotransmission and synaptic plasticity. The UCH-L1 protein localizes to synapses at both pre- and postsynaptic sites, suggesting possible global yet distinct roles for UCH-L1 at the synapse (Cartier et al., 2009, Chen et al., 2010). Additionally, pharmacological inhibition of UCH-L1 activity leads to increased size but decreased density of some dendritic spine populations both pre- and post-synaptically, suggesting UCH-L1 may regulate synaptic structure or maintenance which is consistent with the synaptic terminal degeneration observed in UCH-L1 null mice as described above.

UCH-L1 activity has also been identified as a regulator of hippocampal long-term potentiation (LTP), a cellular correlate of learning and memory. UCH-L1 null mice have deficits in learning behavior as well as in theta burst stimulated LTP (Sakurai et al., 2008), although in a separate study LTP deficits were not observed in hippocampi from UCH-L1 null mice (Walters et al., 2008). In further support of a role for UCH-L1 in synaptic transmission, hippocampal slices treated with the UCH-L1 inhibitor LDN-57444 demonstrated reduced LTP following tetanic stimulation. Moreover, basal synaptic activity was reduced following LDN-57444 treatment, indicating a role for UCH-L1 in normal synaptic function (Gong et al., 2006). Exogenous UCH-L1 expression also rescued deficits in hippocampal LTP in the amyloid precursor protein/presenilin-1 (APP/PS1) mouse model of AD and in hippocampal slices treated with β-amyloid (Gong et al., 2006).

UCH-L1 also plays a critical role in NMJ transmission within the peripheral nervous system, but the mechanism remains unclear. In addition to the NMJ degeneration reported in UCH-L1 null mice (Miura et al., 1993, Chen et al., 2010), age-dependent decreases in spontaneous and evoked synaptic activity at the NMJ have

been reported (Chen et al., 2010). In *ex vivo* muscle tissues, miniature endplate potential (mEPP) frequencies were significantly reduced in UCH-L1 null mice, but mEPP amplitudes were not affected. However, summated EPP amplitudes were reduced in tissue from diseased mice, together suggesting fewer acetylcholine release events at the NMJ (reduced quantal content) rather than alterations in quantal size, or the amount of neurotransmitter released per synaptic vesicle (Chen et al., 2010). Presynaptic denervation and reduced synaptic vesicle density were also observed at the NMJ of UCH-L1 null mice via EM, providing further supporting evidence of reduced acetycholine release. Together these data suggest UCH-L1 may be involved in the trafficking of synaptic vesicles to the terminal or actively participates in neurotransmitter release (Chen et al., 2010). However, it is unknown whether motor endplate deficits are due to disrupted signaling at the NMJ or if they occur as a consequence of motor axon degeneration or some combination of these factors. The structural integrity of the peripheral axons associated with these motor terminals remains undefined and it is also unknown whether EPP deficits measured in isolated muscle preparations correspond with alterations in the *in vivo* compound muscle action potential. Sensory nerve transmission has not previously been reported in this model.

1.5 Role of parkin in neurodegenerative disease pathogenesis

Parkin is commonly mutated in autosomal recessive PD

Parkin is a ubiquitously expressed RING (really interesting new gene) finger containing E3-ubiquitin ligase comprised of 465 amino acids (~52 kDa). Parkin-mediated ubiquitin signaling regulates multiple cellular processes, including UPS-mediated protein turnover (Rankin et al., 2011), the aggresome-autophagy pathway

(Olzmann et al., 2007, Olzmann and Chin, 2008), mitophagy (Narendra et al., 2008, Wang et al., 2011), nuclear factor-κB signaling (Henn et al., 2007, Sha et al., 2010), and endocytic trafficking (Fallon et al., 2006). Parkin-mediated monoubiquitination, K48- and K63-linked have all been reported, which highlights the ability of parkin to regulate diverse cellular pathways through its association with different substrate proteins (Dawson and Dawson, 2009).

Parkin mutations account for almost half of all autosomal recessive PD cases (Kitada et al., 1998, Lucking et al., 2000, West and Maidment, 2004), with the others resulting from mutations in DJ-1 and PTEN-induced putative kinase 1 (PINK1) (Valente et al., 2001, Bonifati et al., 2003a, Bonifati et al., 2003b, Valente et al., 2004). Over 200 human parkin mutations have been reported, including exonic deletions and duplications as well as point mutations. At least 70 pathogenic mutations are causative of autosomal recessive juvenile onset PD (ARJP) and can be homozygous or compound heterozygous mutations (PD mutant database: http://www.molgen.vib-ua.be/PDMutDB/default.cfm?MT=0&ML=0&Page=Home). Patients with ARJP have a similar clinical presentation as sporadic PD patients, except that disease occurs with a much earlier onset, occurring before age 20 and as early as during childhood (Lucking et al., 2000). The pathology observed in postmortem parkin-mutant ARJP patient brain is markedly different from that seen in sporadic or other monogenic forms of the disease. In particular, Lewy bodies are not present in patient samples suggesting that parkin may mediate inclusion body formation (Takahashi et al., 1994, Mori et al., 1998). Parkin has also been identified as a Lewy body component in sporadic PD brain (Schlossmacher et al., 2002, Murakami et al., 2004) and parkin inactivation by oxidative and nitrosative stress is thought to contribute to sporadic PD pathogenesis (Chung et al., 2004, Yao et al., 2004).

Interestingly, parkin loss of function mutations are also observed in several human carcinomas, suggesting that parkin separately functions as a tumor suppressor (Poulogiannis et al., 2010, Tay et al., 2010, Yeo et al., 2012, Sun et al., 2013, Xu et al., 2014). It is unclear how loss of parkin function contributes to cell death in the case of neurodegeneration but cell proliferation in certain cancers. It is possible that unique complements of tissue-specific parkin interactors and substrates contribute to these differences.

Parkin structure and catalytic mechanism

Parkin is a RING-In-Between-RING (RBR) E3-ubiquitin ligase comprised of an N-terminal ubiquitin like domain (UBL), a linker domain, a parkin-unique RING0 domain (Hristova et al., 2009), and two RING finger domains flanking an in-between-RING (IBR) domain region (Kitada et al., 1998, Morett and Bork, 1999). RING fingers are Zn^{2+} coordinating motifs comprised of conserved cysteine and histidine residues, and have been shown to facilitate binding of E2-ubiquitin conjugases during the ubiquitination cascade (Metzger et al., 2012). Thus, mutations that disrupt RING structure and/or Zn^{2+} coordination can have profound effects on catalytic activity. Parkin and other RBR ligases function as HECT/RING hybrids (Wenzel et al., 2011) in regards to ubiquitin transfer. While RING E3s directly transfer Ub from the E2 to a substrate lysine residue without an intermediate RING~Ub reaction, HECT E3s form a thioester-linked ubiquitin intermediate at the active-site cysteine before transferring the Ub to the substrate. The N-terminal region of HECT E3s binds the E2 while the C-terminal region contains the active site cysteine residue (Metzger et al., 2012). Parkin has been classified as an HECT/RING hybrid because it binds E2s at the RING1 domain, but in a HECT-like

fashion forms a thioester intermediate at the active site cysteine (Cys-431) of the RING2 domain before ubiquitin transfer to the substrate (Wenzel et al., 2011).

The crystal structures of full length rat parkin (Trempe et al., 2013) and rat and human parkin C-terminal to RING0 (aa 138-465) (Trempe et al., 2013, Wauer and Komander, 2013) have recently been solved, revealing that complex intramolecular interactions render parkin in an autoinhibited state. The first report of parkin autoinhibition implicated the N-terminal UBL in impeding ligase activity through an intramolecular interaction with the PUB (parkin UBL/Ub-binding) site located within the IBR and RING2 linker region (Chaugule et al., 2011). The crystal structure of rat parkin indicated that the UBL actually binds RING1 which brings it into close proximity of this α-helical linker region (aa 378-410), dubbed the repressor element of parkin (REP) (Trempe et al., 2013). The crystal structure indicates that the REP linker spans between the IBR and RING2 which blocks the E2 binding site in RING1 and renders parkin in an autoinhibited state that could be affected by mutations that effect the structural integrity of the UBL (Trempe et al., 2013, Wauer and Komander, 2013). The higher resolution partial structures of C-terminal human and rat parkin support this overall conformation and reveal an additional mechanism of activity regulation. In particular, the catalytic Cys-431 in RING2 is occluded by interactions between RING0 and RING2 rendering Cys-431 buried inside the RING structure rather than readily accessible (Trempe et al., 2013, Wauer and Komander, 2013). The structure of the drosophila parkin RBR indicates that global parkin structure is conserved across species (Spratt et al., 2013).

The autoinhibited structure suggests that parkin activation requires significant conformational rearrangement and is likely facilitated by interactions with binding partners and/or post-translational modifications that “open” the parkin protein to a catalytically competent structure. Such activation mechanisms are not well understood,

but PINK1-mediated phosphorylation has emerged as a prevailing method of parkin activation, particularly in regards to parkin's role in mitophagy. Following mitochondrial depolarization, PINK1 phosphorylates parkin and recruits it to damaged mitochondria where parkin ubiquitinates outer mitochondrial membrane proteins to signal their proteasomal degradation and promote mitophagy (Narendra et al., 2008, Matsuda et al., 2010). PINK1 phosphorylation of parkin at Ser-65 activates E3 ligase activity and is critical for mitophagy initiation (Kondapalli et al., 2012, Shiba-Fukushima et al., 2012, Kane et al., 2014). Additionally, we have previously shown that PINK1 phosphorylated parkin robustly ubiquitinates the cytosolic substrate IKKγ (Sha et al., 2010), but it is currently unknown if parkin activation toward this substrate (and other cytosolic substrates) is also mediated by Ser-65 phosphorylation as has been reported for mitochondrial substrates.

Mutant parkin pathogenicity

UBL mutants – Some pathogenic parkin mutations disrupt parkin autoinhibition, resulting in aberrant self-ubiquitination and subsequent degradation by proteasomes, which effectively reduces functional parkin availability. For example, several mutations in the N-terminal UBL (R33Q, R42P, K48A, and V56E) have been shown to destabilize parkin and result in their rapid degradation by the proteasome (Henn et al., 2005). In support of this, some pathogenic mutant parkin proteins (K27N, R33Q, R42P, and A46P) do not autoinhibit and indeed self-ubiquitinate more robustly than wild type parkin. Truncated ΔUBL-parkin has been shown to have higher self-ubiquitination activity than wild type, further indicating a regulatory role for this region (Chaugule et al., 2011). It is important to note, however, that other studies have indicated that the ΔUBL-parkin

truncation mutant mediated reduced substrate ubiquitination compared to wild type (Corti et al., 2003, Cha et al., 2005, Henn et al., 2007) and demonstrated weak autoubiquitination activity as well (Wauer and Komander, 2013). Structural analyses via NMR spectroscopy have shown that some mutations (A31D, R42P, A46P, and V56E) cause misfolding of the UBL while most others maintain a normal folded structure (G12R, V15M, D18N, K32T, R33Q, P37L, and K48A) (Safadi et al., 2011). These studies suggest that UBL structural integrity *per se* does not confer pathogenicity, and thus clarifying the role of the UBL in regards to regulation of parkin activity warrants further study.

RING0 mutations – The RING0 domain is involved in parkin inhibition through interaction with RING2 which causes occlusion of the active site cysteine residue. Thus, mutations in this region are predicted to disrupt the hydrophobic RING0/RING2 interface and alter active site accessibility or protein solubility (Trempe et al., 2013, Wauer and Komander, 2013). Synthetic mutations at the RING0/RING2 interface (F146A, F463A) disrupt the hydrophobic interaction and activate parkin autoubiquitination, validating the role of this region in autoinhibition. Some pathogenic RING0 mutations (K161N, M192V) reduce parkin activity which is likely due to their close proximity to the active site cysteine in the folded structure (Trempe et al., 2013). Additionally, pathogenic mutations at RING0 cysteine residues (C166Y, C212Y) are predicted to disrupt Zn^{2+} coordination and thus alter ligase activity, although this has not been directly tested (Wauer and Komander, 2013).

RING1 mutations – The RING1 domain contains the E2 binding site, so mutations in this region are predicted to alter E2/parkin binding dynamics, and therefore catalytic activity. For example, the T240R mutant protein has no ligase activity (Sriram et al., 2005) and is unable to bind the E2 conjugase UbcH7 (Shimura et al., 2000). The

T240 residue is located in a zinc binding loop required for E2 binding, therefore accounting for the observed loss of function (Trempe et al., 2013, Wauer and Komander, 2013). Several RING1 mutations likely disrupt Zn^{2+} coordination (C238Q, C253Y, R256C, H257R, and C289), affecting solubility and ligase function (Wauer and Komander, 2013).

RING2 mutations and C-terminal truncations – Point mutations in RING2 have been shown to alter Zn^{2+} coordination, solubility, and activity of parkin. The T415N mutation abolishes ligase activity (Sriram et al., 2005), but the mechanism is unclear particularly as this residue is surface exposed on RING2 away from the active site (Trempe et al., 2013). Mutation of the catalytic cysteine residue (C431F) reduces parkin solubility and reduces substrate binding and ubiquitination (Sriram et al., 2005). Other cysteine mutations (C418R, C441R) are predicted to disrupt Zn^{2+} coordination and have previously been shown to reduce solubility (Sriram et al., 2005, Wauer and Komander, 2013). C-terminally truncated disease mutants (E453X, E409X, Q331X, and K211X) are catalytically inactive, have reduced solubility, and are prone to aggregation (Henn et al., 2005).

1.6 Summary and organizational overview

UCH-L1 is an abundant neuronal deubiquitinase implicated in neurodegenerative disease and cancer pathogenesis. Loss-of-function mutations in UCH-L1 cause progressive neurodegeneration with somatosensory and motor deficits in humans and mutant mouse models (Chen et al., 2010, Bilguvar et al., 2013). UCH-L1 mutation, down-regulation, and oxidative modification have also been reported in Parkinson disease (Leroy et al., 1998, Choi et al., 2004). Several other studies indicate an

oncogenic function of UCH-L1 in cancer tumorigenesis (Hurst-Kennedy et al., 2012). Despite these clear links between UCH-L1 and human disease, the cellular function and mechanisms regulating the UCH-L1 level remain unclear. In my dissertation work, I examined a novel regulatory mechanism mediating UCH-L1 degradation, and I also assessed the effect of UCH-L1 loss-of-function on peripheral nerve structure and electrophysiology. My studies have demonstrated that degradation of UCH-L1 is regulated by the PD-linked E3 ubiquitin ligase parkin, which K63-polyubiquitinates UCH-L1 and signals for its lysosomal degradation. I have also demonstrated in mice that loss of UCH-L1 causes age-dependent sciatic nerve degeneration and electrophysiological deficits in peripheral nerves, supporting a role of UCH-L1 in axonal maintenance and function.

In Chapter 2, I describe a novel parkin-dependent mechanism for regulating UCH-L1 expression level. UCH-L1 binding is mediated by the C-terminal catalytic domain of parkin spanning aa 237-465. Three representative pathogenic parkin mutations abrogated binding with UCH-L1 whereas neurodegenerative disease-linked UCH-L1 mutations had no effect on the interaction. Moreover, parkin retained binding with a catalytic dead mutant of UCH-L1, indicating that their interaction is not dependent on UCH-L1 DUB activity. In cooperation with the Ubc13/Uev1a E2 conjugating complex, parkin mediated the K63-linked polyubiquitination of UCH-L1. I also show that UCH-L1 degradation is promoted in the presence of parkin, and that its degradation is mediated through the autophagy-lysosomal pathway. In parkin deficient mouse brain, UCH-L1 ubiquitination is decreased while the protein level is significantly increased, further supporting a role for parkin-mediated ubiquitination in regulating UCH-L1 turnover. This is the first study reporting a functional relationship between parkin and UCH-L1, and reveals novel insight into ubiquitin system disruption in PD pathogenesis.

In Chapter 3, I describe the effect of UCH-L1 loss-of-function on the peripheral nervous system using electrophysiological and histological analyses of peripheral nerves from UCH-L1 null mice. I found evidence suggesting that a population of large caliber axons is reduced in the dorsal and ventral roots of diseased mice, although it remains unclear whether this is due to axonal degeneration as gross pathological changes were not apparent in the nerve samples. I also found that age-dependent axonal degeneration occurred in the sciatic nerve of UCH-L1 deficient mice, as well as age dependent reductions in sensory nerve and compound muscle action potential amplitudes with preserved conduction velocities and action potential latencies. Taken together, these data indicate a role for UCH-L1 in axonal maintenance and support a disease model of primary distal-to-proximal axonal degeneration without demyelination in the absence of the UCH-L1 protein.

Overall, my thesis work provides new information about UCH-L1 regulation and the effect of loss-of-function mutations on neurodegenerative disease pathogenesis. In Chapter 4, I will describe the significance of my research and discuss future directions for further study of the UCH-L1 protein.

1.7 Figures and Tables

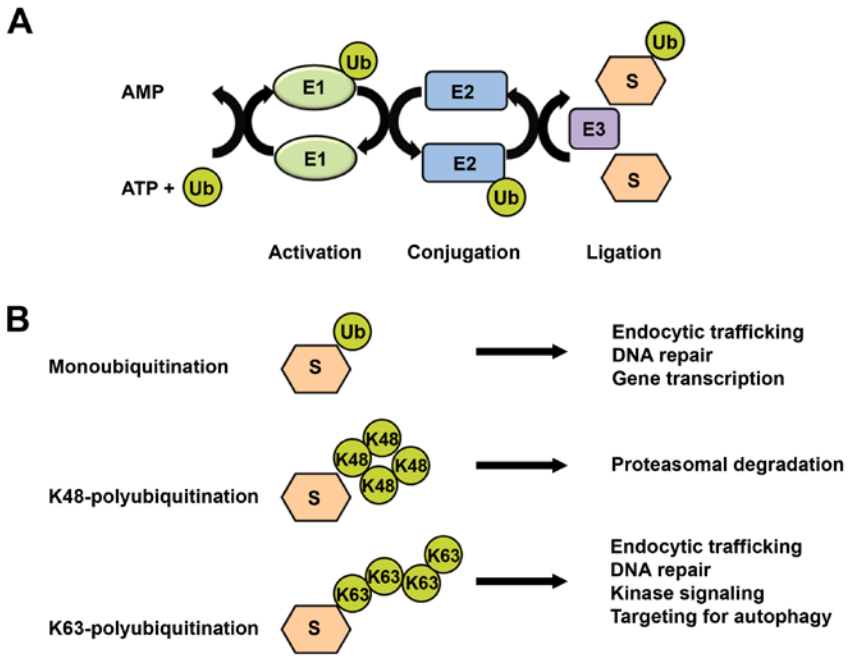

Figure 1.1. Signaling by the ubiquitin system mediates multiple cellular processes. (A) The ubiquitination cascade. Substrate ubiquitination is an ATP-dependent process mediated by the coordinated action of E1-activating, E2-conjugating, and E3-ligating enzymes. Ultimately, the C-terminal glycine of ubiquitin is attached to a lysine residue of the substrate protein via isopeptide bond. Additional ubiquitin moieties can be ligated to one of seven internal lysine residues on ubiquitin to form a polyubiquitin chain. Proteins can be multi-monoubiquitinated, and ubiquitin can also be attached to the N-terminus of the substrate via peptide bond. (B) Different modes of ubiquitination mediate distinct cellular processes. Monoubiquitination typically serves as a signal for DNA repair and gene transcription. Monoubiquitination and multi-monoubiquitination regulate receptor internalization and endocytic trafficking. Polyubiquitin chains differ in

structure which mediates the downstream binding by ubiquitin receptors, a family of proteins containing ubiquitin binding domains (UBDs). K48-linked polyubiquitination signals proteasomal degradation of substrates, whereas K63-linked polyubiquitination regulates multiple processes including DNA repair, trafficking, kinase signaling, and targeting of substrates to the autophagy-lysosomal degradation pathway.

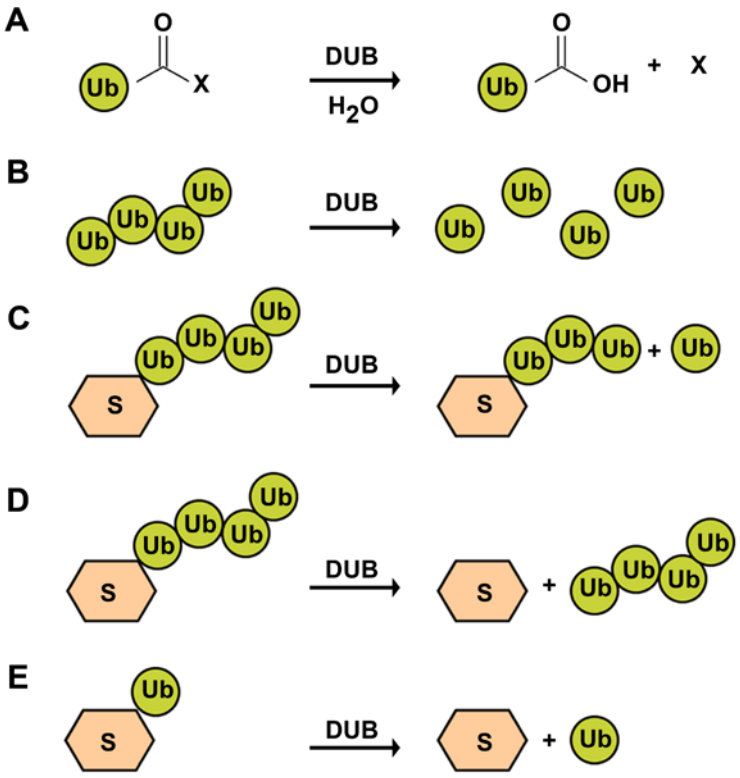

Figure 1.2. Deubiquitinating enzymes (DUBs). The DUBs comprise a family of cysteine proteases and zinc metalloproteases that cleave ubiquitin from substrates; they are also critical for ubiquitin monomer generation and ubiquitin chain disassembly and editing. (A) During the ubiquitination cascade, ubiquitin thiol ester intermediates are often adventitiously attacked by nucleophiles which results in covalent modification at the C-terminus (represented as Ub-X where X represents the ubiquitin adduct bound to the C-terminal glycine residue). The ubiquitin C-terminal hydrolases regenerate ubiquitin monomers by cleaving the Ub~X bond. (B) DUB enzymes process ubiquitin precursors synthesized *de novo* as tandem repeats or as ribosomal fusion proteins, and also disassemble polyubiquitin chains released from substrates to generate monomers. (C) DUBs can also cleave substrate-anchored polyubiquitin chains to edit from the distal

end. Polyubiquitin chain editing serves an important regulatory role as it can “save” proteins from degradation or alter their localization or function. (D,E) Some DUBs cleave the proximal isopeptide bond joining ubiquitin and substrate to release polymeric ubiquitin (D) or monomeric ubiquitin (E). Chain removal is necessary for substrate entry into the catalytic core of the proteasome and monoubiquitin removal regulates downstream signaling events.

Table 1. Genetic PARK loci identified in monogenic PD and related disorders.

Locus	Gene	Inheritance	Encoded Protein Description
PARK1,4	α-synuclein	AD	Synaptic protein of unknown function
PARK2	Parkin	AR	E3-ubiquitin ligase
PARK3	Unknown	AD	Unknown
PARK5	UCH-L1	AD	Deubiquitinating enzyme
PARK6	PTEN induced kinase 1 (PINK1)	AR	Mitochondrial serine/threonine protein kinase
PARK7	DJ-1	AR	Cysteine protease, chaperone, oxidative stress response
PARK8	Leucine-rich repeat kinase 2 (LRRK2)	AD	Serine/threonine protein kinase
PARK9	ATP13A2	AR	Putative lysosomal ATPase
PARK10	Unknown	Risk factor	Unknown
PARK11	Grb-10-Interacting GYF protein (GIGYF2)	AD	Regulation of kinase signaling
PARK12	Unknown	Risk factor	Unknown
PARK13	Omi/HTRA2	AD	Mitochondrial serine protease
PARK14	Phospholipase A2 (PLA2G6)	AR	Cleaves fatty acids from phospholipids
PARK15	F-Box only protein 7 (FBXO7)	AR	Component of SKP1-cullin-F-box family of ubiquitin ligases
PARK16	Unknown	Risk factor	Unknown
PARK17	Vacuolar protein sorting-associated protein 35 (VPS35)	AD	Endosome to Golgi protein trafficking
PARK18	EIF4G1	AD	Regulation of protein translation initiation

Chapter 2: Parkin-mediated K63-polyubiquitination targets ubiquitin C-terminal hydrolase L1 for degradation by the autophagy-lysosome system

Abstract

Ubiquitin C-terminal hydrolase L1 (UCH-L1) is a key neuronal deubiquitinating enzyme which is mutated in Parkinson disease (PD) and in childhood-onset neurodegenerative disorder with optic atrophy. Furthermore, reduced UCH-L1 protein levels are associated with a number of neurodegenerative diseases, whereas up-regulation of UCH-L1 protein expression is found in multiple types of cancer. However, very little is known about how UCH-L1 protein level is regulated in cells. Here, we report that UCH-L1 is a novel interactor and substrate of PD-linked E3 ubiquitin-protein ligase parkin. We find that parkin mediates K63-linked polyubiquitination of UCH-L1 in cooperation with the Ubc13/Uev1a E2 ubiquitin-conjugating enzyme complex and promotes UCH-L1 degradation by the autophagy-lysosome pathway. Targeted disruption of parkin gene expression in mice causes a significant decrease in UCH-L1 ubiquitination with a concomitant increase in UCH-L1 protein level in brain, supporting an *in vivo* role of parkin in regulating UCH-L1 ubiquitination and degradation. Our findings reveal a direct link between parkin-mediated ubiquitin signaling and UCH-L1 regulation, and they have important implications for understanding the roles of these two proteins in health and disease.

2.1 Introduction

Ubiquitin-dependent signaling is required for myriad cellular functions, and disruptions in this system are associated with human disease, including neurodegenerative disorders and cancer (Hussain et al., 2009, Kowalski and Juo, 2012, Satija et al., 2013, McKinnon and Tabrizi, 2014). The ubiquitin system participates in diverse cellular signaling events through the addition or removal of ubiquitin moieties to target proteins. Protein ubiquitination involves the coordinated and sequential action of three proteins – E1-activating, E2-conjugating, and E3-ligating enzymes that together mediate isopeptide bond formation between the ubiquitin C-terminal glycine and substrate lysine residue, after which additional ubiquitin moieties can be joined at one of ubiquitin's seven internal lysine residues to form a polyubiquitin chain (Pickart and Eddins, 2004, Pickart and Fushman, 2004, van Tijn et al., 2008). The nature of the ubiquitin linkage dictates downstream signaling. For example, K48-linked polyubiquitination is the canonical signal for proteasomal degradation (Thrower et al., 2000), whereas K63-linked polyubiquitination plays a signaling role in regulation of various proteasome-independent cellular processes, including endocytosis, DNA repair, and protein trafficking for lysosomal degradation (Olzmann et al., 2007, Olzmann and Chin, 2008, Chen and Sun, 2009). Deubiquitinating enzymes (DUBs) remove ubiquitin from ubiquitinated proteins or cleave C-terminal adducts of ubiquitin to regenerate the ubiquitin monomer, and therefore play an important role in regulating ubiquitin-dependent signaling events as well as in ubiquitin recycling (Reyes-Turcu et al., 2009, Eletr and Wilkinson, 2014).

Ubiquitin C-terminal hydrolase L1 (UCH-L1) is a neuronal DUB with a critical role in the control of cellular ubiquitin homeostasis (Wilkinson et al., 1989, Larsen et al., 1998, Osaka et al., 2003, Wang et al., 2004, Case and Stein, 2006). Human genetic

studies reveal that UCH-L1 is mutated in a rare form of autosomal dominant Parkinson disease (PD) (Leroy et al., 1998) and in the recently described childhood-onset neurodegenerative disorder with optic atrophy (NDGOA) (Bilguvar et al., 2013). The PD-linked I93M mutation reduces UCH-L1 activity by around 50% (Leroy et al., 1998, Nishikawa et al., 2003, Bilguvar et al., 2013) while the NDGOA-linked E7A mutation reduces activity by over 90% (Bilguvar et al., 2013). Furthermore, we have shown that UCH-L1 is oxidatively damaged and down-regulated in sporadic PD and Alzheimer disease (Choi et al., 2004). In mice, loss-of-function mutations in UCH-L1 cause a severe neurodegenerative phenotype dubbed gracile axonal dystrophy which is characterized by progressive ataxia and hindlimb paralysis (Yamazaki et al., 1988, Saigoh et al., 1999, Walters et al., 2008, Chen et al., 2010). Although predominantly expressed in neurons (Doran et al., 1983, Day and Thompson, 2010), UCH-L1 protein is up-regulated in multiple tumors and cancer cells and is likely to have an oncogenic role in tumorigenesis (Tezel et al., 2000, Chen et al., 2002, Mastoraki et al., 2009, Hurst-Kennedy et al., 2012). Despite these established links between UCH-L1 and human diseases, little is known about how UCH-L1 is regulated in cells.

Another ubiquitin system component involved in PD pathogenesis is parkin, an E3 ubiquitin-protein ligase whose mutations cause autosomal recessive juvenile Parkinsonism (ARJP) (Kitada et al., 1998, Lucking et al., 2000, West and Maidment, 2004). Parkin mutations and down-regulation are also found in several types of cancer, supporting a function of parkin as a tumor suppressor (Cesari et al., 2003, Picchio et al., 2004, Poulogiannis et al., 2010, Veeriah et al., 2010). Although UCH-L1 and parkin have been linked to PD and cancer, the relationship between these two proteins remains unknown.

In this study, we investigated the interaction of UCH-L1 with parkin and the role of parkin in UCH-L1 regulation. Our results reveal that parkin binds and facilitates K63-linked polyubiquitination of UCH-L1, and the parkin-mediated ubiquitination promotes UCH-L1 degradation through the autophagy-lysosomal pathway.

2.2 Experimental Procedures

Expression constructs and antibodies - Conventional molecular biological techniques were used to generate the following expression constructs: N-terminal Myc- and His-tagged human wild-type or mutant UCH-L1; N-terminal S-, GFP-, or GST-tagged human wild-type or mutant parkin. Other expression constructs used in this study include N-terminally HA-tagged Ub-WT, Ub-K48, Ub-K63, Ub-K0 (provided by T. Dawson, Johns Hopkins University, Baltimore, MD) and Ub-K48R and Ub-K63R (provided by M. Wooten, Auburn University, Auburn, AL). Polyclonal anti-UCH-L1 antibody against a synthetic peptide (residues 201-219) of human UCH-L1 was generated in rabbit and affinity-purified as described (Chin et al., 2000). Other antibodies used in this study include anti-actin (clone C4, Millipore), anti-HA (clone 12CA5), anti-Myc (clone 9E10), anti-S-tag (Abcam), anti-ubiquitin (clone P4G7, Abcam), anti-GST (clone B14, Santa Cruz), and anti-parkin (Cell Signaling). Horseradish peroxidase-conjugated secondary antibodies were from Jackson ImmunoResearch.

Cell Culture and Transfection - SH-SY5Y or HeLa cells were cultured in DMEM (Gibco) supplemented with 10% fetal bovine serum (Atlanta Biologicals) and 1% penicillin/streptomycin (Fisher). Cell transfections were performed using LipofectAMINE

2000 transfection reagent (Invitrogen) according to the manufacturer's protocol. Lysates were harvested at 24-72 hr post-transfection for subsequent analyses.

Coimmunoprecipitation and S-tag pulldown assays – For coimmunoprecipitation analysis of the interaction between endogenous UCH-L1 and parkin, anti-UCH-L1 antibodies or rabbit serum IgG controls were cross-linked to G-Sepharose agarose (Millipore) using 25 mM dimethyl pimelimidate dihydrochloride (Thermo Scientific). Immunoprecipitation was carried out as described (Giles et al., 2009) by incubation of the cross-linked anti-UCH-L1 or IgG beads with SH-SY5Y cell lysates prepared in Triton lysis buffer (50 mM Tris HCl pH 7.6, 150 mM NaCl, 0.1% Triton-X-100, 1% IGEPAL CA630 supplemented with proteinase and phosphatase inhibitors). Immunocomplexes were eluted with 100 mM glycine (pH = 2.8) followed by immunoblotting with anti-parkin and anti-UCH-L1 antibodies. For coimmunoprecipitation analyses of the interaction between Myc-tagged UCH-L1 WT or mutant and GFP-tagged parkin, lysates from transfected HeLa cells were subjected to immunoprecipitation with anti-Myc antibody followed by recovery of protein complexes with protein G-Sepharose and subsequent immunoblotting analyses. S-tag pulldown assays were performed as described (Hackbarth et al., 2004) by incubation of lysates from HeLa cells coexpressing S-tagged parkin WT or mutant and Myc-UCH-L1 with S-protein-agarose (Novagen), and the pulled down protein complexes were analyzed by immunoblotting with anti-UCH-L1 and anti-S-tag antibodies.

Recombinant protein purification and in vitro binding assays – Recombinant His-UCH-L1, glutathione S-transferase (GST), and GST-tagged parkin proteins were expressed in *E. coli* BL21 or Arctic Express cells and purified as previously described

(Li et al., 2001, Lee et al., 2012). *In vitro* binding assays were performed as described (Li et al., 2001, Webber et al., 2008) by incubation of GST-parkin and GST proteins immobilized on glutathione agarose with mouse brain lysate or soluble His-UCH-L1 for 2 hr at 4 °C. Bound proteins were analyzed by SDS-PAGE and immunoblotting.

In vivo and in vitro ubiquitination assays – *In vivo* ubiquitination assays were performed as previously described (Olzmann et al., 2007, Sha et al., 2010). In brief, lysates from HeLa cells coexpressing S-tagged parkin, Myc-tagged UCH-L1, and HA-tagged wild type or mutant ubiquitin plasmids as indicated were immunoprecipitated under denaturing conditions with anti-Myc antibody, and ubiquitinated UCH-L1 was detected by immunoblotting with anti-HA antibody. *In vitro* ubiquitination assays were performed as described (Olzmann et al., 2007, Sha et al., 2010) by incubation of purified His-UCH-L1 (1 µg) with E1 enzyme (18 nM), E2 enzyme (UbcH7, UbcH8, or UbcH13/Uev1a; 250 nM), ubiquitin (10 µg) and GST or GST-parkin (1 µg) in reaction buffer (50 mM Tris-HCl, pH 7.6, 5 mM $MgCl_2$, 100 mM NaCl, 25 µM $ZnCl_2$, 2 mM dithiothreitol, and 4 mM ATP) for 2 hr at 37 °C. Ubiquitin, E1, and E2 enzymes were from Boston Biochem, and the total volume of the reaction was 100 µL. Ubiquitinated UCH-L1 was detected by immunoblotting with anti-ubiquitin antibody.

Parkin$^{-/-}$ mice and analysis of UCH-L1 ubiquitination and protein levels in parkin$^{-/-}$ mice – A breeding colony of parkin knockout (*parkin$^{-/-}$*) mice was established from breeding pairs provided by R. Palmiter, University of Washington, Seattle, WA (Perez et al., 2005, Perez and Palmiter, 2005). For assessment of endogenous UCH-L1 ubiquitination in *parkin$^{-/-}$* and *parkin$^{+/+}$* mouse brain, immobilized GST-tagged, tandem ubiquitin binding entities (TUBEs, LifeSensors) were used as described (Hjerpe et al.,

2009) to isolate ubiquitinated proteins from brain extracts from 4-month-old male *parkin*$^{-/-}$ mice and parkin$^{+/+}$ controls, followed by immunoblotting with anti-UCH-L1 and anti-GST antibodies. For analysis of total UCH-L1 protein levels, brains from 3-month-old *parkin*$^{-/-}$ and *parkin*$^{+/+}$ mice were homogenized in 1% SDS and then subjected to SDS–PAGE and immunoblotting with anti-UCH-L1 and anti-β-actin antibodies. The relative level of UCH-L1 was determined as described (Giles et al., 2009) by normalizing the immunoblot intensity of UCH-L1 against that of β-actin using Image J software.

Treatment of cells with proteasomal and lysosomal degradation inhibitors – SH-SY5Y cells expressing S-parkin or the S-vector control were subjected to 24 hr treatments with the proteasome inhibitor MG132 (20 μM, Sigma), chloroquine (CQ, 100 μM, Sigma), 3-methyl-adenine (3MA, 10 mM, Sigma), or 0.1% Me_2SO (DMSO, Fisher) vehicle control. Equal amounts of whole cell lysates were subjected to SDS-PAGE followed by immunoblotting with anti-UCH-L1 and anti-β-actin antibodies. Relative UCH-L1 levels were quantified as described above.

UCH-L1 degradation assays– For analysis of UCH-L1 degradation, SH-SY5Y cells expressing S-parkin or the S-vector control were treated with protein synthesis inhibitor cyclohexamide (10 μg/mL) for the indicated lengths of time. Cells were lysed at the indicated time points, and equal protein fractions from each lysate were analyzed by immunoblotting with anti-UCH-L1 and anti-S-tag antibodies.

Statistical analyses – Data were analyzed by Student's t-test or 2-way ANOVA followed by Tukey's posttests where $p < 0.05$ was considered statistically significant. Results were expressed as mean ± SEM from three independent experiments.

2.3 Results

UCH-L1 interacts with parkin in vitro and in vivo – UCH-L1 was identified as a potential interactor of parkin in a recent proteomic screen (Davison et al., 2009), but this result has not yet been validated and it is unknown if these two proteins interact either *in vitro* or *in vivo*. To test if UCH-L1 and parkin can physically interact with each other, we performed *in vitro* binding assays with purified recombinant proteins. We found that His-tagged UCH-L1 bound selectively to GST-tagged parkin but not to GST alone (Fig. 2.1 A), indicating a direct interaction between UCH-L1 and parkin. To confirm this interaction, we performed GST pulldown assays and found that purified GST-parkin, but not the GST control, was able to pulldown endogenous UCH-L1 from mouse brain homogenates (Fig. 2.1 B), further supporting a specific interaction between these two proteins. We then performed coimmunoprecipitation analysis to examine the association of endogenous UCH-L1 and parkin in dopaminergic SH-SY5Y cells (Fig. 2.1 C). Anti-UCH-L1 antibody, but not the IgG control, was able to coimmunoprecipitate UCH-L1 and parkin from cell lysates (Fig. 2.1 C), indicating that UCH-L1 interacts with parkin *in vivo*.

The parkin-UCH-L1 interaction is impaired by PD-linked parkin mutations but not by UCH-L1 mutations – Because UCH-L1 binds monoubiquitin (Osaka et al., 2003), we hypothesized that the parkin-UCH-L1 interaction may be mediated by the ubiquitin-like domain (UBL) at the N-terminus of parkin. To test this hypothesis, we examined the interaction of UCH-L1 with N- or C-terminal truncation mutants of parkin (Fig 2.2 A). We

found that parkin ΔUBL, a mutant form of parkin lacking the UBL domain, retained the ability to bind UCH-L1 (Fig. 2.2 B), arguing against the involvement of the UBL domain in mediating the parkin-UCH-L1 interaction. In addition, the parkin N-terminal region (PKN), which contains the UBL and RING0 domains, was virtually incapable of binding UCH-L1 (Fig. 2.2 B), indicating that parkin UBL and RING0 domains are dispensable for the parkin-UCH-L1 interaction. In contrast, the parkin C-terminal region (PKC), which contains the RING1, RING2, and in-between RING-finger (IBR) domains, was able to bind UCH-L1 (Fig. 2.2 B), indicating that the UCH-L1-binding region is located between amino acid residues 237-465 of parkin.

We next examined the effects of several familial PD-linked parkin mutations (Fig. 2.2 A) on the parkin-UCH-L1 interaction by performing S-pulldown assays using lysates from HeLa cells coexpressing Myc-tagged UCH-L1 and S-tagged parkin WT or pathogenic mutant. We found that the ability of parkin to bind UCH-L1 is abrogated by parkin T240R and T415N mutations (Fig. 2.2 B). Consistent with previous reports that parkin R42P mutant is misfolded and rapidly degraded by the proteasome (Schlehe et al., 2008), we observed low levels of parkin R42P mutant in cells (Fig. 2.2 B). Our results showed an apparent lack of UCH-L1 binding to parkin R42P mutant (Fig. 2.2 B).

We then assessed the effects of several UCH-L1 mutations (Fig. 2.3 A) on the parkin-UCH-L1 interaction and found that the ability of UCH-L1 to interact with parkin is not affected by the PD-linked UCH-L1 I93M mutation or by the NDGOA-associated E7A mutation (Fig. 2.3 B). In addition, UCH-L1 S18Y substitution, a polymorphism in UCH-L1 which is thought to confer protection against sporadic PD (Satoh and Kuroda, 2001, Elbaz et al., 2003, Maraganore et al., 2004, Carmine Belin et al., 2007), also had no apparent effect on the parkin-UCH-L1 interaction (Fig. 2.3 B). Furthermore, the UCH-L1 catalytic site-specific C90S mutation did not disrupt the ability of UCH-L1 to interact with

parkin (Fig. 2.3 B), indicating that the DUB activity of UCH-L1 is not required for its interaction with parkin.

Parkin mediates K63-linked polyubiquitination of UCH-L1 – Our finding of an interaction between UCH-L1 and parkin (Fig. 2.1) raises the possibility that UCH-L1 may be a substrate of parkin E3 ligase. To test this possibility, we assessed the ability of parkin to promote UCH-L1 ubiquitination in cells by using a well-established *in vivo* ubiquitination assay (Wheeler et al., 2002, Lee et al., 2008). We found that ectopic parkin expression in HeLa cells, which lack endogenous parkin, resulted in enhanced ubiquitination of Myc-tagged UCH-L1 compared to the vector-transfected control (Fig. 2.4 A), supporting a role of parkin in facilitating UCH-L1 ubiquitination *in vivo*. We next performed *in vitro* ubiquitination analyses with recombinant proteins to test if UCH-L1 is ubiquitinated by parkin in the presence of various E2 ubiquitin-conjugating enzymes (UbcH7, UbcH8, or the Ubc13/Uev1a complex) which are known to facilitate parkin E3 ligase activity (Olzmann et al., 2007). We observed UCH-L1 ubiquitination by parkin in the presence of Ubc13/Uev1a, but not in the presence of either UbcH7 or UbcH8 (Fig. 2.4 B, 2.4 C). These results, together with our previous finding that Ubc13/Uevla is the cognate E2 enzyme for parkin-mediated K63-linked polyubiquitination, whereas UbcH7 and UbcH8 are the cognate E2 enzymes for parkin-mediated K48-linked polyubiquitination (Olzmann et al., 2007), suggest that parkin cooperates with the Ubc13/Uev1a E2 enzyme to catalyze K63-linked polyubiquitination of UCH-L1.

To determine if parkin-mediated K63-linked polyubiquitination of UCH-L1 takes places in cells, we performed *in vivo* ubiquitination assays using ubiquitin mutants, Ub-K48 and Ub-K63, which permit only the formation of K48-linked and K63-linked polyubiquitin chains, respectively, because all other lysine residues of ubiquitin were mutated to arginine. We detected robust UCH-L1 polyubiquitination by parkin in cells

expressing Ub-WT or Ub-K63, but not in cells expressing Ub-K48 (Fig. 2.5 A), supporting that parkin-mediated UCH-L1 polyubiquitination occurs via the K63-linkage. To further confirm this linkage, we used ubiquitin mutants, Ub-K48R and Ub-K63R, which contain a single lysine-to-arginine mutation at the indicated residues and are therefore incapable of forming K48-linked and K63-linked polyubiquitin chains, respectively. We found that parkin-mediated UCH-L1 polyubiquitination was abolished by replacement of Ub-WT with Ub-K63R but not by the replacement with Ub-K48R (Fig. 2.5 B). In addition, parkin-mediated UCH-L1 polyubiquitination was not detected in cells expressing Ub-K0, an ubiquitin mutant which is incapable of forming polyubiquitin chains because all its lysine residues were mutated to arginines (Fig. 2.5 B). Together, these data provide strong support for a function of parkin in facilitating K63-linked polyubiquitination of UCH-L1.

Parkin is required for polyubiquitination of endogenous UCH-L1 in the brain – To further assess the role of parkin in regulation of UCH-L1 ubiquitination *in vivo*, we examined the ubiquitination status of endogenous UCH-L1 in brains from wild type (*parkin*$^{+/+}$) and parkin knockout (*parkin*$^{-/-}$) mice (Perez et al., 2005, Perez and Palmiter, 2005) by using the tandem ubiquitin binding entities (TUBEs) approach. Previous studies have shown that GST-tagged TUBEs, such as GST-tagged TUBE2 based on the UBA1 domain from human RAD23A, preferentially capture endogenous polyubiquitnated proteins, but bind monubiquitnated proteins at much lower affinity (Hjerpe et al., 2009). Our analysis of UCH-L1 ubiquitination with GST-tagged TUBE2 revealed that endogenous UCH-L1 in mouse brain was polyubiquitinated and the UCH-L1 polyubiquitination was significantly reduced by targeted disruption of parkin expression in mice (Fig. 2.6 A, 2.6 B). In addition to polyubiquitinated UCH-L1 forms, we also observed a ubiquitinated UCH-L1 species at ~40 kDa, which could represent UCH-L1

diubiquitination or monoubiquitination at two different sites (Fig. 2.6 A). The level of this ubiquitinated UCH-L1 species was not significantly changed in the *parkin*$^{-/-}$ mouse brain compared to that in the *parkin*$^{+/+}$ mouse brain (Fig. 2.6 A, 2.6 C). These findings indicate that parkin is required for regulation of UCH-L1 polyubiquitination but not UCH-L1 diubiquitination or monoubiquitination *in vivo*.

Parkin promotes UCH-L1 degradation through the autophagy-lysosome pathway – Next, we assessed the effect of targeted parkin deletion on the total level of endogenous UCH-L1 in mouse brain by performing quantitative Western blot analysis. We found that the total UCH-L1 level in the brain was significantly higher in *parkin*$^{-/-}$ mice than that in the *parkin*$^{+/+}$ controls (Fig. 2.7 A, 2.7 B), suggesting a role for parkin in regulation of UCH-L1 degradation. To test this possibility, we analyzed the effect of parkin overexpression on the turnover rate of endogenous UCH-L1 protein in SH-SY5Y cells. We found that the UCH-L1 protein turnover rate was increased by parkin overexpression (Fig. 7C) and protein half-life reduced (Fig. 7D), supporting a function of parkin in promoting UCH-L1 degradation.

There are two major protein degradation pathways in cells: the ubiquitin-proteasome pathway and the autophagy–lysosome pathway (Ciechanover, 2005, Rubinsztein, 2006). To determine which degradation pathway is involved in the clearance of UCH-L1 protein, we assessed the effects of proteasome, lysosome and autophagy inhibition on the steady-state level of endogenous UCH-L1 in SH-SY5Y cells in the absence or presence of exogenous parkin. We found that the steady-state level of endogenous UCH-L1 was significantly decreased in the presence of exogenous parkin as compared with the UCH-L1 level in the absence of exogenous parkin (Fig 2.8), consistent with a role of parkin in promoting UCH-L1 degradation. The parkin-induced degradation of UCH-L1 was blocked by the lysosome inhibitor chloroquine (CQ) or the

autophagy inhibitor 3MA but not by the proteasome inhibitor MG132 (Fig 2.8). Together, these results support that parkin promotes UCH-L1 degradation through the autophagy-lysosome pathway but not the proteasome pathway.

DISCUSSION:

While both parkin and UCH-L1 have both been implicated in the pathogenesis of PD and cancer, it is not established whether there is a physical or functional link between these two proteins. Our work described in this study shows that UCH-L1 is a substrate of parkin E3 ligase and reveals a function of parkin as a regulator of UCH-L1 degradation.

Despite ample evidence indicating the importance of UCH-L1 in health and disease, our knowledge of UCH-L1 post-translational modifications and their roles in UCH-L1 regulation is limited. A previous study reported that His-tagged UCH-L1 in transfected COS-7 monkey kidney cells is monoubiquitinated, with a ~33 kDa ubiquitinated UCH-L1 species which corresponds to monoubiquitination at a single site (Meray and Lansbury, 2007). However, the E3 ligase for mediating UCH-L1 monoubiquitination remains unidentified, and the ubiquitination status of endogenous UCH-L1 is unknown. Our TUBE analysis of endogenous UCH-L1 ubiquitination in mouse brain revealed the presence of multiple polyubiquitinated UCH-L1 forms as well as a ~40 kDa diubiquitinated UCH-L1 species (which could also represent UCH-L1 monoubiquitination at two sites), but no ~33 kDa monoubiquitinated UCH-L1 species. Interestingly, we found that the levels of the polyubiquitinated UCH-L1 forms, but not ~40 kDa diubiquitinated UCH-L1 species, were significantly reduced by targeted parkin deletion in mice, indicating a role for parkin in regulation of endogenous UCH-L1 polyubiquitination but not UCH-L1 diubiquitination or monoubiquitination.

Because ubiquitin has seven internal lysine residues, polyubiquitination can occur via different linkages, leading to distinct outcomes. For example, K48-linked polyubiquitination targets protein to the proteasome for degradation, whereas K63-linked polyubiquitination acts in a proteasome-independent manner to regulate a number of cellular processes, including protein trafficking and autophagosome formation (Pickart and Fushman, 2004, Chen and Sun, 2009).We and others have previously shown that, through its association with different E2 enzymes, parkin is capable of mediating multiple forms of ubiquitination, including K48-linked polyubiquitination and K63-linked polyubiquitnation(Olzmann et al., 2007, Dawson and Dawson, 2009, Chin et al., 2010). Our *in vivo* ubiquitination studies revealed that, in cells, parkin-mediated UCH-L1 polyubiquitination occurs via the K63 linkage but not the K48 linkage. Furthermore, by using *in vitro* ubiquitination assays with recombinant proteins, we obtained evidence that parkin cooperates with the UbcH13/Uevla E2 ubiquitin-conjugating complex to facilitate K63-linked polyubiquitination of UCH-L1.

Emerging evidence indicates that K63-linked polyubiquitination could serve as a signal for targeting protein or other cargo to the autophagy machinery for subsequent degradation by the lysosome (Kirkin et al., 2009b, Chin et al., 2010). The recognition of this targeting signal is thought to be mediated by adaptor proteins, such as p62, which binds simultaneously to K63-polyubiquitinated cargo via its ubiquitin-binding UBA domain and to the autophagy machinery component LC3 via its LC3-interacting region (LIR) to induce autophagosome formation (Pankiv et al., 2007, Wooten et al., 2008). The autophagosome then fuses with the lysosome, leading to degradation of the cargo by lysosomal hydrolases. Consistent with this view, our findings support that parkin-mediated K63-linked polyubiquitination of UCH-L1 promotes the degradation of UCH-L1

by the autophagy-lysosome pathway. These findings provide new insights into the mechanism that control UCH-L1 degradation in cells.

Protein degradation plays an important role in regulating the expression levels of specific proteins and consequently the cellular processes in which these proteins participate (Ciechanover, 2005) UCH-L1 has a well-characterized deubiquitinating activity for catalyzing the hydrolysis of C-terminal esters and amides of ubiquitin to generate monomeric ubiquitin (Larsen et al., 1996) and might also possess dimerization-dependent E3 ligase activity (Liu et al., 2002). Although the exact function of UCH-L1 remains unclear, UCH-L1 has been shown to control the cellular pool of free ubiquitin (Osaka et al., 2003, Walters et al., 2008), and thereby could affect many ubiquitin-dependent cellular processes. Recent studies in *Drosophila* showed that overexpression of UCH-L1 in the eye imaginal discs induces caspase-dependent apoptosis and interferes with photoreceptor cell differentiation, resulting in a rough eye phenotype (Thao et al., 2012). Our analysis reveals that targeted disruption of parkin gene expression in mice causes a significant increase in UCH-L1 protein level in the brain. Taken together, these results suggest that loss of parkin-mediated UCH-L1 regulation may be a pathogenic mechanism contributing to neurodegeneration in human ARJP patients with parkin mutations.

Acknowledgements

We thank Dr. Samuel M. Lee and Soe Thein for assistance with parkin and UCH-L1 protein purifications, Drs. Ted Dawson and Marie Wooten for providing plasmids, and Richard Palmiter for providing breeding pairs of parkin$^{-/-}$ mice. This work was supported in part by the National Institutes of Health (NS067950 to J.E.M, GM103613 to L.L., and AG034126 to L.S.C.) and the Emory University Research Committee (SK46673 to L.L.).

2.5 Figures

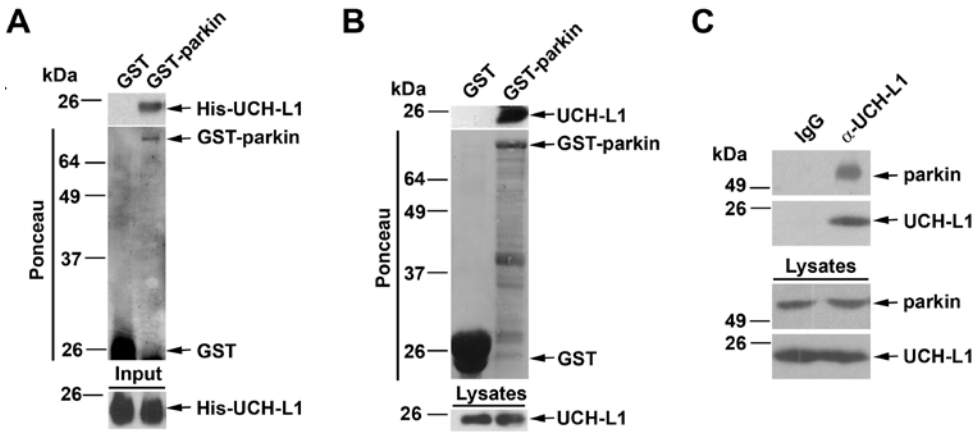

Figure 2.1. Specific interaction of UCH-L1 with parkin. (A) *In vitro* binding assays were performed by incubation of soluble His-tagged UCH-L1 (input) with immobilized GST or GST-parkin proteins (shown by Ponceau staining). Analysis of bound UCH-L1 by immunoblotting with anti-UCH-L1 antibody reveals direct binding of UCH-L1 to parkin. (B) GST pulldown assays were performed by incubation of equal amounts of mouse brain lysates with immobilized GST or GST-parkin (Ponceau staining) followed by immunoblotting with anti-UCH-L1 antibody to detect binding of endogenous UCH-L1 to parkin. (C) Coimmunoprecipitation of endogenous parkin with UCH-L1. SH-SY5Y cell lysates were subjected to immunoprecipitation with anti-UCH-L1 antibody cross-linked to G-protein agarose or with the IgG beads. The immuoprecipitated proteins were eluted and analyzed by immuoblotting with anti-parkin and anti-UCH-L1 antibodies.

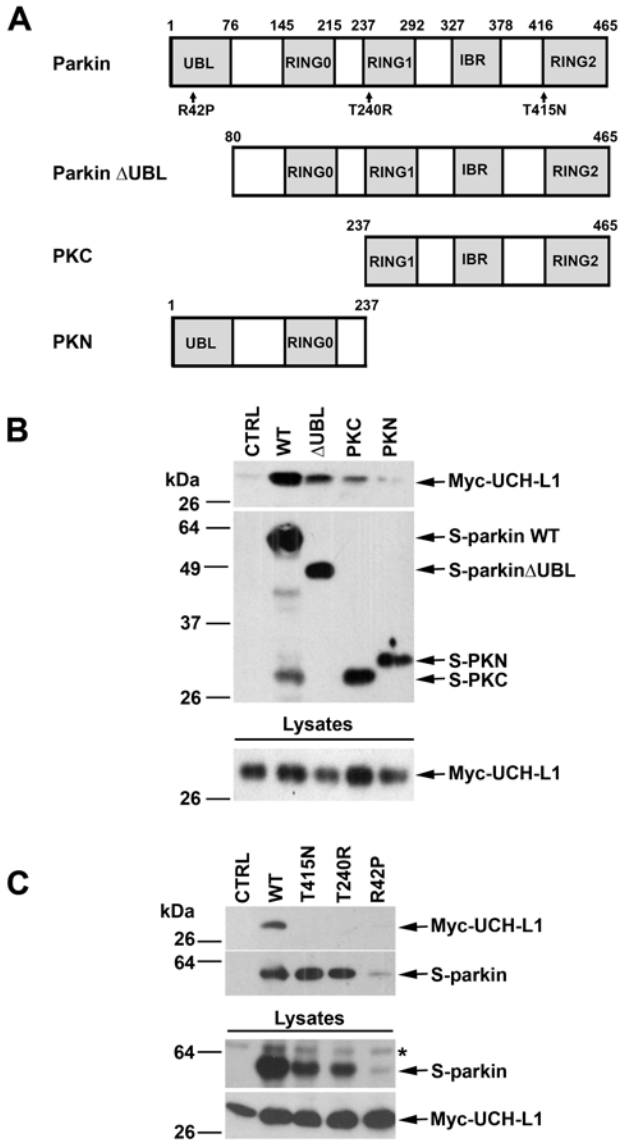

Figure 2.2. Pathogenic mutations and C-terminal truncation of parkin disrupt the interaction with UCH-L1. (A) Schematic representation of parkin and its mutants used in this study. The location of PD-linked parkin mutations are indicated on the domain structure. UBL, ubiquitin like domain; IBR, in between RING-finger domain; PKC, C-terminal parkin; PKN, N-terminal parkin. (B) The interaction of parkin with UCH-L1 occurs within the C-terminal portion of parkin. S-pulldown assays were performed with lysates from HeLa cells coexpressing Myc-UCH-L1 and S-parkin WT or deletion mutant

or the S-vector control, followed by immunoblotting with anti-Myc and anti-S-tag antibodies. (C) Impairment of the parkin-UCH-L1 interaction by PD-linked parkin mutations. S-pulldown assays were performed using lysates from HeLa cells coexpressing Myc-UCH-L1 and S-vector or S-parkin WT or mutant as indicated, followed by immunoblotting with anti-Myc and anti-S-tag antibodies. Asterisk indicates a nonspecific band.

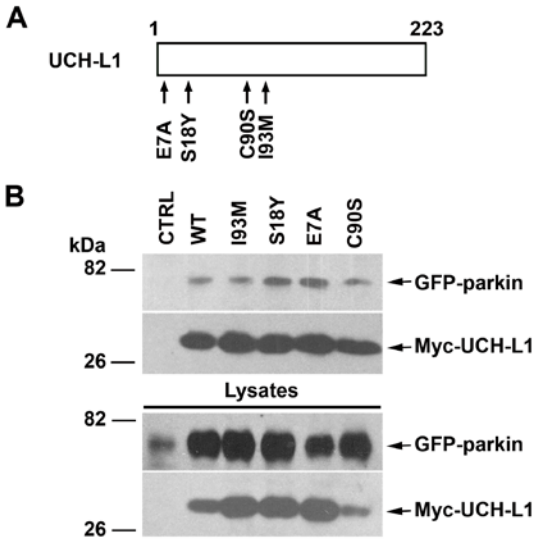

Figure 2.3. Interaction of parkin with wild-type and mutant UCH-L1. (A) Schematic representation of UCH-L1 and its mutants used in this study. The locations of neurodegenerative disease-linked UCH-L1 mutations (E7A and I93M), protective polymorphism (S18Y), and catalytically inactive mutation (C90S) are indicated. (B) Lysates from HeLa cells coexpressing GFP-parkin and the indicated Myc-UCH-L1 WT or mutant were immunoprecipitated with anti-Myc antibodies followed by immunoblotting with anti-Myc and anti-parkin antibodies.

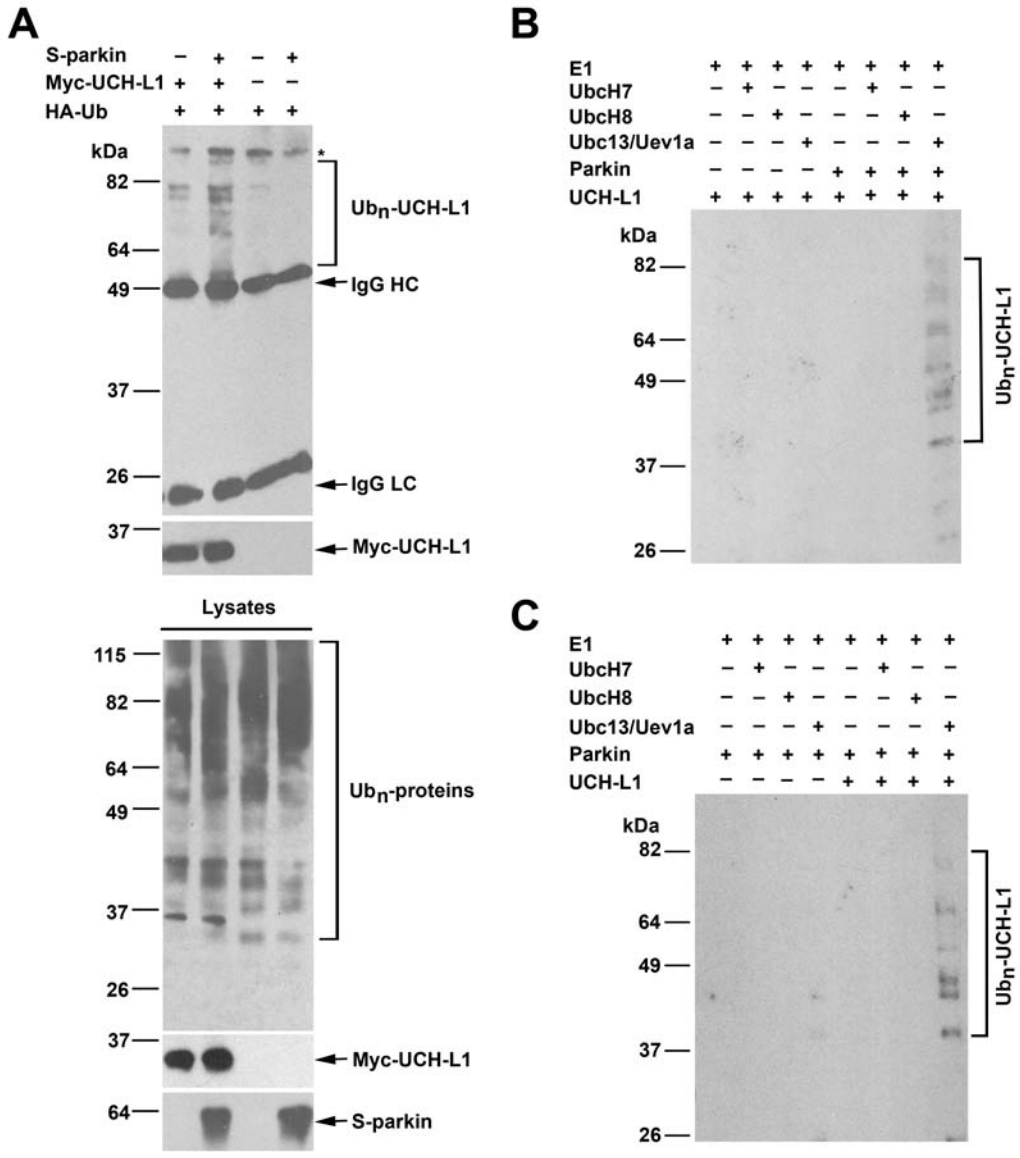

Figure 2.4. UCH-L1 is a substrate of parkin E3 ubiquitin ligase. (A) Parkin ubiquitinates UCH-L1 *in vivo.* Parkin-mediated ubiquitination of UCH-L1 was assessed in HeLa cells expressing HA-tagged ubiquitin, Myc-UCH-L1, and S-parkin as indicated. *In vivo* ubiquitination of UCH-L1 was determined by immunoprecipitation with anti-Myc antibody followed by immunoblotting with anti-HA and anti-Myc antibodies. Ub_n-UCH-L1, polyubiquitinated UCH-L1; IgG HC, immunoglobulin heavy chain; IgG LC, immunoglobulin light chain. Asterisk indicates a nonspecific band. (B and C) Parkin

ubiquitinates UCH-L1 *in vitro* in cooperation with the Ubc13/Uevla E2 enzyme. *In vitro* ubiquitination assays were performed with recombinant His-tagged UCH-L1 in the presence of E1, E2 (UbcH7, UbcH8, or the Ubc13/Uev1a complex), GST-parkin, and ubiquitin as indicated. Ubiquitinated UCH-L1 was detected by immunoblotting with anti-ubiquitin antibody.

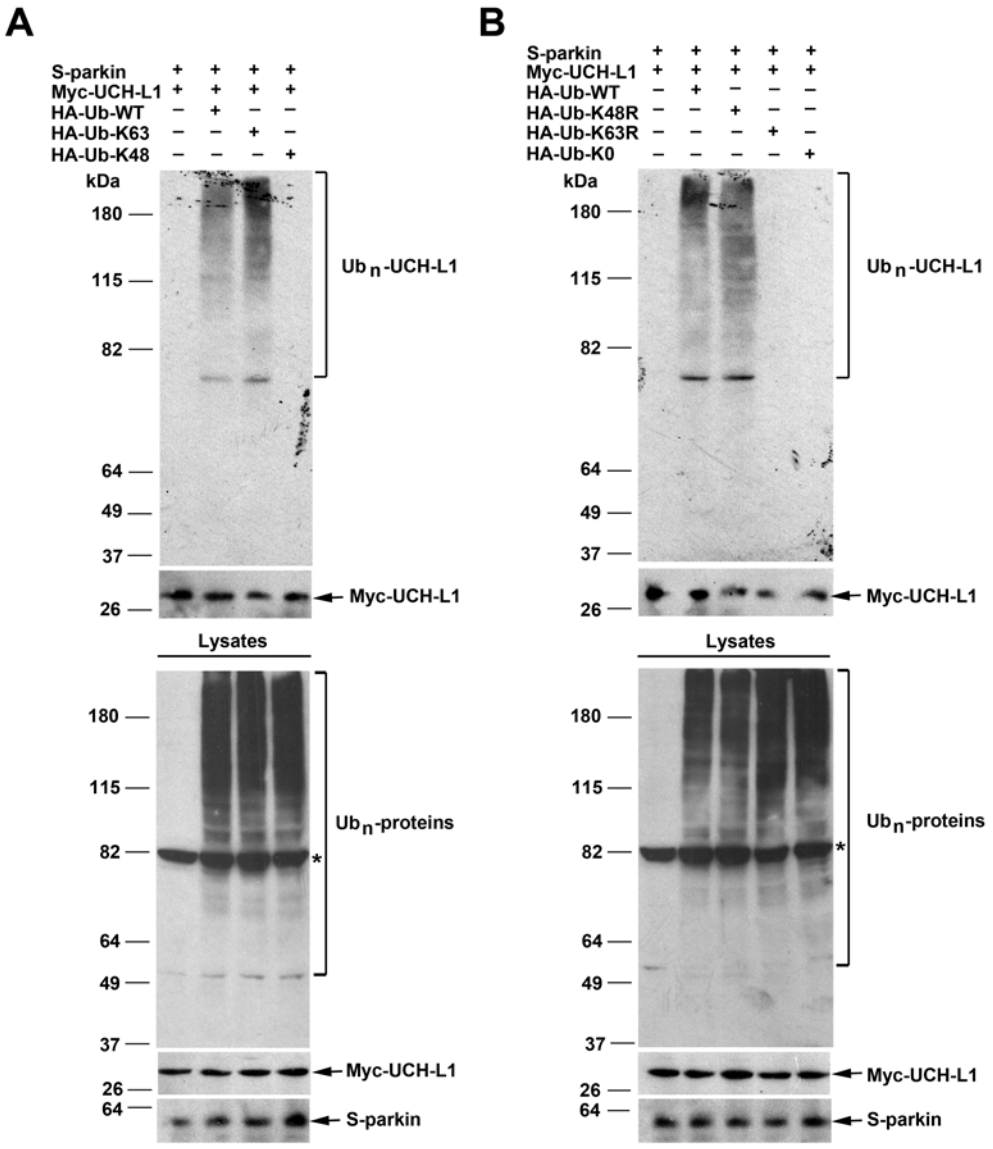

Figure 2.5. Parkin-mediated UCH-L1 polyubiquitination occurs via the K63 linkage. (A and B) HeLa cells were transfected with S-parkin, Myc-UCH-L1, and HA-tagged wild-type or mutant ubiquitin as indicated. Polyubiquitinated UCH-L1 (Ub_n-UCH-L1) was detected by immunoprecipitation with anti-Myc antibody under denaturing conditions followed by immunoblotting with anti-HA and anti-Myc antibodies. The expression of S-parkin, Myc-UCH-L1, and HA-ubiquitin-conjugated proteins (Ub_n-

proteins) in the cell lysates were confirmed by immunoblotting with anti-parkin, anti-Myc, and anti-HA antibodies. Asterisk indicates a nonspecific band.

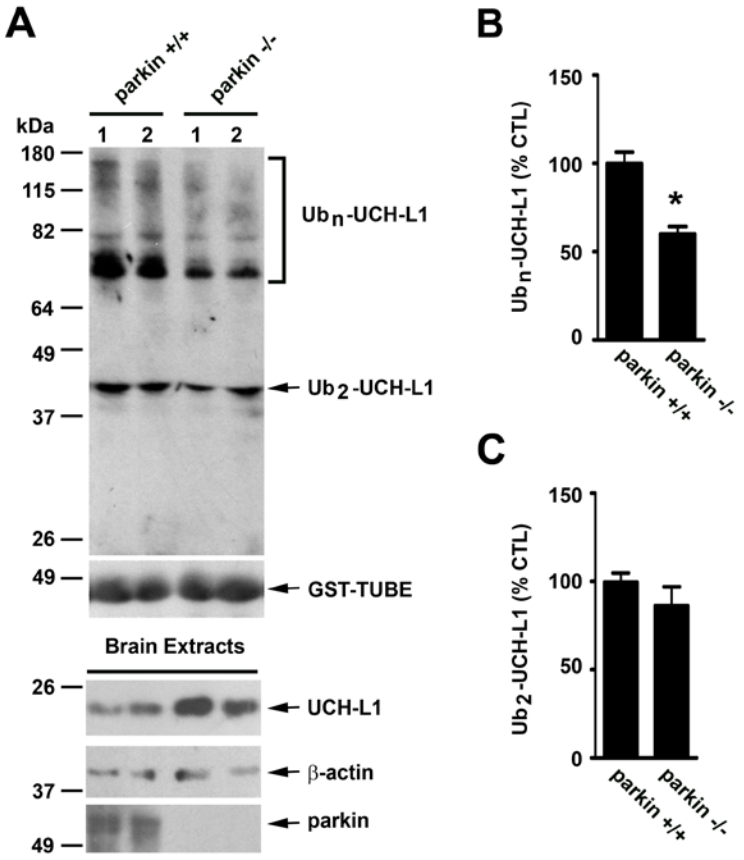

Figure 2.6. UCH-L1 polyubiquitination is reduced in parkin$^{-/-}$ mouse brain. (A) Brain extracts (500 µg) from two individual *parkin*$^{+/+}$ or *parkin*$^{-/-}$ mice were subjected to pull-down using GST-TUBEs, and ubiquitinated UCH-L1 was detected by immunoblotting with anti-UCH-L1 antibodies. (B and C) The level of polyubiquitinated UCH-L1 (Ub_n-UCH-L1) (B) and the level of diubiquitinated UCH-L1 (Ub_2-UCH-L1) (C) were quantified using Image J software and expressed as a percentage of the corresponding control level in the *parkin*$^{+/+}$ mice. Data represent mean ± SEM (n = 3 animals per genotype). *, $p < 0.05$ versus the *parkin*$^{+/+}$ control, unpaired two-tailed student's *t* test.

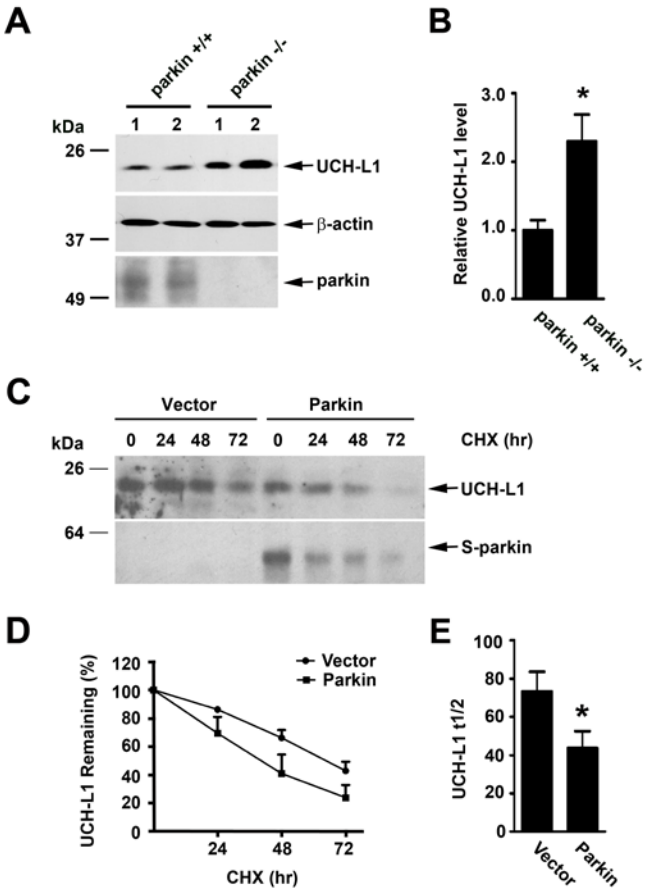

Figure 2.7. Regulation of endogenous UCH-L1 degradation by parkin. (A and B) Total brain UCH-L1 levels are elevated in *parkin*$^{-/-}$ mice. Immunoblot analysis of brain homogenates from two individual *parkin*$^{+/+}$ or *parkin*$^{-/-}$ mice with anti-UCH-L1, anti-β-actin and anti-parkin antibodies (A). The relative level of total UCH-L1 was normalized to the β-actin level and expressed relative to the normalized UCH-L1 level in the *parkin*$^{+/+}$ brain homogenate (B). Data represent mean ± SEM (n = 5 animals per genotype). *, $p < 0.05$ versus the *parkin*$^{+/+}$ control, unpaired two-tailed student's *t* test. (C) SH-SY5Y cells expressing S-tag vector or S-parkin were treated with cycloheximide (10 µg/mL) for 0-72 hr with lysates collected at 24 hr intervals in 1.1% SDS. Equal lysate fractions were subjected to SDS-PAGE followed by immunoblotting with anti-UCH-L1 and anti S-parkin antibodies. (D) UCH-L1 degradation rates were assessed by normalizing UCH-L1 band

intensity at each time point to the corresponding t_0 timepoint for either vector or parkin expressing cells. (E) UCH-L1 $t_{1/2}$ was calculated from the 48 hr and 72 hr data points and analyzed by student's t-test. Results are displayed as the mean ± SEM determined from three independent experiments.

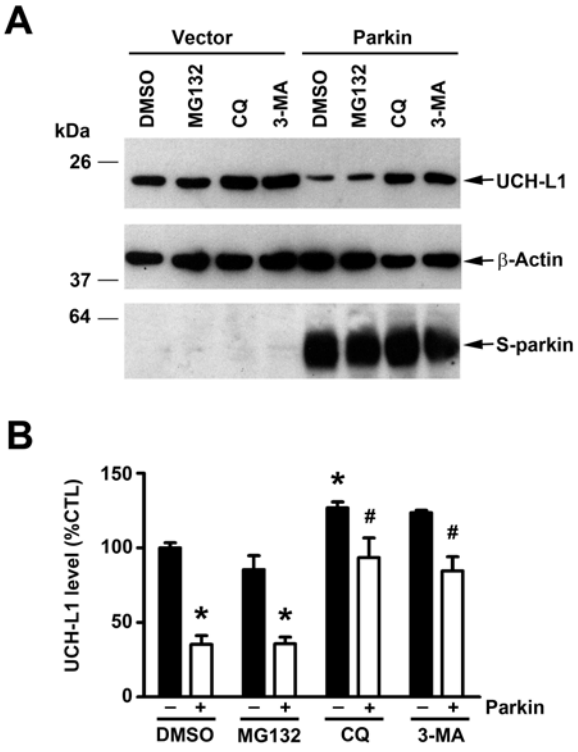

Figure 2.8. Parkin targets UCH-L1 for degradation by the autophagy-lysosome pathway. (A) SH-SY5Y cells expressing S-tag vector or S-parkin were treated for 24 hr with the indicated protein degradation inhibitors or vehicle (DMSO), and cell lysates were analyzed by immunoblotting with anti-UCH-L1, anti-S-tag, and anti-β-actin antibodies. (B) The level of endogenous UCH-L1 was normalized to the β-actin level and expressed as a percentage of the normalized UCH-L1 level in the DMSO-treated, vector-transfected control cells. Results are shown as mean ± SEM from three independent experiments. *, $p < 0.05$ versus the DMSO-treated, vector-transfected control; #, $p < 0.05$ versus the DMSO-treated, parkin-transfected control, two-way ANOVA with a Tukey's post-hoc test.

Chapter 3: UCH-L1 is required for maintenance and function of sensory and motor axons in the peripheral nervous system

Abstract

Loss-of-function mutations in ubiquitin C-terminal hydrolase L1 (UCH-L1) cause gracile axonal dystrophy (*gad)* in mice and childhood-onset neurodegeneration with optic atrophy (NDGOA) in humans. These disorders are characterized by progressive neurodegeneration in the central nervous system (CNS) and sensory and motor ataxia. Although UCH-L1 localizes to sensory and motor nerve terminals in the peripheral nervous system (PNS) and progressive terminal degeneration is observed in UCH-L1 deficient mice, the role UCH-L1 plays in the peripheral nervous system remains undefined. Thus, we examined distal (sciatic nerve and tail nerve) and proximal peripheral nerves (L4 dorsal and ventral roots) from young and aged animals to determine if loss-of-UCH-L1 function causes peripheral nerve degeneration and functional conduction deficits. We report evidence supporting an age-dependent distal-to-proximal mode of nerve degeneration in the PNS, accompanied by age-dependent reductions in sensory nerve and compound muscle potential amplitudes, but preserved nerve conduction velocities. We also observed normal myelination and structural integrity at the nodes of Ranvier, supporting a disease model of primary axonal degeneration without demyelination. Taken together, the data described in this chapter support a role for UCH-L1 in the maintenance and transmission of peripheral axons, and provide novel insight into PNS pathologies resulting from UCH-L1 loss-of-function.

3.1 Introduction

An autosomal recessive mutation in the neuronal deubiquitinase UCH-L1 was recently reported in three siblings from consanguineous parents exhibiting neurodegeneration with optic atrophy (NDGOA)(OMIM 615491) (Bilguvar et al., 2013). Symptoms worsened with age and included childhood onset blindness, nystagmus, head tremor, cerebellar ataxia, spasticity, and reduced proprioceptive sense. Cortical, cerebellar, and optic atrophy were also apparent. Additionally, evoked somatosensory potential amplitudes were diminished upon electrical stimulation (Bilguvar et al., 2013) suggesting degeneration of peripheral fibers. Moreover, loss of function mutations in UCH-L1 cause gracile axonal dystrophy (*gad*) in mice (Saigoh et al., 1999, Walters et al., 2008), a neurodegenerative phenotype characterized by progressive degeneration in the gracile nucleus and gracile fasciculi associated with age-dependent sensorimotor ataxia and paralysis that first develops in the hindlimbs. (Yamazaki et al., 1988, Kikuchi et al., 1990). In UCH-L1 deficient mice, muscle spindle and motor terminal loss has also been reported at sensory and motor nerve endings, respectively, with muscle spindle degeneration preceding motor terminal loss (Oda et al., 1992, Miura et al., 1993, Chen et al., 2010). Taken together, the pathological findings in both humans and mice indicate that the UCH-L1 protein is required for axon maintenance and synaptic terminal integrity in the periphery. In support of this hypothesis, UCH-L1 is localized to the neuromuscular junction (NMJ) and central synapses (Cartier et al., 2009, Chen et al., 2010) and mice deficient in UCH-L1 expression demonstrate electrophysiological deficits in long term potentiation (Sakurai et al., 2008) and acetylcholine release at motor endplates (Chen et al., 2010). However, the role UCH-L1 plays in nerve transmission and axonal maintenance in the peripheral nervous system remains unknown.

In this study, we used electrophysiological and histological analyses to examine the effect of UCH-L1 loss-of-function on distal and proximal peripheral nerves. We observed age-dependent axonal degeneration in the sciatic nerve, characterized by altered area and diameter distributions in symptomatic animals. We examined the L4 dorsal and ventral roots of symptomatic mice, and found selective reductions in the large caliber axon population in UCH-L1 null animals suggestive of axonal atrophy. Additionally, sensory nerve and compound muscle action potentials were reduced in symptomatic animals while conduction velocities and action potential latencies were unchanged, supporting a disease model of primary axonal degeneration without demyelination. Taken together, these data indicate a critical role for UCH-L1 in axonal maintenance and neurotransmission in the PNS, and support a distal-to-proximal mode of degeneration in the absence of UCH-L1 expression. This report provides novel insight into the role of UCH-L1 in the PNS and is the first to report *in vivo* functional nerve deficits in UCH-L1 deficient mice, which has important implications for understanding mechanisms underlying NDGOA pathology.

3.2 Experimental Procedures

UCH-L1$^{-/-}$ mice – Heterozygous mice (B6;129P2-*Uchl1^{tm1Dgen}*,011642-UNC) - containing targeted deletion of exons 6-8 and a portion of exon 9 in the UCH-L1 gene were obtained from the Mutant Mouse Regional Resource Center (MMRRC, University of North Carolina at Chapel Hill). The strain was originally produced by the Deltagen Corporation and deposited to the MMRRC. Mutant mice were generated through heterozygous breeding and genotypes were determined via PCR using primers as described (Chen et al., 2010).

Peripheral nerve histology and morphometric analyses – Mice were deeply anesthetized with choral hydrate followed by transcardial perfusion with ice cold 2.5% glutaraldehyde in 0.1 M phosphate buffer (pH 7.4). Sciatic nerves and the L4 dorsal and ventral roots were removed and postfixed in 2.5% glutaraldehyde overnight at 4 °C, washed with phosphate buffer and then embedded in paraffin. Semithin sections (0.5 µm) were cut in longitudinal and cross section followed by toluidine blue staining. Whole slide images were generated via digital scanning of the glass slides with the NanoZoomer 2.0-HT digital slide scanner (Hamamatsu Photonics, Shizuoka Pref., Japan) and visualized with the NanoZoomer Digital Pathology (NDP) software. Axon diameter (minimum Feret's), axon area, and circularity were measured from 8-10 randomly selected 100 µm x 100 µm fields at 40x magnification of the toluidine blue stained semithin sections. Three mice were examined for each genotype at either 1 month or 4.5 months of age, with approximately 750-1360 fibers counted per nerve per animal. Circularity is defined by the equation $(4\pi \times \text{area})/(\text{perimeter}^2)$ where a maximum value of 1 represents a perfect circle. Measurements were made using the particle analysis feature in ImageJ and quantitative analyses were performed after manual exclusion of Schwann cell nuclei and other non-axonal structures from the data set.

Nerve conduction studies – Motor and sensory nerve conduction were analyzed in UCH-L1 wild type and mutant mice at 1 month (presymptomatic) and 3-5 months of age (symptomatic). Studies were conducted using the Nicolet VikingQuest (Natus Medical Incorporated, San Carlos, CA) system as described (Lee et al., 2013). Briefly, mice were anesthetized with 4% chloral hydrate dissolved in saline (400 mg/kg of body weight, i.p.) and kept under ambient heat to prevent hypothermia. Compound muscle

action potentials (CMAPs) were measured from the interosseous muscles of the left foot following stimulation (19.2 mA) at the sciatic notch and ankle. Motor nerve conduction (MNCV) was calculated as the quotient of the distance between stimulus sites over the difference between action potential latencies. Sensory nerve action potential (SNAP) and sensory nerve conduction velocity (SNCV) were measured from the tail nerve with recording electrodes inserted at the base of the tail and stimulating electrodes 30-40 mm distal to the recording electrodes. Amplitude and velocity measurements were calculated as the average from 20 repeated stimulations (3.1 mA).

Antibodies and western blot analyses – The UCH-L1 antibody used in this study was previously described (Chapter 2). Other antibodies used include anti-β-actin (Millipore), anti-neurofilament H (Millipore), anti-MBP (myelin basic protein) (Millipore) and anti-Caspr (contactin-associated protein) (Abcam). Secondary antibodies were from Jackson ImmunoResearch. For examination of protein expression by western blot, soluble protein homogenates of brain and sciatic nerve were prepared from 3 month old UCH-L1$^{+/+}$ and UCH-L1$^{-/-}$ mice in Triton lysis buffer (50 mM Tris HCl pH 7.6, 150 mM NaCl, 0.1% Triton-X-100, 1% IGEPAL CA630 supplemented with proteinase and phosphatase inhibitors). Sciatic nerves were combined from 3-4 animals prior to homogenization to ensure sufficient protein levels for subsequent analyses. Protein expression was assessed using SDS-PAGE followed by immunoblotting with the indicated antibodies and detection with enhanced chemiluminescence (ECL).

Teased fiber staining and confocal microscopy – Mice were perfused with 4% paraformaldehyde (PFA) in 0.1 M phosphate buffer (pH 7.4). The L4 dorsal roots, L4 ventral roots, and sciatic nerves were dissected and postfixed in 4% PFA overnight and then transferred to 0.1 M phosphate buffer. To separate individual fibers, samples were teased with fine tweezers in glycerol under a dissecting microscope, followed by immersion in cold acetone (10 min) and rehydration in PBS. Samples were blocked for 1 hr at room temperature in PBS containing 10% horse serum and 0.5% Triton X-100 followed by incubation with primary antibodies in the blocking solution at 4 °C overnight. After washing, fibers were incubated with fluorophore-conjugated secondary antibodies for 1 hr at room temperature and subsequently mounted on glass slides using ProLong Gold (Invitrogen). Nile red staining was performed as previously described (Lee et al., 2013). Confocal images were acquired on a Nikon Eclipse C1 confocal microscope at 60X magnification and visualized with Nikon EZ-C1 Viewer software.

Statistical analyses – To generate frequency histograms of axon area, diameter, and circularity for the dorsal root, ventral root, and sciatic nerve samples, total measurements were grouped into bins as indicated and graphed as percentage of total fibers corresponding to each bin. Frequency histograms were compared via chi-square goodness-of-fit analysis followed by comparisons of the individual bin means using Fisher's exact tests of the raw data, and statistical significance was assessed after Bonferroni correction. To assess differences between the average axon density, area, and diameter, data were analyzed via Student's t-test where $p < 0.05$ was considered statistically significant.

3.3 Results

UCH-L1 is highly expressed in the sciatic nerve – We assessed UCH-L1 expression in the brain and sciatic nerve of UCH-L1$^{+/+}$ and UCH-L1$^{-/-}$ mice by western blot. As expected, there were no bands detected in UCH-L1$^{-/-}$ lysates probed with anti-UCH-L1 antibody (Fig. 3.1 A). We also examined the axonal localization of UCH-L1 via immunostaining of teased sciatic nerve fibers and found that UCH-L1 colocalizes with NF-H, indicating a predominant axonal localization of UCH-L1 (Fig. 3.1 B).

Age-dependent neurodegeneration in the sciatic nerve of symptomatic UCH-L1$^{-/-}$ animals – We next examined the structure of sciatic nerves from the 4.5 m/o symptomatic animals and observed pathological alterations indicative of axonal degeneration in the UCH-L1$^{-/-}$ mice (Fig. 3.2 A, Fig. 3.3). Surprisingly, the average axon fiber density was not altered in UCH-L1$^{-/-}$ sciatic nerve (Fig. 3.2 B), but we did find a significant reduction in average axonal area (Fig. 3.2 C) and in the distribution of axons binned by area (Fig. 3.2 D). The frequency histogram for axon area shows a greater proportion of small caliber axons (0-5 μm^2) in UCH-L1$^{-/-}$ sciatic nerve and reduced proportions of larger caliber axons compared to the UCH-L1$^{+/+}$ samples. These findings are supported by our observation of significantly reduced average axon diameter (Fig. 3.2 E) and a similarly shifted frequency histogram of percentage of axons binned by diameter (Fig. 3.2 F). Fiber shape as measured by axon circularity was similar between the genotypes (Fig. 2G). We observed degenerating axons in the UCH-L1$^{-/-}$ sciatic nerve cross sections (Fig 3B) while axons from UCH-L1$^{+/+}$ sciatic nerve were normal in appearance (Fig. 3A). In the longitudinal plane, we observed densely packed wild type

axons that were healthy in appearance (Fig. 3.3 C), whereas myelin debris from degenerated axons was evident in the UCH-L1$^{-/-}$ sections (Fig. 3.3 D).

To determine whether the pathological alterations in UCH-L1$^{-/-}$ sciatic nerve are age dependent, we next examined sections from presymptomatic 1 m/o animals. We did not detect evidence of neurodegeneration (Fig. 3.4 A). The axon densities (Fig 3.4 B) and average axon areas (Fig. 3.4 C) were not altered by loss of UCH-L1 expression. We also found no significant differences in axon diameter (Fig. 3.4 E) and in the distributions of axons binned by area (Fig. 3.4 D) or perimeter (Fig. 3.4 F). There were also no differences in the axon circularity distributions (Fig. 3.4 G). Thus, our data suggest that the axonal degeneration observed in UCH-L1$^{-/-}$ sciatic nerve is progressive with age and corresponds to disease severity.

Reduction in the proportion of large caliber axons in ventral and dorsal roots of symptomatic UCH-L1$^{-/-}$ mice – Because we did not detect evidence of degeneration in the 1 m/o sciatic nerve samples, we opted to only examine the L4 dorsal and ventral roots from symptomatic animals. Although gross pathological changes were not apparent in ventral root (Fig. 3.5 A) and the overall fiber density was unaltered (Fig. 3.5 B), we found that the average axon area was significantly decreased in the UCH-L1$^{-/-}$ samples (Fig. 3.5 C), suggesting a potential decrease in the relative proportion of small and large caliber axons in these mice. We next analyzed the frequency histograms of axon area grouped into 5 μm^2 incremental bins (Fig. 3.5 D) by chi square goodness-of-fit analysis and found a significant difference in the distributions. We next examined each bin between UCH-L1$^{+/+}$ and UCH-L1$^{-/-}$ mice and found that the population of axons over 50 μm^2 was significantly decreased in UCH-L1 deficient animals. However, we did not

find any statistically significant differences in average axon diameter (Fig. 3.5 E) or distribution (Fig. 3.5 F). Axon morphology (circularity) distributions were also not significantly different between genotypes (Fig. 3.5 G).

We next analyzed the L4 dorsal roots and again found a reduction in the relative proportion of a population of high caliber axons in the UCH-L1$^{-/-}$ animals. Similar to the ventral root, gross pathological alterations were not apparent in the dorsal roots of symptomatic UCH-L1$^{-/-}$ animals (Fig. 3.6 A) and fiber density was not altered (Fig. 3.6 B). However, although the differences in average axon area (Fig. 3.6 C) and diameter (Fig. 3.6 D) were not statistically significant, we did observe significant differences between the area and diameter frequency histograms. In particular, we found that the proportion of axons >40 μm^2 in area and ≥ 6 μm in diameter were reduced in the UCH-L1$^{-/-}$ dorsal root sections (Fig. 3.6 D, 3.6 F). However, axon circularity distributions were similar between genotypes (Fig. 3.6 G).

Functional deficit of sensory and motor nerves in symptomatic animals – To determine whether the degenerative changes observed in symptomatic UCH-L1$^{-/-}$ sciatic nerve were associated with a functional deficit, we assessed CMAPs and MNCVs following stimulation at the sciatic notch and ankle. In presymptomatic UCH-L1$^{-/-}$ animals, CMAP amplitude was not significantly different compared to the UCH-L1$^{+/+}$ controls. In symptomatic UCH-L1$^{-/-}$ animals between 3 and 5 months of age, however, the CMAP amplitude was significantly decreased, in accord with our histopathology data (Fig. 3.7 A). The MNCV (Fig. 3.7 B) and distal and proximal action potential latencies (Fig. 3.7 C, 3.7 D) were not significantly different at either age group.

We also recorded from the tail nerve to assess sensory nerve function and found that SNAP amplitudes were similar in 1 m/o UCH-L1$^{+/+}$ and UCH-L1$^{-/-}$ mice, but significantly reduced in the symptomatic cohort of mice between 3-5 m/o of age (Fig. 3.8 A). Similar to our motor conduction findings, we did not detect differences in SNCV (Fig. 3.8 B) or action potential latency (Fig. 3.8 C) between genotypes at either age group. Taken together, our electrophysiology and histology data demonstrate age-dependent distal-to-proximal degeneration in UCH-L1$^{-/-}$ animals and support a role for the UCH-L1 protein in peripheral nerve maintenance and transmission.

Myelin appearance and morphology at the nodes of Ranvier are not altered in symptomatic UCH-L1$^{-/-}$ animals – In accord with our conduction velocity data, we did not detect pathological changes at the nodes of Ranvier or in the myelination of sciatic nerves from symptomatic UCH-L1$^{-/-}$ animals. We examined structural integrity at the nodes of Ranvier using anti-Caspr immunostaining of teased fibers and toluidine blue staining of semithin longitudinal sciatic nerve sections. Caspr/paranodin is a transmembrane glycoprotein localized to the paranodal axon compartment of myelinated axons and plays a critical role in maintaining nodal structure and facilitating efficient salutatory conduction. We found similar Caspr staining in teased fibers from UCH-L1$^{+/+}$ and symptomatic UCH-L1$^{-/-}$ mice (Fig. 3.9 A) and likewise observed normal nodal morphologies in the toluidine blue stained semithin sections (Fig. 3.9 B). These findings suggest that although UCH-L1 is localized to axons, it is dispensable for maintaining structural integrity at the nodes of Ranvier. We also observed similar anti-MBP immunostaining and Nile red staining patterns in both genotypes (Fig. 3.9 C) suggesting that the axons remaining in the sciatic nerve of symptomatic animals are normally

myelinated. These data support our electrophysiology findings of normal conduction velocities but reduced action potential amplitudes.

3.4 Discussion

In this study, we found age dependent sciatic nerve degeneration as well as evidence of altered small and large caliber axon distributions in the ventral and dorsal roots of symptomatic animals. The reduced proportion of large caliber axons in the dorsal and ventral roots of symptomatic mice was an unexpected finding, particularly as there were no overt signs of axonal degeneration. We speculate that these fibers are showing early axonal atrophy, and thus are moderately reduced in size. However, it is unclear how changes in the large caliber axon distribution in the roots may contribute to the disease phenotype. We also find alterations in motor and sensory nerve transmission, specifically reduced CMAP and SNAP amplitudes in symptomatic animals, but normal conduction velocities and action potential latencies, as well as normal myelin staining and preserved nodal structure in sciatic nerve. This is the first report of functional nerve deficits in UCH-L1 deficient mice, and together supports a model of progressive primary axonal degeneration without demyelination in peripheral nerves in the absence of UCH-L1. Our finding that UCH-L1 expression in sciatic nerve is over 10-fold higher than in brain is consistent with the pronounced peripheral neuropathy phenotype observed in these animals.

Our findings in motor nerves are consistent with prior electrophysiological studies showing age-dependent reductions in mEPP frequency and EPP amplitude in isolated leg muscles of UCH-L1$^{-/-}$ animals (Chen et al., 2010). Progressive denervation at NMJs beginning around postnatal day 60 has also been reported (Miura et al., 1993),

supporting a role for UCH-L1 in the synaptic initiation of motor transmission. Our studies complement these reports as we see age-dependent reductions in CMAP amplitude and pathological alterations in the sciatic nerve, indicating motor axon degeneration. Aside from hindlimb clasping when suspended by the tail, 1 m/o UCH-L1$^{-/-}$ mice are phenotypically normal and are considered presymptomatic (Yamazaki et al., 1988). mEPP frequencies and EPP amplitudes are also normal in 1 m/o mice (Chen et al., 2010), and in this study we found preserved CMAP amplitudes and no evidence of sciatic nerve degeneration at this age. These findings support a correlation between sciatic nerve structure and function and disease severity, but whether transmission deficits at the NMJ precede axonal degeneration or occur as a direct consequence of axon degeneration remains to be determined.

The sciatic nerve is composed of both motor and sensory fibers, and although we did not examine sensory nerve transmission in the sciatic nerve, we found reduced SNAP amplitudes in the mouse tail nerve. Inferring from these results and prior reports of muscle spindle denervation at Ia sensory afferents and proprioceptive deficits reported in UCH-L1$^{-/-}$ mice (Yamazaki et al., 1988, Mukoyama et al., 1989, Kikuchi et al., 1990, Oda et al., 1992), it is likely that both sensory and motor nerve degeneration occur in the sciatic nerve of symptomatic animals. In agreement with our motor nerve findings, we found age-dependent reductions in SNAP amplitude but normal SNCV in the tail nerve of UCH-L1$^{-/-}$ animals. This is the first report of a functional sensory nerve deficit in UCH-L1 deficient animals and is in accord with the reduced somatosensory-evoked potentials but normal conduction velocities observed in NDGOA patients (Bilguvar et al., 2013).

Although genetic mutations in UCH-L1 have not been reported in Charcot-Marie-Tooth (CMT) disease patients, our electrophysiological recordings reveal similarities between the UCH-L1$^{-/-}$ mouse phenotype and CMT2, the axonal degenerating subtype of CMT without significant demyelination (Jani-Acsadi et al., 2008, Patzko and Shy, 2011). CMT2 has been linked to mutations in several diverse genes, including neurofilament light chain, mitofusin 2, dynamin 2, kinesin family member 1B (Kif1b), and Rab7 (Patzko and Shy, 2011, Shy and Patzko, 2011). UCH-L1 may function in the same pathways as CMT2 disease-linked proteins or may indirectly affect these proteins or pathways through the UCH-L1 dependent regulation of monomeric ubiquitin homeostasis. Aberrant protein and mitochondria accumulation has been reported in dystrophic axons along the gracile tract of UCH-L1$^{-/-}$ animals, which suggests a potential axonal transport defect (Mukoyama et al., 1989, Ichihara et al., 1995, Wu et al., 1995, Wang et al., 2004). Stagnation in axonal transport has been hypothesized as a major contributor to axonal degeneration and many of the CMT2 proteins are linked to altered transport (Coleman, 2005, Conforti et al., 2014). In cultured neurons, pharmacological inhibition of UCH-L1 inhibits BDNF retrograde trafficking while UCH-L1 overexpression rescues transport deficits induced by β-amyloid (Poon et al., 2013), supporting a potential role for UCH-L1 in the regulation of axonal transport. Thus, the UCH-L1$^{-/-}$ mouse is a robust model for mechanistic studies of age dependent primary axonal degeneration in the peripheral nervous system and may also have potential utility as a novel model of CMT2 in addition to NDGOA.

Acknowledgements

We thank the Emory Electron Microscopy Core Facility for processing of semithin nerve sections and the Winship Cancer Institute Pathology CoreLab at Emory for whole slide digital scanning. This work was supported in part by the National Institutes of Health (NS067950 to J.E.M, GM103613 to L.L., and AG034126 to L.S.C.) and the Emory University Research Committee (SK46673 to L.L.).

3.5 Figures

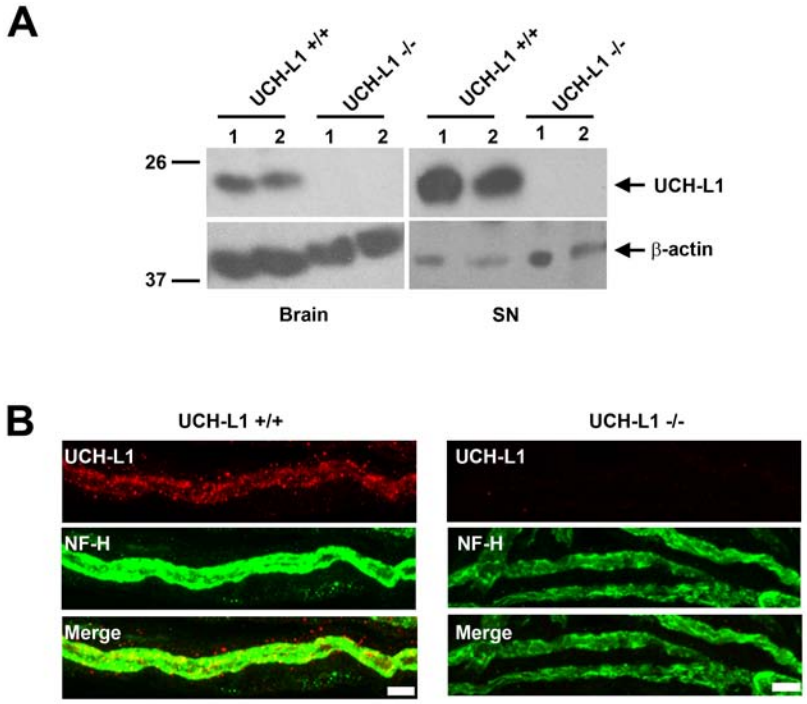

Figure 3.1. UCH-L1 is highly expressed in PNS axons. (A) Whole brain and sciatic nerve lysates prepared from 3 m/o UCH-L1$^{+/+}$ and UCH-L1$^{-/-}$ animals were subjected to SDS-PAGE and subsequently analyzed by immunoblotting with anti-UCH-L1 and anti-β-actin antibodies. (B) Representative images of teased sciatic nerve fibers from 4.5 m/o UCH-L1$^{+/+}$ and UCH-L1$^{-/-}$ animals immunostained with anti-UCH-L1 and anti-NF-H antibodies. UCH-L1 colocalizes with NF-H in UCH-L1$^{+/+}$ sciatic nerve, indicating the axonal localization of UCH-L1. As expected, a fluorescent signal was not detected in UCH-L1$^{-/-}$ nerve, demonstrating antibody staining specificity. Scale bar = 5 µm.

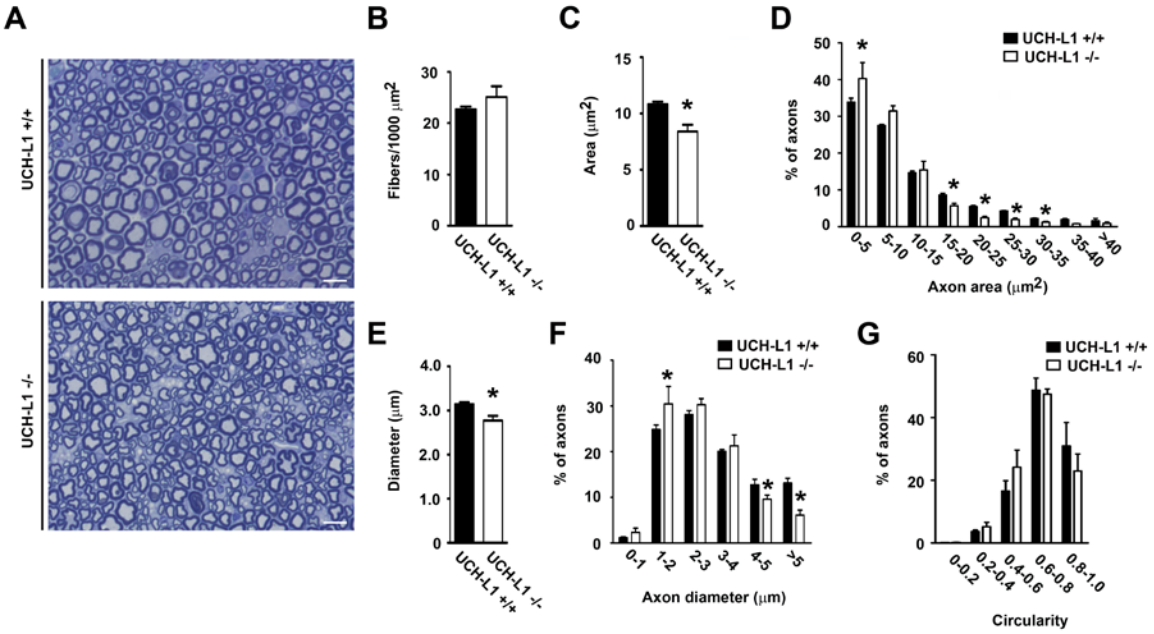

Figure 3.2. Sciatic nerve degeneration in symptomatic UCH-L1$^{-/-}$ animals. (A) Representative images of toluidine blue stained sciatic nerve sections from 4.5 month old UCH-L1$^{+/+}$ and UCH-L1$^{-/-}$ mice. (B) The average total fiber density (fibers/1000 μm^2) was not altered in UCH-L1 deficient animals. (C) However, the average axon area (μm^2) was significantly reduced in UCH-L1$^{-/-}$ mice (Student's t-test, *p = 0.02). (D) Frequency histograms of the percentage of axons in 5 μm^2 incremental bins of axon area indicate reduced proportions of large caliber axons in UCH-L1$^{-/-}$ sciatic nerve. Chi square analysis for goodness of fit demonstrated a significant difference between the distributions (χ^2 = 97.5, df = 8, p < 0.001), and post-tests after Bonferroni correction revealed significant differences in the 0-5 μm^2, 15-20 μm^2, 20-25 μm^2, and 25-30 μm^2 bins (*p < 0.001). (E) The average axon diameter (minimum Feret's) was significantly reduced in UCH-L1$^{-/-}$ animals (Student's t-test, *p = 0.036). (F) The frequency histograms of diameter were also significantly different (χ^2 = 100.15, df = 5, p < 0.001). The percentage of axons between 1-2 μm, 4-5 μm, and >5 μm was significantly

decreased in UCH-L1$^{-/-}$ mice. (G) Axon circularity distributions were similar between groups. All data are expressed as average ± SEM from 3 animals per genotype with average counts of 1339 fibers/animal for UCH-L1$^{+/+}$ and 1202 fibers/animal for the UCH-L1$^{-/-}$ samples). Scale bar = 10 µm.

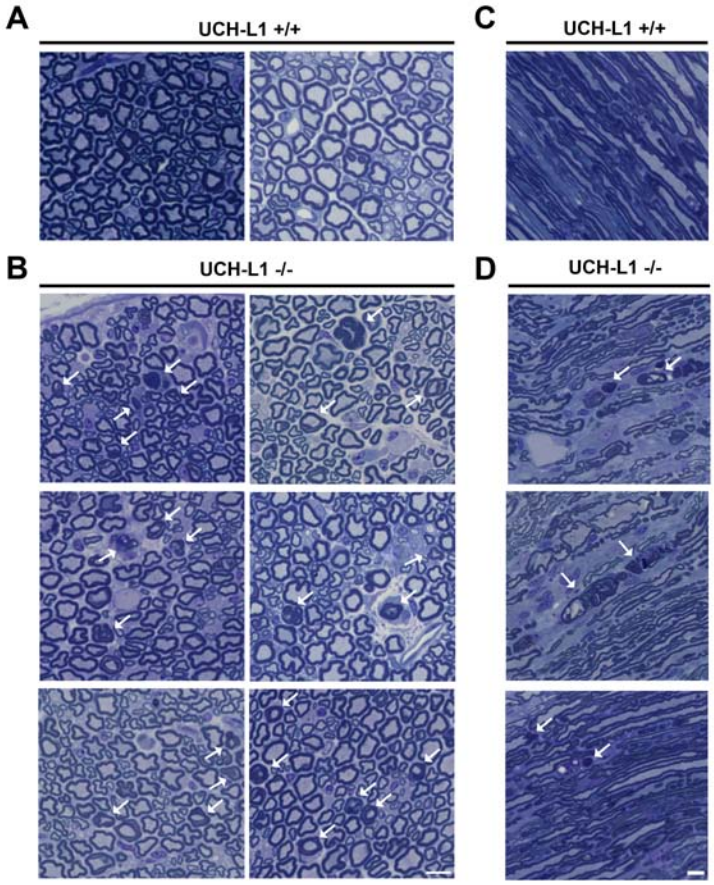

Figure 3.3. Examples of axonal degeneration observed in sciatic nerve of symptomatic UCH-L1 deficient animals. (A) Toluidine blue stained sciatic nerve cross sections from 4.5 m/o UCH-L1$^{+/+}$ showing no evidence of axonal pathology. (B) Degeneration of myelinated axons (arrows) is observed in several UCH-L1$^{-/-}$ sciatic nerve cross sections. (C) Toluidine blue stained sciatic nerve longitudinal section from UCH-L1$^{+/+}$ mouse showing densely packed axons with no evident pathology. (D) Myelin debris (arrows) from degenerating axons is apparent in sciatic nerve of UCH-L1$^{-/-}$ animals. Sections are from the same animals used for morphometry analyses described in Figure 3.2. Scale bar = 10 µm.

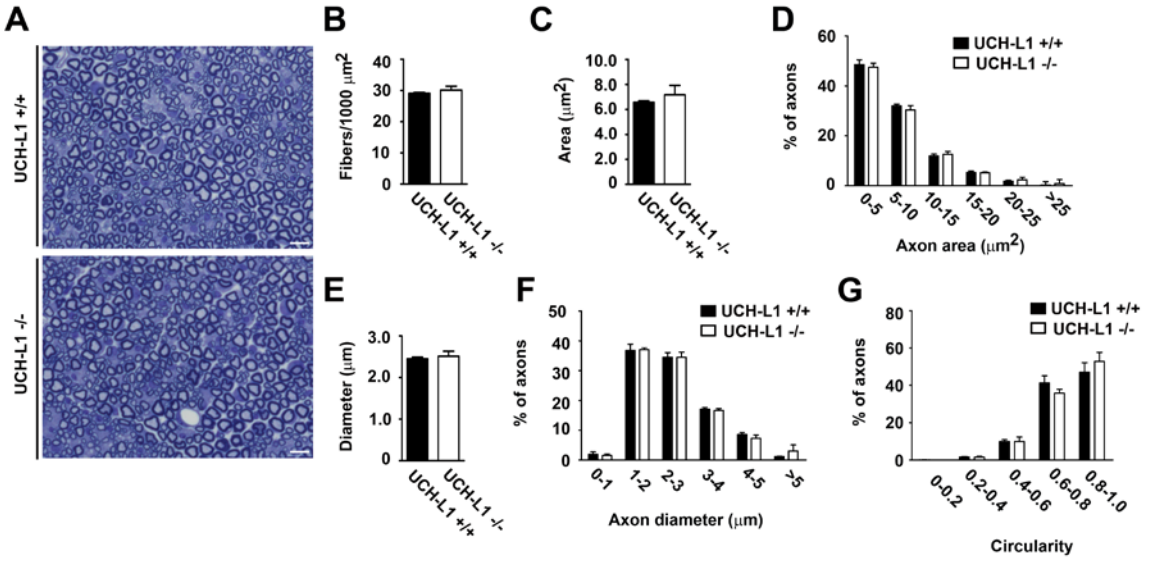

Figure 3.4. Presymptomatic UCH-L1-/- animals show no signs of axonal degeneration in the sciatic nerve. (A) Representative images of toluidine blue stained sciatic nerve sections from presymptomatic 1 month old UCH-L1$^{+/+}$ and UCH-L1$^{-/-}$ animals. (B) The average total fiber density (fibers/1000 μm^2), (C) axon area (μm^2), and (E) diameter were not significantly different in the young animals. The frequency distributions for (D) area, (F) diameter (minimum Feret's), and (G) circularity were also similar between groups. All data are expressed as average ± SEM from 3 animals per genotype (average counts of 1001 fibers/animal for UCH-L1$^{+/+}$ and 1018 fibers/animal for UCH-L1$^{-/-}$ samples). Scale bar = 10 μm.

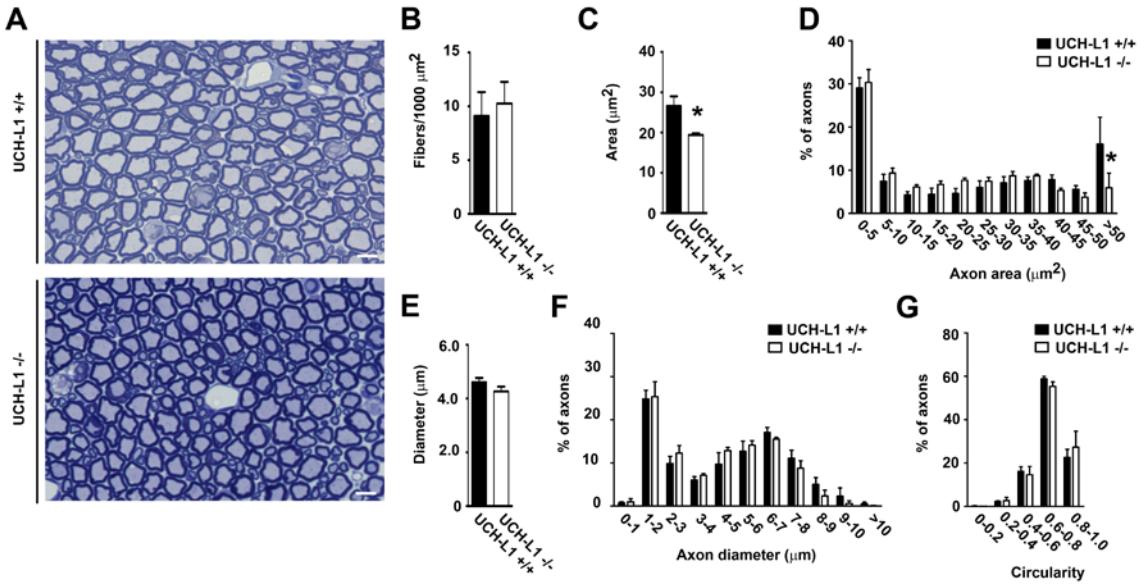

Figure 3.5. Reduced frequency in a population of large caliber axons in the L4 ventral root of symptomatic UCH-L1$^{-/-}$ mice. (A) Representative images of toluidine blue stained L4 ventral root sections from 4.5 m/o UCH-L1$^{+/+}$ and UCH-L1$^{-/-}$ animals. (B) The average fiber density (fibers/1000 μm^2) was not altered in UCH-L1 deficient animals. (C) The average axon area (μm^2) was significantly reduced (Student's t-test, *p = 0.042) in UCH-L1$^{-/-}$ samples. (D) The distribution of axons graphed as a frequency histogram of the percentage of axons from the total in each 5 μm^2 incremental bin. Chi square analysis for goodness of fit demonstrated a significant difference between the distributions (χ^2 = 101.807, df = 10, p < 0.001), and post-tests after Bonferroni correction revealed a significant difference in the >50 μm^2 bin (*p < 0.001). (E) Differences between average axon diameter (minimum Feret's) and frequency histograms of diameter (F) were not statistically significant. (G) Axon shape as assessed by measurement of circularity was normal in the UCH-L1$^{-/-}$ animals. All data are expressed as average ± SEM from 3 animals per genotype with average counts of 746 fibers/animal for UCH-L1$^{+/+}$ and 761 fibers/animal for UCH-L1$^{-/-}$ samples. Scale bar = 10 μm.

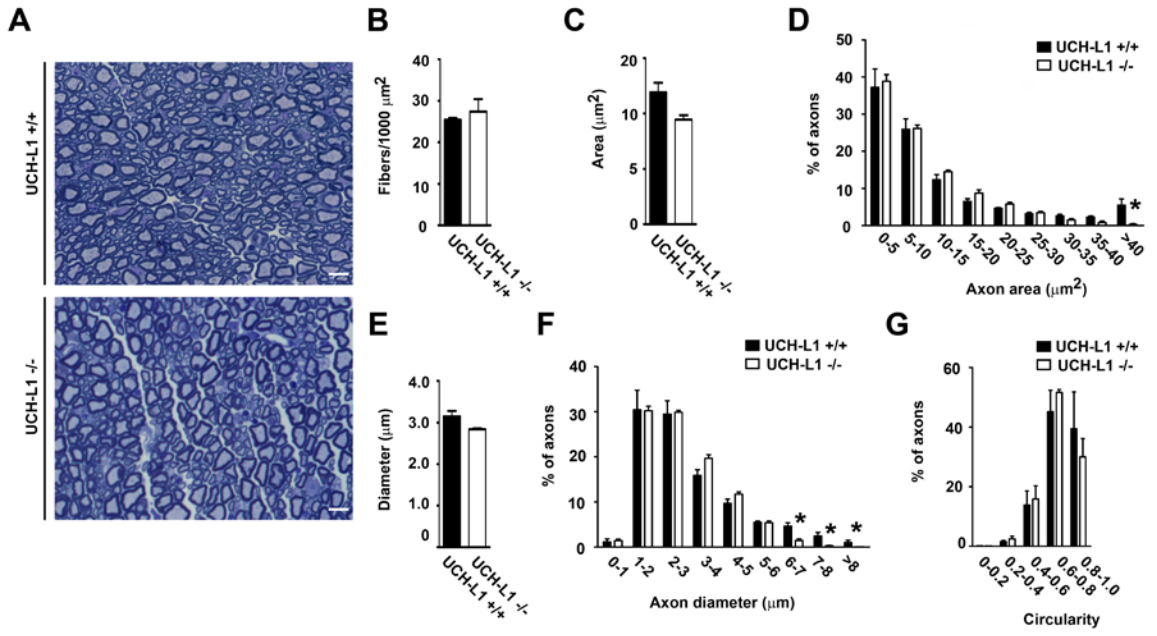

Figure 3.6. Reduced frequency in a population of large caliber axons in the L4 dorsal root of symptomatic UCH-L1$^{-/-}$ mice. (A) Representative images of toluidine blue stained L4 dorsal root sections from 4.5 month old UCH-L1$^{+/+}$ and UCH-L1$^{-/-}$ animals. (B) The average total fiber density (fibers/1000 μm^2) was not altered in UCH-L1 deficient animals. (C) The average axon area (μm^2) was slightly reduced in UCH-L1$^{-/-}$ mice, but this difference did not reach statistical significance (Student's t-test, p = 0.063). (D) Frequency histograms of the percentage of axons in 5 μm^2 incremental bins of axon area. Chi square analysis for goodness of fit demonstrated a significant difference between the distributions (χ^2 = 93.46, df = 8, p < 0.001), and post-tests after Bonferroni correction revealed a significant difference in the >40 μm^2 bin (*p < 0.001). (E) The difference between average axon diameter (minimum Feret's) was not significant but (F) there was a significant difference in the frequency histograms of diameter length (χ^2 = 80.13, df = 8, p < 0.001) with post-tests revealing significant differences at the 6-7 μm, 7-8 μm, and >8 μm bins (*p < 0.001) (G) Axon shape as

assessed by measurement of circularity was normal in the UCH-L1$^{-/-}$ animals. All data are expressed as average ± SEM from 3 animals per genotype with average counts of 1361 fibers/animal for UCH-L1$^{+/+}$ and 1281 fibers/animal for UCH-L1$^{-/-}$ samples. Scale bar = 10 µm.

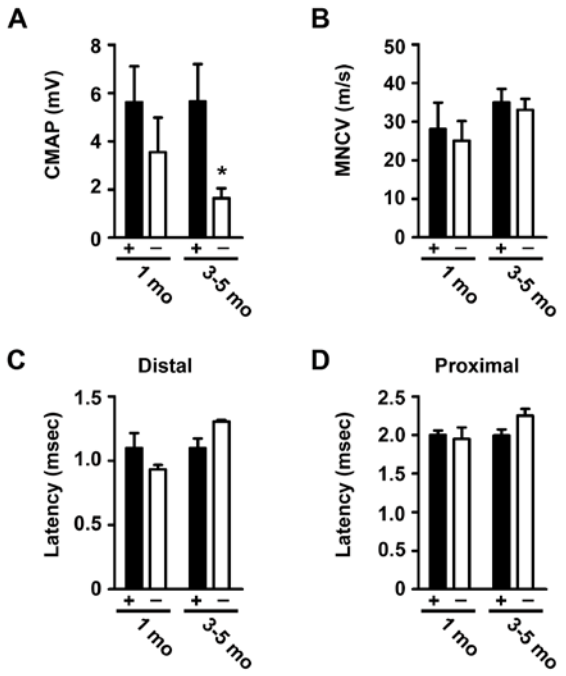

Figure 3.7. Age-dependent decrease in compound muscle action potential amplitude in symptomatic UCH-L1$^{-/-}$ animals. (A) CMAPs were measured from the interosseous muscles of the left foot following electrical stimulation at the sciatic notch and ankle. The CMAP measurements were averaged for each animal prior to analysis. We did not detect a significant difference in CMAP amplitude in the 1 m/o presymptomatic animals (n = 3-4 per genotype) but did find a significant reduction in CMAP amplitude in the symptomatic animals ranging from 3 to 5 months of age (n = 8 per genotype) (B-D) The MNCV and proximal (sciatic notch) and distal (ankle) action potential latencies were not significantly different between genotypes at either age. Data were analyzed by Student's t-test where a p-value < 0.05 (*) was considered statistically significant.

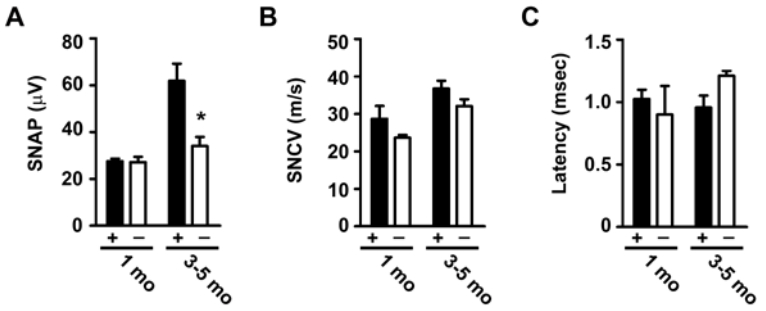

Figure 3.8. Age-dependent decrease in sensory nerve action potential amplitudes in symptomatic UCH-L1$^{-/-}$ animals. (A) SNAPs were measured from the base of the tail following electrical stimulation of the tail nerve 30-40 mm distal to the recording electrodes. We did not detect a significant difference in SNAP amplitude in presymptomatic 1 m/o animals (n = 3-4 per genotype) but found a significant reduction of SNAP amplitude in the 3-5 m/o symptomatic animals (n = 7-8 per genotype). (C-D) SNCVs and action potential latencies were not significantly different at either age group. Measurements were made from the averaged trace from 20 repeated stimulations. Data were analyzed by Student's t-test where a p-value < 0.05 (*) was considered statistically significant.

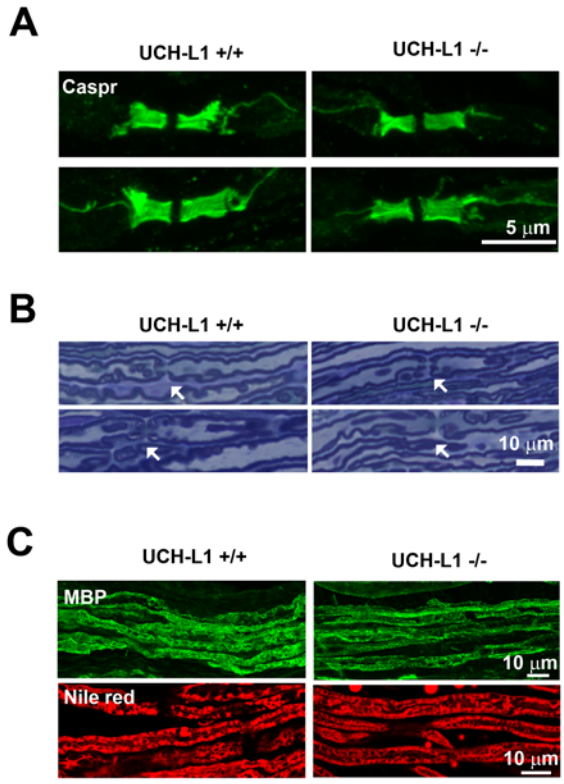

Figure 3.9. Nodal morphology and myelination appear normal in symptomatic UCH-L1$^{-/-}$ animals. (A) Nodes of Ranvier from 4.5 m/o UCH-L1$^{-/-}$ animals are grossly normal in appearance. Representative images from teased sciatic nerve fibers immunostained with anti-Caspr antibody showing similar nodal structure between genotypes. (B) Representative images of toluidine blue stained semithin sciatic nerve longitudinal sections, with nodes of Ranvier indicated by arrows. (C) Representative images of myelin basic protein (MBP) immunohistochemistry and Nile red staining of myelinated axons from 4.5 m/o UCH-L1$^{+/+}$ and UCH-L1$^{-/-}$ mice demonstrating similar staining patterns between genotypes. Scale bars as indicated.

Chapter 4: Summary, Implications, and Future Directions

4.1 Summary of findings

Genetic studies have revealed that missense mutation in UCH-L1 causes autosomal dominant PD (Leroy et al., 1998) and loss-of-function mutations in UCH-L1 trigger progressive neurodegeneration and somatosensory deficits in both mice and humans (Yamazaki et al., 1988, Saigoh et al., 1999, Walters et al., 2008, Chen et al., 2010, Bilguvar et al., 2013), indicating a critical role for UCH-L1 in neuronal health and survival. Additionally, aberrant upregulation of UCH-L1 has been observed in several human malignancies (Tezel et al., 2000, Chen et al., 2002, Mastoraki et al., 2009, Hurst-Kennedy et al., 2012). Thus, elucidating mechanisms that regulate UCH-L1 protein level and understanding the pathological consequences of UCH-L1 loss-of-function has important implications for understanding the role UCH-L1 plays in human health and disease. My thesis work has revealed a novel regulatory mechanism mediating UCH-L1 degradation and has demonstrated a critical role for UCH-L1 in peripheral nerve maintenance and transmission.

In Chapter 2, I described my work validating UCH-L1 as a substrate of parkin ubiquitination and linking parkin-mediated ubiquitin signaling to the regulation of UCH-L1 degradation. Prior to these studies, UCH-L1 and parkin had not been functionally linked although both proteins operate in the ubiquitin system and are implicated in PD and cancer pathogenesis. I found that UCH-L1 interacts with wild type parkin, but does not appear to bind representative pathogenic PD mutants (T415N, T240R, and R42P), suggesting disrupted parkin and UCH-L1 interaction dynamics may contribute to pathogenesis in ARJP. Disease-associated mutations and catalytic dead mutation in UCH-L1, however, did not abrogate binding with parkin indicating that the interaction does not require the DUB activity of UCH-L1. I also found that parkin utilizes the

Ubc13/Uev1a E2-conjugating complex to mediate the K63-polyubiquitination of UCH-L1. My data indicate that UCH-L1 is a long-lived protein and that parkin-mediated K63-polyubiquitination of UCH-L1 targets it for degradation by the autophagy lysosome pathway. I also found that UCH-L1 protein expression and ubiquitination are disrupted in parkin deficient mouse brain, further supporting an *in vivo* role for parkin in regulating UCH-L1 degradation through ubiquitin signaling.

In Chapter 3, I examined if the UCH-L1 protein plays a role in the axonal maintenance and function of peripheral nerves. Loss-of-function mutations in UCH-L1 cause progressive sensory and motor terminal degeneration, axonal dystrophy, and sensorimotor ataxia in mice (Yamazaki et al., 1988, Kikuchi et al., 1990, Oda et al., 1992, Miura et al., 1993, Saigoh et al., 1999, Walters et al., 2008, Chen et al., 2010). In humans, a loss-of-function mutation in UCH-L1 causes NDGOA which manifests with progressive neurodegeneration and sensorimotor ataxia along with atrophy of the optic nerve, cortex, and cerebellum (Bilguvar et al., 2013). The findings in both mice and humans indicate a critical role for UCH-L1 in relaying motor and proprioceptive signals between the peripheral and central nervous systems. However, although UCH-L1 null mice exhibit progressive hindlimb paralysis and somatosensory deficits, it is unknown if peripheral motor or sensory nerve action potentials and conduction velocities are altered in these animals, and if any observed deficits are progressive with age. Additionally, peripheral nerve histopathology has not been thoroughly examined in this model, so the extent and time course of axonal degeneration in the peripheral nervous system is undefined. To address these matters, I performed electrophysiological recordings from muscles innervated by the sciatic nerve as well as structural analyses of sciatic nerve from cohorts of pre-symptomatic and symptomatic animals. I also assessed sensory nerve conduction using recordings from the mouse tail nerve in these same animals.

Additionally, I examined the distribution of small and large caliber axons in the L4 dorsal and ventral roots of symptomatic UCH-L1$^{-/-}$ mice. I observed age-dependent alterations in CMAP and SNAP amplitudes which provides evidence of widespread peripheral axonal degeneration in UCH-L1$^{-/-}$ animals and is the first report of a functional nerve deficit in this model. Degenerating axons were observed in the sciatic nerve from symptomatic animals, which was accompanied by an altered distribution of large and small caliber axons. However, we did not find evidence of axonal degeneration in the sciatic nerve from presymptomatic mice, supporting the progressive nature of neuropathy. Pathological changes were not visually evident in the dorsal and ventral roots, but our analyses of axon distributions by size indicated the absence of a small population of large caliber axons in these structures, which may be indicative of axonal atrophy. Finally, myelination and nodal structure were normal in appearance and MNCVs and SNCVs were not reduced. Taken together, these data indicate a primary age-dependent distal to proximal axonopathy without demyelination, and support a role for UCH-L1 in peripheral axon maintenance.

4.2 Insight into UCH-L1 function in health and disease

Implications for Parkinson disease

My thesis work has demonstrated a novel relationship between parkin E3 ligase and UCH-L1 which implicates parkin in the baseline regulation of UCH-L1 turnover and suggests that this regulatory mechanism may be disrupted in PD. Prior reports indicate that in postmortem sporadic PD and AD brain, the soluble UCH-L1 protein level is reduced compared to age-matched controls (Choi et al., 2004, Barrachina et al., 2006). UCH-L1 is also found in Lewy bodies (LBs) and neurofibrillary tangles (Lowe et al.,

1990, Choi et al., 2004), indicating that a subpopulation of UCH-L1 is potentially aggregated and insoluble in neurodegenerative disease brain, but it is presently unclear if this accounts for the reduced expression levels observed in solubilized brain tissues. To our knowledge, the UCH-L1 level in parkin mutant ARJP brain has not been examined, but we find elevated UCH-L1 levels in parkin$^{-/-}$ mouse brain suggesting that UCH-L1 levels may also be dysregulated in ARJP. These findings are in accord with a prior proteomics study that reported increased UCH-L1 levels in parkin$^{-/-}$ mouse striatum (Periquet et al., 2005). We also found altered binding between UCH-L1 and pathogenic parkin mutants, but the contribution of dysregulated parkin and UCH-L1 binding dynamics to disease pathogenesis remains unknown. Additionally, to better inform on the relationship between parkin and UCH-L1 in ARJP, it will be important to determine whether the expression of pathogenic PD mutant parkin affects UCH-L1 ubiquitination and expression levels. Future research should also try to determine if altered UCH-L1 levels resulting from parkin inactivation alter global protein degradation through disruptions of the monomeric ubiquitin pool and whether this directly or indirectly contributes to inclusion body formation or neurodegeneration in PD.

Biochemically, how do we reconcile the observed UCH-L1 decrease in sporadic PD brain but an increase in the parkin$^{-/-}$ ARJP mouse model, and potentially in ARJP itself? A drawback of the brain studies is that they only examined soluble protein levels, so a substantial population of UCH-L1 may be present in insoluble Lewy body structures that were not accounted for in these studies. In support of this, we have previously shown an inverse correlation between the soluble UCH-L1 level and neurofibrillary tangle number in sporadic AD brain (Choi et al., 2004). Whether or not a similar correlation exists between soluble UCH-L1 level and LB pathology in PD brain remains unknown. In ARJP brain, however, LB pathology is typically not observed (Takahashi et

al., 1994, Mori et al., 1998) suggesting that alterations in UCH-L1 level would not be due to UCH-L1 accumulation in aggregates. Thus, the protein level may be elevated as a direct consequence of abrogated parkin-mediated targeting of UCH-L1 for lysosomal degradation.

Another possibility is that in sporadic PD, parkin activity may be reduced by the nitrosative and oxidative stress characteristic of PD (Chung et al., 2004, Yao et al., 2004), but a population of functional ligase is still present to ubiquitinate and signal for UCH-L1 degradation. Elevated oxidative stress may also serve a double blow to the parkin and UCH-L1 relationship. Parkin inactivation resulting from nitrosative and oxidative stress may initially contribute to increased UCH-L1 levels. As UCH-L1 accumulates, it likely acquires oxidative modifications, as has been observed in sporadic PD brain (Choi et al., 2004), potentially causing a toxic gain-of-function. Carbonyl-modified UCH-L1 proteins have reduced solubility and demonstrate aberrant binding with other proteins, similar to the PD-linked mutant UCH-L1 (Kabuta et al., 2008a, Kabuta et al., 2008b). These changes may precipitate inclusion body formation and reduce the relative population of soluble UCH-L1. As LBs do not form in ARJP brain, this may in part account for the reduced soluble UCH-L1 in PD brains but the increased total UCH-L1 observed in our study of parkin$^{-/-}$ mice.

The absence of LBs in ARJP suggests that parkin is involved in inclusion body formation. In support of this, our lab has previously shown that parkin plays an active role in recruiting misfolded L166P DJ-1 protein into aggresomes through K63-polyubiquitination to facilitate lysosomal degradation (Olzmann et al., 2004, Olzmann and Chin, 2008, Chin et al., 2010). UCH-L1 is a component of LBs (Lowe et al., 1990) and has been found in cellular aggresomes following proteotoxic stress (Ardley et al., 2004). However, although parkin mediates the normal lysosomal degradation of UCH-L1

as demonstrated in this thesis, it is unknown if mutant or damaged UCH-L1 is recruited to aggresomes by parkin. It will also be interesting to determine if selective parkin mediated degradation of I93M mutant and oxidatively damaged toxic UCH-L1 proteins is potentially neuroprotective in cellular PD models. My thesis work examined parkin-mediated UCH-L1 ubiquitination and degradation under basal conditions; thus, the above studies are important lines of future research. Gaining a better understanding of how disruptions in parkin-mediated ubiquitination and degradation of UCH-L1 contributes to altered UCH-L1 distribution and degradation in PD will reveal novel mechanisms underlying disease pathogenesis.

Implications for peripheral sensory and motor neuropathies

Although neurodegeneration caused by UCH-L1 loss-of-function has been described in the CNS, the effect of UCH-L1 loss-of-function on PNS axons was undefined. The work described in Chapter 3 provides compelling evidence that supports a disease model where neuropathy associated with UCH-L1 loss-of-function is caused, at least in part, by progressive axonal degeneration of peripheral nerves. This inference is supported by our observation of degenerating axons and myelin debris, altered axonal size (area and perimeter) distributions, and reduced CMAPs in the sciatic nerve of symptomatic, but not presymptomatic, UCH-L1$^{-/-}$ animals. NMJ denervation has previously been reported in this mouse model, beginning as early as postnatal day 60 (Miura et al., 1993), a pathological alteration accompanied by reduced mEPP frequencies and reduced EPP amplitudes in isolated EDL muscles of mice aged 2 months or older (Chen et al., 2010). However, prior to this report, it was unknown whether CMAP and MNCV were also affected in the UCH-L1$^{-/-}$ model. We observed an

age-dependent decrease in CMAP amplitude, which is consistent with these previously reported progressive reductions in mEPP frequency and EPP amplitude. We also show, for the first time, that the MNCV is not altered in UCH-L1$^{-/-}$ sciatic nerve, indicating a primary axonal degenerative phenotype without demyelination. We also find a normal structural appearance of the nodes of Ranvier as evidenced by Caspr immunolabeling and toluidine blue staining. We also found a normal myelin staining pattern, in support of our MNCV findings.

The first pathological sign in UCH-L1$^{-/-}$ mice is abnormal hindlimb clasping when animals are suspended by the tail, beginning around day 30 (Yamazaki et al., 1988). Interestingly, mEPP frequency and EPP amplitude are unaffected at this age (Chen et al., 2010), and moreover, we find normal CMAP amplitudes and no evidence of sciatic nerve degeneration. These findings support a correlation between sciatic nerve structure and NMJ and motor nerve transmission with disease severity. However, it is still unclear whether NMJ transmission deficits precede axonal degeneration or if reduced NMJ transmission is a direct consequence of axonal degeneration. A finer examination of the time course between CMAP deficits and sciatic nerve degeneration would be needed to answer this question, and is certainly an interesting avenue for future research.

The major pathological alterations in UCH-L1$^{-/-}$ mice occur in the gracile nucleus, gracile fasiculi, and spinocerebellar tract which is accompanied by muscle spindle degeneration at Ia afferent sensory nerve fibers (Yamazaki et al., 1988, Mukoyama et al., 1989, Kikuchi et al., 1990, Oda et al., 1992). Muscle spindle degeneration begins as early as postnatal day 20 before the onset of CNS pathology, suggesting that degeneration in these brain structures may be driven by reduced proprioceptive inputs

from the periphery (Oda et al., 1992). However, it was previously unknown whether sensory nerve conduction was altered as a result of UCH-L1 loss-of-function. Thus, we measured SNAPs and SNCV from the tail nerve in presymptomatic and aged UCH-L1$^{-/-}$ mice. In accord with our motor nerve findings, we found that symptomatic animals have significantly reduced SNAP amplitudes and SNCVs within the normal range. This is the first report of a functional sensory nerve deficit in UCH-L1$^{-/-}$ animals and is in accord with the reduced somatosensory-evoked potentials but normal conduction velocities observed in NDGOA patients (Bilguvar et al., 2013). Our findings are also consistent with clinical features seen in CMT2, the axonal subtype of CMT, namely the reduced action potential amplitudes but preservation of nerve conduction velocities.

An interesting and unexpected finding was the reduced proportions of large caliber axons in the dorsal and ventral roots of symptomatic mice, particularly as there were no overt signs of axonal degeneration. There are several possible interpretations of these data. Due to their higher energy demands, large caliber axons typically degenerate before small caliber axons, so it is possible that a subpopulation of large caliber axons in the dorsal and ventral roots are in the early stages of degeneration, which can include axonal atrophy and shrinkage away from the myelin sheath, and thus are mildly dystrophic in appearance. Additionally, as UCH-L1 is localized to the axon and colocalizes with the heavy neurofilament subunit, it raises the possibility that UCH-L1 plays a role in maintaining axonal size. The neurofilaments are neuronal intermediate filament proteins that compose the axonal cytoskeleton and thus their proper assembly regulates axon diameter (Hoffman et al., 1984, Yuan et al., 2012). Mice with autosomal recessive mutations in the heavy and mid-sized neurofilament subunits undergo age-dependent axonal atrophy in the dorsal and ventral roots without evidence of axonal degeneration until 2 years of age (Elder et al., 1999). However, we

did not find any axonal size differences in the sciatic nerve of the younger presymptomatic animals, suggesting that UCH-L1 does not actively regulate the axonal cytoskeleton as the neurofilaments do.

Additional histological studies on presymptomatic animals and mice in more advanced stages of the disease would need to be performed to determine whether the altered axonal distributions we see in the dorsal and ventral roots result from neurodegeneration or are potentially due to developmental or structural differences in the absence of UCH-L1. However, as UCH-L1 deficient animals typically die between 5 and 6 months, the 4.5 m/o UCH-L1$^{-/-}$ animals used for these studies were already approaching end stage and thus examination of older mice may not reveal any additional differences. Nevertheless, our findings in the sciatic nerve and proximal roots support a distal-to-proximal or dying back mode of neurodegeneration in the PNS as has been reported in the gracile tract of the CNS. Because we only examined the pathology in sciatic nerve from 1 m/o and 4.5 m/o cohorts of UCH-L1$^{-/-}$ mice, it is unclear when sciatic nerve degeneration begins in these animals. However, we have defined a window of pre- and post-degenerative changes in the sciatic nerve corresponding with disease severity, which opens the possibility of using this mouse model for examining genetic or pharmacological interventions that may slow axonal degeneration and delay disease progression.

Comments on UCH-L1 gain of function vs loss of function in conferring different neurodegenerative disease outcomes

The linking of UCH-L1 abnormalities to diseases with decidedly different CNS and PNS phenotypes raises the possibility that UCH-L1 gain of function vs loss of function manifests as different pathological conditions. UCH-L1 loss of function causes peripheral nerve terminal degeneration and primary axonal degeneration, whereas gain of function through mutation or oxidative modification is likely more pertinent to PD pathogenesis. Although the I93M PD mutation causes approximately 50% reduction in hydrolase activity *in vitro* (Leroy et al., 1998, Nishikawa et al., 2003), it is unknown what effect this may have on familial PD patient pathology. The I93M mutation is autosomal dominant, so there is one wild type allele encoded in heterozygous individuals which may compensate for some of the lost activity. Oxidative modification by carbonylation of UCH-L1 reduces hydrolase activity (Nishikawa et al., 2003) which may be a contributing factor in sporadic PD, particularly as we have previously reported extensive oxidative modification of the UCH-L1 protein in sporadic PD brain (Choi et al., 2004). Additionally, the I93M mutant UCH-L1 and oxidatively modified UCH-L1 proteins undergo abnormally increased protein/protein interactions, including aberrant binding with tubulins and CMA degradation machinery which may drive a toxic gain of function (Kabuta et al., 2008a, Kabuta et al., 2008b). Transgenic mice overexpressing the I93M mutant display dopaminergic degeneration and are more susceptible to MPTP treatment, further supporting a role for this mutation in PD (Setsuie et al., 2007).

Autosomal recessive UCH-L1 loss-of-function mutations in mice and humans do not result in a PD phenotype but rather sensory and motor nerve terminal retraction and axonal degeneration, suggesting an alternate mode of pathogenicity that results from the loss of UCH-L1 expression. UCH-L1$^{-/-}$ mice have reduced monomeric ubiquitin levels in neuronal tissues (Osaka et al., 2003, Walters et al., 2008), but it is presently unclear if disrupted ubiquitin homeostasis directly causes the neurodegenerative phenotypes

observed in these mice. Abnormal protein and organelle accumulation in the dystrophic axons of UCH-L1$^{-/-}$ animals suggests that axonal transport may be disrupted which may result in aggregation and transport blockages that ultimately contribute to axon degeneration (Mukoyama et al., 1989, Ichihara et al., 1995, Wu et al., 1995, Wang et al., 2004) as has been reported in other peripheral neuropathies (Coleman, 2005, Conforti et al., 2014). It is unclear if the hydrolase activity of UCH-L1 is required for normal axonal transport, but pharmacological inhibition of UCH-L1 reduces retrograde BDNF trafficking in axons of cultured neurons (Poon et al., 2013). Future studies examining axonal transport in primary neurons from UCH-L1 null animals will help determine what role, if any, UCH-L1 plays in the regulation of axonal transport.

Implications for cancer pathogenesis

In recent years, an appreciation for potential alternative roles of PD-linked genes in PD and cancer pathogenesis has been recognized, suggesting that one disease associated with neuronal cell death and another with aberrant cell proliferation may converge on a common pathway that regulates cell health and/or cell cycle. Parkin and UCH-L1 are familial PD proteins that are also implicated in cancer pathogenesis; thus, further studying their relationship in PD may have important implications for elucidating mechanisms in cellular malignancies. Parkin has a putative tumor suppressor function, while UCH-L1 is a putative oncogene. Thus, these proteins may have opposing roles in cancer pathogenesis, and an interesting unexplored possibility is that disruption of the parkin mediated regulation of UCH-L1 level is linked to tumorigenesis as well as PD pathogenesis. It is important to note, however, that UCH-L1 is not upregulated in all

cancers, as reduced mRNA levels and promoter hypermethylation have been observed in some prostrate, breast, and nasopharyngeal cancers (Wang et al., 2008, Li et al., 2010, Ummanni et al., 2011, Xiang et al., 2012) suggesting a potential tumor suppressor function. However, as UCH-L1 expression is typically low or absent in non-neuronal tissues, it is unclear how reduced UCH-L1 levels would exert a tumor suppressor function in cells that do not normally express the protein (Hurst-Kennedy et al., 2012). The preponderance of evidence points toward UCH-L1 as an oncogene that when upregulated in non-neuronal cells promotes cancerous transformation and tumor cell invasion, but the mechanisms underlying enhanced tumorigenesis remain unknown (Tezel et al., 2000, Chen et al., 2002, Miyoshi et al., 2006, Liu et al., 2009a, Mastoraki et al., 2009). Additionally, transgenic mice expressing UCH-L1 under a ubiquitous promoter are prone to spontaneous tumor generation, particularly in the lymph nodes and lungs (Hussain et al., 2010) supporting an *in vivo* oncogenic role for UCH-L1. The manner by which UCH-L1 promotes tumorigenesis and whether this requires the hydrolase activity of UCH-L1 remains unclear. Future studies utilizing pharmacological inhibitors of UCH-L1 will help determine whether or not the DUB activity is required for driving oncogenesis. It will also be interesting to see if in future any UCH-L1 mutations are reported that are linked to cancer rather than neurological disease.

In contrast to UCH-L1, parkin has a reported tumor suppressor function, meaning that parkin mutation and loss of function are linked to both neurodegeneration and cancer pathogenesis. Parkin mutations have been observed in multiple tumor types including cervical cancer, lung cancer, and colorectal cancer (Cerami et al., 2012, Gao et al., 2013, Xu et al., 2014). Additionally, parkin promoter hypermethylation, as well as mRNA and protein downregulation have also been reported in several transformed cells and tumors (Xu et al., 2014), further supporting a role for parkin inactivation in

tumorigenesis. Moreover, parkin null mice develop γ-irradiation-induced tumors at a higher rate than control animals (Zhang et al., 2011). It will be of interest to examine whether cancers associated with parkin mutation or reduced expression also demonstrate elevated UCH-L1 levels, or vice versa. Additionally, it would be particularly interesting to examine if parkin overexpression is protective in tumors and transformed cells associated with elevated levels of UCH-L1.

4.3 Future Directions

I discussed many unknown issues in the previous discussion section, but several additional unanswered questions remain. Here I propose experiments that can address these unknowns and potentially increase our understanding of UCH-L1 function and regulation in health and disease.

Does PINK1 phosphorylation of parkin stimulate the ubiquitination of UCH-L1?

As described in Chapter 1, the crystal structure of parkin indicates that it normally exists in an autoinhibited structure (Trempe et al., 2013, Wauer and Komander, 2013) that likely requires activation by an external mechanism, such as cofactor binding or posttranslational modification which opens the structure to allow E2 and/or substrate binding. For example, the PD-linked kinase PINK1 is upstream of parkin in the mitophagy pathway. In response to mitochondrial depolarization, PINK1 phosphorylates parkin at Ser-65 in the N-terminal UBL, which activates parkin and leads to the ubiquitination and subsequent proteasomal degradation of several outer mitochondrial membrane proteins, signaling for mitophagy (Narendra et al., 2008, Matsuda et al.,

2010, Kondapalli et al., 2012, Shiba-Fukushima et al., 2012, Kane et al., 2014). Thus, PINK1 phosphorylation is a required step for parkin activation during mitophagy. However, it remains unclear whether PINK1 phosphorylation specifically regulates parkin activity toward mitochondrial substrates. We have previously shown that PINK1 phosphorylation facilitates robust ubiquitination of the cytosolic protein IKKγ (Sha et al., 2010). Together these studies suggest that PINK1 activates parkin activity toward both mitochondrial and cytosolic proteins, but whether PINK1 activates parkin-mediated ubiquitination of UCH-L1 remains unknown. It is important to determine whether PINK1 phosphorylation is a global mechanism of parkin activation, or whether parkin targets individual substrates in response to different modifications. This information will potentially facilitate development of drugs that selectively target, for example, mitophagy related substrates without affecting ubiquitination of other proteins.

To test whether PINK1 phosphorylation activates the parkin-mediated ubiquitination of UCH-L1, several experiments can be performed. Ubiquitination assays as described in Chapter 2 can be conducted in the presence and absence of wild type PINK1 or kinase-inactive mutants. If PINK1 phosphorylation of parkin is critical for UCH-L1 ubiquitination, then ubiquitination will be increased following wild type PINK1 overexpression compared to parkin expression alone, whereas kinase-inactive PINK1 expression should not elevate UCH-L1 ubiquitination. Because PINK1 mutations cause autosomal recessive PD, it is perhaps of greater interest to examine UCH-L1 ubiquitination and expression level in PINK1 null mice and/or PINK1 knockdown cells. Absent or reduced PINK1 expression is predicted to block parkin activation, thus reducing parkin-mediated UCH-L1 ubiquitination, which may cause increased levels of UCH-L1 protein in PINK1 deficient cells. Additionally, as the PINK1 phosphorylation site on parkin (Ser-65) has been determined, mutant parkin S65A plasmids can be

generated and expressed in cells to determine if UCH-L1 ubiquitination is affected. Alternative mechanisms may exist that prompt the parkin-mediated ubiquitination of UCH-L1. For example, a posttranslational modification (PTM) on UCH-L1 may act to enhance binding with active parkin which triggers its ubiquitination and lysosomal degradation.

What are other mechanisms that regulate the UCH-L1 protein?

Identification of other UCH-L1 regulatory mechanisms has important consequences for understanding the role of UCH-L1 dysfunction in disease. The elucidation of such mechanisms may also facilitate the identification of potential drug targets that may be therapeutic in neurodegenerative disease or cancer. Aside from monoubiquitination (Meray and Lansbury, 2007) and the polyubiquitination described in this thesis, other PTMs of UCH-L1 have been described which include farnesylation (Liu et al., 2009b) and O-glycosylation (Cole and Hart, 2001). Although a predominantly cytosolic protein, farnesylation of C-terminal Cys-220 appears to alter UCH-L1 solubility by increasing its association with endoplasmic reticulum membranes. The role of UCH-L1 farnesylation on neuronal health is unclear, but blocking farnesylation by mutation or pharmacological manipulations reduces toxicity associated with α-synuclein overexpression and thus may be a therapeutic target in PD (Liu et al., 2009b).

UCH-L1 is also O-glycosylated with β-D-*N*-acetylglucosamine (O-GlcNac) at synaptic nerve terminals, but the functional outcome of this modification has not been defined (Cole and Hart, 2001). O-GlcNAcylation occurs at serine and threonine residues of cytosolic and nuclear proteins, frequently at the same serines and threonines that undergo phosphorylation. Depending on cellular health and nutritional status, O-

GlcNAcylation can block phosphorylation and vice versa, allowing cellular cross talk in various signaling pathways (Hart et al., 2011). The reciprocal relationship between O-GlcNAcylation and phosphorylation raises that possibility that UCH-L1 is also phosphorylated. However, there have been no reports of UCH-L1 phosphorylation, and signaling events mediated by UCH-L1 O-GlcNAcylation have yet to be elucidated.

What are other PTMs of UCH-L1 and how do we identify them? First, it will be important to identify neuronal binding partners of UCH-L1. This can be achieved using a combined immunoprecipitation and mass spectrometry approach. The UCH-L1 protein can be immunoprecipitated from cultured neuronal cells or brain lysates, which will also retrieve proteins bound to UCH-L1. The immunoprecipitated materials can be analyzed by mass spectrometry to identify potential binding partners, and then confirmed using coimmunoprecipitation assays. If enzymatic binding partners are identified, experiments can then be performed to determine if they mediate PTM of UCH-L1 and what the functional consequences of the PTM are, such as increased or decreased hydrolase activity. Additionally, these experiments can be performed with wild type and C90S hydrolase-dead mutant to potentially identify activity-dependent interactors of UCH-L1. Another method toward identifying UCH-L1 PTMs and/or binding partners can be achieved through empirical testing of putative modification sites revealed by UCH-L1 coding sequence analysis.

Does UCH-L1 regulate axonal transport?

Observations of neurodegeneration associated with UCH-L1 loss-of-function mutations have been well characterized. However, it remains unknown how UCH-L1

loss-of-function promotes neurodegeneration which ultimately results in disease. Abnormal protein aggregates and mitochondrial accumulation has been described in degenerating axons of UCH-L1-/- mice, leading to speculation that UCH-L1 is involved in axonal transport. Reduced quantities of synaptic vesicles have been observed at NMJs of UCH-L1-/- animals (Chen et al., 2010), suggesting a potential disruption of synaptic vesicle transport to terminals. Additionally, inhibition of UCH-L1 activity reduces BDNF trafficking in cultured neurons (Poon et al., 2013), supporting a role for UCH-L1 in axonal transport. Although pharmacological inhibitors selectively reduce UCH-L1 activity (Liu et al., 2003), it is unknown whether these drugs have off-target effects that may have contributed to this phenotype. Thus, in order to directly test whether axonal transport is altered by UCH-L1 loss-of-function, transport rates of fluorescently labeled cargos can be measured in primary neurons cultured from UCH-L1$^{-/-}$ animals using live cell imagining. If UCH-L1 plays a role in axonal transport as has been hypothesized, then we would expect to observe reduced transport rates and potentially evidence of stalled cargos in neuronal processes. Assuming a defect is observed, rescue experiments should then be conducted to determine whether reintroduction of UCH-L1 protein improves transport rates and whether the DUB activity of UCH-L1 is required in transport regulation. Another important issue to address is whether any transport deficits observed in UCH-L1-/- neurons results from disruption of the monomeric ubiquitin pool or through an independent mechanism. To assess this, the transport rescue experiments should be repeated using ubiquitin overexpression rather than UCH-L1 overexpression. These experiments have precedent as ubiquitin overexpression has been found to rescue dendritic spine structural alterations associated with UCH-L1 inhibition (Cartier et al., 2009). Additionally, cell based death assays can be conducted in primary UCH-L1$^{-/-}$ neurons transfected with ubiquitin to determine whether this confers

cytoprotection. Finally, alterations in axonal degeneration and phenotype severity can be assessed *in vivo* by generating and analyzing ubiquitin overexpressing transgenic mice crossed with UCH-L1$^{-/-}$ mice.

4.4 Hypothesized model of UCH-L1 dysfunction in neurological disease and closing remarks

Although many questions remain unanswered, we can begin to put my thesis research into context with previous studies to suggest a potential model of UCH-L1 dysfunction in neurodegenerative disease (Fig. 4.1). In healthy neuronal cells, UCH-L1 levels are maintained through basal parkin-mediated K63-polyubiquitination and lysosomal turnover. In ARJP, however, parkin activity is lost or severely reduced which blocks K63-polyubiquitination of UCH-L1, which in turn reduces the lysosomal degradation of UCH-L1 causing elevated UCH-L1 level. Although it is unclear how elevated UCH-L1 promotes neurodegeneration, one possibility is that accumulated UCH-L1 may become oxidatively damaged and take on a toxic gain-of-function, thereby contributing to pathogenesis. In sporadic PD, parkin activity itself is reduced by oxidative and nitrosative stress which can also inhibit the K63-polyubiquitination of UCH-L1 and cause a similar chain of events as described for ARJP. However, in sporadic PD, damaged UCH-L1 is sequestered in Lewy bodies (a process potentially mediated by parkin) which may account for the reduced soluble UCH-L1 levels observed in sporadic PD brain tissues. Loss-of-function mutations in UCH-L1 cause gracile axonal dystrophy in mice and NDGOA in humans. My research has also revealed a critical role for UCH-L1 peripheral axon maintenance and neurotransmission and shows that loss-of-function results in progressive distal-to-proximal degeneration in the PNS. The mechanism by

which UCH-L1 loss-of-function results in PNS axon degeneration remains unclear, but pathological disruptions in axonal transport have been hypothesized and should be tested. Further elucidation of mechanisms that regulate UCH-L1 protein level and gaining a better understanding of the pathological consequences of UCH-L1 loss-of-function will reveal novel insight into the role that UCH-L1 dysfunction plays in neurological disease.

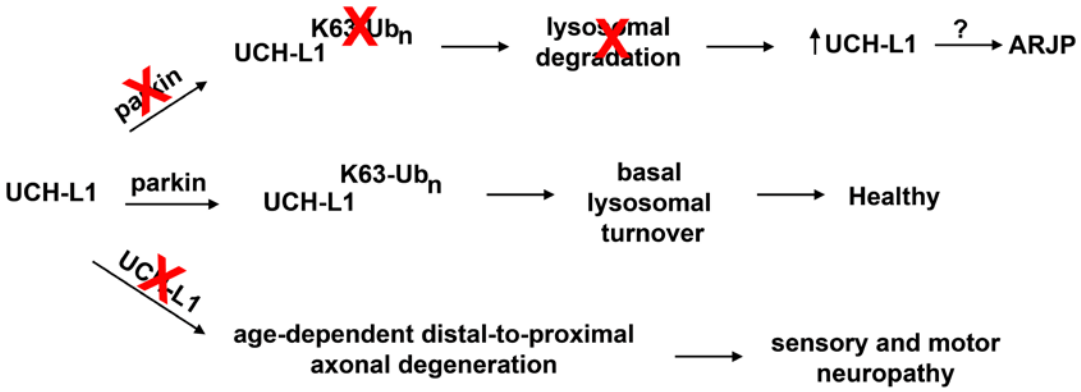

Figure 4.1. Proposed model of the role of UCH-L1 dysfunction in neurological disease. Different neurodegenerative disease outcomes are mediated by disruptions to UCH-L1 protein homeostasis. Loss of parkin function through genetic mutation or potentially through oxidative stress reduces the K63-polyubiquitination and lysosomal degradation of UCH-L1 leading to increased protein level. Dysregulation of UCH-L1 homeostasis may be a pathogenic mechanism in ARJP. UCH-L1 loss-of-function mutations cause sensory and motor neuropathy in mice, which is caused, at least in part, by age-dependent distal-to-proximal axonal degeneration in the peripheral nervous system.

References

Amm I, Sommer T, Wolf DH (2014) Protein quality control and elimination of protein waste: the role of the ubiquitin-proteasome system. Biochimica et biophysica acta 1843:182-196.

Ardley HC, Scott GB, Rose SA, Tan NG, Robinson PA (2004) UCH-L1 aggresome formation in response to proteasome impairment indicates a role in inclusion formation in Parkinson's disease. Journal of neurochemistry 90:379-391.

Azhary H, Farooq MU, Bhanushali M, Majid A, Kassab MY (2010) Peripheral neuropathy: differential diagnosis and management. American family physician 81:887-892.

Baba M, Nakajo S, Tu PH, Tomita T, Nakaya K, Lee VM, Trojanowski JQ, Iwatsubo T (1998) Aggregation of alpha-synuclein in Lewy bodies of sporadic Parkinson's disease and dementia with Lewy bodies. The American journal of pathology 152:879-884.

Baker RT, Board PG (1987) The human ubiquitin gene family: structure of a gene and pseudogenes from the Ub B subfamily. Nucleic acids research 15:443-463.

Balastik M, Ferraguti F, Pires-da Silva A, Lee TH, Alvarez-Bolado G, Lu KP, Gruss P (2008) Deficiency in ubiquitin ligase TRIM2 causes accumulation of neurofilament light chain and neurodegeneration. Proceedings of the National Academy of Sciences of the United States of America 105:12016-12021.

Barrachina M, Castano E, Dalfo E, Maes T, Buesa C, Ferrer I (2006) Reduced ubiquitin C-terminal hydrolase-1 expression levels in dementia with Lewy bodies. Neurobiol Dis 22:265-273.

Barrett AJ, Rawlings ND (2001) Evolutionary lines of cysteine peptidases. Biol Chem 382:727-733.

Barsottini OG, Albuquerque MV, Braga Neto P, Pedroso JL (2014) Adult onset sporadic ataxias: a diagnostic challenge. Arquivos de neuro-psiquiatria 72:232-240.

Bernal-Pacheco O, Limotai N, Go CL, Fernandez HH (2012) Nonmotor manifestations in Parkinson disease. Neurologist 18:1-16.

Bernasconi R, Molinari M (2011) ERAD and ERAD tuning: disposal of cargo and of ERAD regulators from the mammalian ER. Current opinion in cell biology 23:176-183.

Bilguvar K, Tyagi NK, Ozkara C, Tuysuz B, Bakircioglu M, Choi M, Delil S, Caglayan AO, Baranoski JF, Erturk O, Yalcinkaya C, Karacorlu M, Dincer A, Johnson MH, Mane S, Chandra SS, Louvi A, Boggon TJ, Lifton RP, Horwich AL, Gunel M (2013) Recessive loss of function of the neuronal ubiquitin hydrolase UCHL1 leads to early-onset progressive neurodegeneration. Proceedings of the National Academy of Sciences of the United States of America 110:3489-3494.

Bonifati V, Rizzu P, Squitieri F, Krieger E, Vanacore N, van Swieten JC, Brice A, van Duijn CM, Oostra B, Meco G, Heutink P (2003a) DJ-1(PARK7), a novel gene for autosomal recessive, early onset parkinsonism. Neurol Sci 24:159-160.

Bonifati V, Rizzu P, van Baren MJ, Schaap O, Breedveld GJ, Krieger E, Dekker MC, Squitieri F, Ibanez P, Joosse M, van Dongen JW, Vanacore N, van Swieten JC, Brice A, Meco G, van Duijn CM, Oostra BA, Heutink P (2003b) Mutations in the DJ-1 gene associated with autosomal recessive early-onset parkinsonism. Science 299:256-259.

Bosco G, Poppele RE (2001) Proprioception from a spinocerebellar perspective. Physiological reviews 81:539-568.

Boudreaux DA, Maiti TK, Davies CW, Das C (2010) Ubiquitin vinyl methyl ester binding orients the misaligned active site of the ubiquitin hydrolase UCHL1 into productive conformation. Proceedings of the National Academy of Sciences of the United States of America 107:9117-9122.

Boya P, Reggiori F, Codogno P (2013) Emerging regulation and functions of autophagy. Nature cell biology 15:713-720.

Butterfield DA (2004) Proteomics: a new approach to investigate oxidative stress in Alzheimer's disease brain. Brain Res 1000:1-7.

Carmine Belin A, Westerlund M, Bergman O, Nissbrandt H, Lind C, Sydow O, Galter D (2007) S18Y in ubiquitin carboxy-terminal hydrolase L1 (UCH-L1) associated with decreased risk of Parkinson's disease in Sweden. Parkinsonism Relat Disord 13:295-298.

Cartier AE, Djakovic SN, Salehi A, Wilson SM, Masliah E, Patrick GN (2009) Regulation of synaptic structure by ubiquitin C-terminal hydrolase L1. J Neurosci 29:7857-7868.

Case A, Stein RL (2006) Mechanistic studies of ubiquitin C-terminal hydrolase L1. Biochemistry 45:2443-2452.

Cerami E, Gao J, Dogrusoz U, Gross BE, Sumer SO, Aksoy BA, Jacobsen A, Byrne CJ, Heuer ML, Larsson E, Antipin Y, Reva B, Goldberg AP, Sander C, Schultz N (2012) The cBio cancer genomics portal: an open platform for exploring multidimensional cancer genomics data. Cancer discovery 2:401-404.

Cesari R, Martin ES, Calin GA, Pentimalli F, Bichi R, McAdams H, Trapasso F, Drusco A, Shimizu M, Masciullo V, D'Andrilli G, Scambia G, Picchio MC, Alder H, Godwin AK, Croce CM (2003) Parkin, a gene implicated in autosomal recessive juvenile parkinsonism, is a candidate tumor suppressor gene on chromosome

6q25-q27. Proceedings of the National Academy of Sciences of the United States of America 100:5956-5961.

Cha GH, Kim S, Park J, Lee E, Kim M, Lee SB, Kim JM, Chung J, Cho KS (2005) Parkin negatively regulates JNK pathway in the dopaminergic neurons of Drosophila. Proceedings of the National Academy of Sciences of the United States of America 102:10345-10350.

Chartier-Harlin MC, Kachergus J, Roumier C, Mouroux V, Douay X, Lincoln S, Levecque C, Larvor L, Andrieux J, Hulihan M, Waucquier N, Defebvre L, Amouyel P, Farrer M, Destee A (2004) Alpha-synuclein locus duplication as a cause of familial Parkinson's disease. Lancet 364:1167-1169.

Chaugule VK, Burchell L, Barber KR, Sidhu A, Leslie SJ, Shaw GS, Walden H (2011) Autoregulation of Parkin activity through its ubiquitin-like domain. EMBO J 30:2853-2867.

Chen F, Sugiura Y, Myers KG, Liu Y, Lin W (2010) Ubiquitin carboxyl-terminal hydrolase L1 is required for maintaining the structure and function of the neuromuscular junction. Proceedings of the National Academy of Sciences of the United States of America 107:1636-1641.

Chen G, Gharib TG, Huang CC, Thomas DG, Shedden KA, Taylor JM, Kardia SL, Misek DE, Giordano TJ, Iannettoni MD, Orringer MB, Hanash SM, Beer DG (2002) Proteomic analysis of lung adenocarcinoma: identification of a highly expressed set of proteins in tumors. Clinical cancer research : an official journal of the American Association for Cancer Research 8:2298-2305.

Chen ZJ, Sun LJ (2009) Nonproteolytic functions of ubiquitin in cell signaling. Mol Cell 33:275-286.

Chin LS, Nugent RD, Raynor MC, Vavalle JP, Li L (2000) SNIP, a novel SNAP-25-interacting protein implicated in regulated exocytosis. J Biol Chem 275:1191-1200.

Chin LS, Olzmann JA, Li L (2010) Parkin-mediated ubiquitin signalling in aggresome formation and autophagy. Biochemical Society transactions 38:144-149.

Choi J, Levey AI, Weintraub ST, Rees HD, Gearing M, Chin LS, Li L (2004) Oxidative modifications and down-regulation of ubiquitin carboxyl-terminal hydrolase L1 associated with idiopathic Parkinson's and Alzheimer's diseases. J Biol Chem 279:13256-13264.

Choi J, Rees HD, Weintraub ST, Levey AI, Chin LS, Li L (2005) Oxidative modifications and aggregation of Cu,Zn-superoxide dismutase associated with Alzheimer and Parkinson diseases. J Biol Chem 280:11648-11655.

Choi J, Sullards MC, Olzmann JA, Rees HD, Weintraub ST, Bostwick DE, Gearing M, Levey AI, Chin LS, Li L (2006) Oxidative damage of DJ-1 is linked to sporadic Parkinson and Alzheimer diseases. J Biol Chem 281:10816-10824.

Chung KK, Thomas B, Li X, Pletnikova O, Troncoso JC, Marsh L, Dawson VL, Dawson TM (2004) S-nitrosylation of parkin regulates ubiquitination and compromises parkin's protective function. Science 304:1328-1331.

Ciechanover A (2005) Intracellular protein degradation: from a vague idea thru the lysosome and the ubiquitin-proteasome system and onto human diseases and drug targeting. Cell death and differentiation 12:1178-1190.

Cole RN, Hart GW (2001) Cytosolic O-glycosylation is abundant in nerve terminals. Journal of neurochemistry 79:1080-1089.

Coleman M (2005) Axon degeneration mechanisms: commonality amid diversity. Nature Reviews Neuroscience.

Conforti L, Gilley J, Coleman MP (2014) Wallerian degeneration: an emerging axon death pathway linking injury and disease. Nature reviews Neuroscience 15:394-409.

Corti O, Hampe C, Koutnikova H, Darios F, Jacquier S, Prigent A, Robinson JC, Pradier L, Ruberg M, Mirande M, Hirsch E, Rooney T, Fournier A, Brice A (2003) The p38 subunit of the aminoacyl-tRNA synthetase complex is a Parkin substrate: linking protein biosynthesis and neurodegeneration. Human molecular genetics 12:1427-1437.

Cuervo AM (2004) Autophagy: many paths to the same end. Mol Cell Biochem 263:55-72.

Cuervo AM, Stefanis L, Fredenburg R, Lansbury PT, Sulzer D (2004) Impaired degradation of mutant alpha-synuclein by chaperone-mediated autophagy. Science 305:1292-1295.

Cuervo AM, Wong E (2014) Chaperone-mediated autophagy: roles in disease and aging. Cell research 24:92-104.

Davison EJ, Pennington K, Hung CC, Peng J, Rafiq R, Ostareck-Lederer A, Ostareck DH, Ardley HC, Banks RE, Robinson PA (2009) Proteomic analysis of increased Parkin expression and its interactants provides evidence for a role in modulation of mitochondrial function. Proteomics 9:4284-4297.

Dawson TM, Dawson VL (2009) The role of parkin in familial and sporadic Parkinson's disease. Movement disorders : official journal of the Movement Disorder Society 25 Suppl 1:9.

Day IN, Thompson RJ (2010) UCHL1 (PGP 9.5): neuronal biomarker and ubiquitin system protein. Progress in neurobiology 90:327-362.

Doran JF, Jackson P, Kynoch PA, Thompson RJ (1983) Isolation of PGP 9.5, a new human neurone-specific protein detected by high-resolution two-dimensional electrophoresis. Journal of neurochemistry 40:1542-1547.

Dorsey ER, Constantinescu R, Thompson JP, Biglan KM, Holloway RG, Kieburtz K, Marshall FJ, Ravina BM, Schifitto G, Siderowf A, Tanner CM (2007) Projected number of people with Parkinson disease in the most populous nations, 2005 through 2030. Neurology 68:384-386.

Dorsey ER, George BP, Leff B, Willis AW (2013) The coming crisis: obtaining care for the growing burden of neurodegenerative conditions. Neurology 80:1989-1996.

Douglas PM, Dillin A (2010) Protein homeostasis and aging in neurodegeneration. J Cell Biol 190:719-729.

Dueñas A, Goold R, Giunti P (2006) Molecular pathogenesis of spinocerebellar ataxias. Brain : a journal of neurology 129:1357-1370.

Durr A, Brice A (2000) Clinical and genetic aspects of spinocerebellar degeneration. Current opinion in neurology 13:407-413.

Elbaz A, Levecque C, Clavel J, Vidal JS, Richard F, Correze JR, Delemotte B, Amouyel P, Alperovitch A, Chartier-Harlin MC, Tzourio C (2003) S18Y polymorphism in the UCH-L1 gene and Parkinson's disease: evidence for an age-dependent relationship. Mov Disord 18:130-137.

Elder GA, Friedrich VL, Jr., Margita A, Lazzarini RA (1999) Age-related atrophy of motor axons in mice deficient in the mid-sized neurofilament subunit. J Cell Biol 146:181-192.

Eletr ZM, Wilkinson KD (2014) Regulation of proteolysis by human deubiquitinating enzymes. Biochimica et biophysica acta 1843:114-128.

England JD, Asbury AK (2004) Peripheral neuropathy. Lancet 363:2151-2161.

Eskelinen EL, Saftig P (2009) Autophagy: a lysosomal degradation pathway with a central role in health and disease. Biochimica et biophysica acta 1793:664-673.

Fahn S (2003) Description of Parkinson's disease as a clinical syndrome. Ann N Y Acad Sci 991:1-14.

Fallon L, Belanger CM, Corera AT, Kontogiannea M, Regan-Klapisz E, Moreau F, Voortman J, Haber M, Rouleau G, Thorarinsdottir T, Brice A, van Bergen En Henegouwen PM, Fon EA (2006) A regulated interaction with the UIM protein Eps15 implicates parkin in EGF receptor trafficking and PI(3)K-Akt signalling. Nature cell biology 8:834-842.

Fang Y, Fu D, Shen XZ (2010) The potential role of ubiquitin c-terminal hydrolases in oncogenesis. Biochimica et biophysica acta 1806:1-6.

Farrer MJ (2006) Genetics of Parkinson disease: paradigm shifts and future prospects. Nat Rev Genet 7:306-318.

Fortun J, Li J, Go J, Fenstermaker A, Fletcher BS, Notterpek L (2005) Impaired proteasome activity and accumulation of ubiquitinated substrates in a hereditary neuropathy model. Journal of neurochemistry 92:1531-1541.

Gao J, Aksoy BA, Dogrusoz U, Dresdner G, Gross B, Sumer SO, Sun Y, Jacobsen A, Sinha R, Larsson E, Cerami E, Sander C, Schultz N (2013) Integrative analysis of complex cancer genomics and clinical profiles using the cBioPortal. Science signaling 6:pl1.

Giles LM, Li L, Chin LS (2009) Printor, a novel torsinA-interacting protein implicated in dystonia pathogenesis. J Biol Chem 284:21765-21775.

Gilman S (2002) Joint position sense and vibration sense: anatomical organisation and assessment. Journal of neurology, neurosurgery, and psychiatry 73:473-477.

Gong B, Cao Z, Zheng P, Vitolo OV, Liu S, Staniszewski A, Moolman D, Zhang H, Shelanski M, Arancio O (2006) Ubiquitin hydrolase Uch-L1 rescues beta-amyloid-induced decreases in synaptic function and contextual memory. Cell 126:775-788.

Guernsey DL, Jiang H, Bedard K, Evans SC, Ferguson M, Matsuoka M, Macgillivray C, Nightingale M, Perry S, Rideout AL, Orr A, Ludman M, Skidmore DL, Benstead T, Samuels ME (2010) Mutation in the gene encoding ubiquitin ligase LRSAM1 in patients with Charcot-Marie-Tooth disease. PLoS genetics 6.

Hackbarth JS, Lee SH, Meng XW, Vroman BT, Kaufmann SH, Karnitz LM (2004) S-peptide epitope tagging for protein purification, expression monitoring, and localization in mammalian cells. BioTechniques 37:835-839.

Hamani C, Lozano AM (2003) Physiology and pathophysiology of Parkinson's disease. Ann N Y Acad Sci 991:15-21.

Hart GW, Slawson C, Ramirez-Correa G, Lagerlof O (2011) Cross talk between O-GlcNAcylation and phosphorylation: roles in signaling, transcription, and chronic disease. Annual review of biochemistry 80:825-858.

Hatcher JM, Pennell KD, Miller GW (2008) Parkinson's disease and pesticides: a toxicological perspective. Trends Pharmacol Sci 29:322-329.

Healy DG, Abou-Sleiman PM, Casas JP, Ahmadi KR, Lynch T, Gandhi S, Muqit MM, Foltynie T, Barker R, Bhatia KP, Quinn NP, Lees AJ, Gibson JM, Holton JL, Revesz T, Goldstein DB, Wood NW (2006) UCHL-1 is not a Parkinson's disease susceptibility gene. Ann Neurol 59:627-633.

Henn IH, Bouman L, Schlehe JS, Schlierf A, Schramm JE, Wegener E, Nakaso K, Culmsee C, Berninger B, Krappmann D, Tatzelt J, Winklhofer KF (2007) Parkin

mediates neuroprotection through activation of IkappaB kinase/nuclear factor-kappaB signaling. J Neurosci 27:1868-1878.

Henn IH, Gostner JM, Lackner P, Tatzelt J, Winklhofer KF (2005) Pathogenic mutations inactivate parkin by distinct mechanisms. Journal of neurochemistry 92:114-122.

Hickey P, Stacy M (2011) Available and emerging treatments for Parkinson's disease: a review. Drug design, development and therapy 5:241-254.

Hjerpe R, Aillet F, Lopitz-Otsoa F, Lang V, England P, Rodriguez MS (2009) Efficient protection and isolation of ubiquitylated proteins using tandem ubiquitin-binding entities. EMBO Rep 10:1250-1258.

Hoffman PN, Griffin JW, Price DL (1984) Control of axonal caliber by neurofilament transport. J Cell Biol 99:705-714.

Hristova VA, Beasley SA, Rylett RJ, Shaw GS (2009) Identification of a novel Zn2+-binding domain in the autosomal recessive juvenile Parkinson-related E3 ligase parkin. J Biol Chem 284:14978-14986.

Hu M, Li P, Li M, Li W, Yao T, Wu JW, Gu W, Cohen RE, Shi Y (2002) Crystal structure of a UBP-family deubiquitinating enzyme in isolation and in complex with ubiquitin aldehyde. Cell 111:1041-1054.

Hurst-Kennedy J, Chin LS, Li L (2012) Ubiquitin C-terminal hydrolase l1 in tumorigenesis. Biochemistry research international 2012:123706.

Hussain S, Foreman O, Perkins SL, Witzig TE, Miles RR, van Deursen J, Galardy PJ (2010) The de-ubiquitinase UCH-L1 is an oncogene that drives the development of lymphoma in vivo by deregulating PHLPP1 and Akt signaling. Leukemia 24:1641-1655.

Hussain S, Zhang Y, Galardy PJ (2009) DUBs and cancer: the role of deubiquitinating enzymes as oncogenes, non-oncogenes and tumor suppressors. Cell cycle 8:1688-1697.

Hutter CM, Samii A, Factor SA, Nutt JG, Higgins DS, Bird TD, Griffith A, Roberts JW, Leis BC, Montimurro JS, Kay DM, Edwards KL, Payami H, Zabetian CP (2008) Lack of evidence for an association between UCHL1 S18Y and Parkinson's disease. Eur J Neurol 15:134-139.

Ichihara N, Wu J, Chui DH, Yamazaki K, Wakabayashi T, Kikuchi T (1995) Axonal degeneration promotes abnormal accumulation of amyloid beta-protein in ascending gracile tract of gracile axonal dystrophy (GAD) mouse. Brain Res 695:173-178.

Iwahashi CK, Yasui DH, An HJ, Greco CM, Tassone F, Nannen K, Babineau B, Lebrilla CB, Hagerman RJ, Hagerman PJ (2006) Protein composition of the intranuclear inclusions of FXTAS. Brain : a journal of neurology 129:256-271.

Jani-Acsadi A, Krajewski K, Shy ME (2008) Charcot-Marie-Tooth neuropathies: diagnosis and management. Seminars in neurology 28:185-194.

Kabuta T, Furuta A, Aoki S, Furuta K, Wada K (2008a) Aberrant interaction between Parkinson disease-associated mutant UCH-L1 and the lysosomal receptor for chaperone-mediated autophagy. J Biol Chem 283:23731-23738.

Kabuta T, Setsuie R, Mitsui T, Kinugawa A, Sakurai M, Aoki S, Uchida K, Wada K (2008b) Aberrant molecular properties shared by familial Parkinson's disease-associated mutant UCH-L1 and carbonyl-modified UCH-L1. Human molecular genetics 17:1482-1496.

Kabuta T, Wada K (2008) Insights into links between familial and sporadic Parkinson's disease: physical relationship between UCH-L1 variants and chaperone-mediated autophagy. Autophagy 4:827-829.

Kane L, Lazarou M, Fogel A, Li Y, Yamano K, Sarraf S, Banerjee S, Youle R (2014) PINK1 phosphorylates ubiquitin to activate Parkin E3 ubiquitin ligase activity. The Journal of cell biology.

Kanthasamy AG, Kitazawa M, Kanthasamy A, Anantharam V (2005) Dieldrin-induced neurotoxicity: relevance to Parkinson's disease pathogenesis. Neurotoxicology 26:701-719.

Kaushik S, Cuervo AM (2006) Autophagy as a cell-repair mechanism: activation of chaperone-mediated autophagy during oxidative stress. Molecular aspects of medicine 27:444-454.

Kayagaki N, Phung Q, Chan S, Chaudhari R, Quan C, O'Rourke KM, Eby M, Pietras E, Cheng G, Bazan JF, Zhang Z, Arnott D, Dixit VM (2007) DUBA: a deubiquitinase that regulates type I interferon production. Science 318:1628-1632.

Kiffin R, Christian C, Knecht E, Cuervo AM (2004) Activation of chaperone-mediated autophagy during oxidative stress. Molecular biology of the cell 15:4829-4840.

Kikuchi T, Mukoyama M, Yamazaki K, Moriya H (1990) Axonal degeneration of ascending sensory neurons in gracile axonal dystrophy mutant mouse. Acta neuropathologica 80:145-151.

Kim J, Kundu M, Viollet B, Guan KL (2011) AMPK and mTOR regulate autophagy through direct phosphorylation of Ulk1. Nature cell biology 13:132-141.

Kirkin V, Lamark T, Johansen T, Dikic I (2009a) NBR1 cooperates with p62 in selective autophagy of ubiquitinated targets. Autophagy 5:732-733.

Kirkin V, McEwan DG, Novak I, Dikic I (2009b) A role for ubiquitin in selective autophagy. Molecular cell 34:259-269.

Kish-Trier E, Hill CP (2013) Structural biology of the proteasome. Annual review of biophysics 42:29-49.

Kitada T, Asakawa S, Hattori N, Matsumine H, Yamamura Y, Minoshima S, Yokochi M, Mizuno Y, Shimizu N (1998) Mutations in the parkin gene cause autosomal recessive juvenile parkinsonism. Nature 392:605-608.

Komander D, Clague MJ, Urbe S (2009) Breaking the chains: structure and function of the deubiquitinases. Nature reviews Molecular cell biology 10:550-563.

Kondapalli C, Kazlauskaite A, Zhang N, Woodroof H, Campbell D, Gourlay R, Burchell L, Walden H, Macartney T, Deak M, Knebel A, Alessi D, Muqit M (2012) PINK1 is activated by mitochondrial membrane potential depolarization and stimulates Parkin E3 ligase activity by phosphorylating Serine 65. Open biology 2:120080.

Kowalski JR, Juo P (2012) The role of deubiquitinating enzymes in synaptic function and nervous system diseases. Neural plasticity 2012:892749.

Kruger R, Kuhn W, Muller T, Woitalla D, Graeber M, Kosel S, Przuntek H, Epplen JT, Schols L, Riess O (1998) Ala30Pro mutation in the gene encoding alpha-synuclein in Parkinson's disease. Nat Genet 18:106-108.

Kyratzi E, Pavlaki M, Stefanis L (2008) The S18Y polymorphic variant of UCH-L1 confers an antioxidant function to neuronal cells. Human molecular genetics 17:2160-2171.

Lam YA, Xu W, DeMartino GN, Cohen RE (1997) Editing of ubiquitin conjugates by an isopeptidase in the 26S proteasome. Nature 385:737-740.

Lamark T, Kirkin V, Dikic I, Johansen T (2009) NBR1 and p62 as cargo receptors for selective autophagy of ubiquitinated targets. Cell cycle 8:1986-1990.

Larsen CN, Krantz BA, Wilkinson KD (1998) Substrate specificity of deubiquitinating enzymes: ubiquitin C-terminal hydrolases. Biochemistry 37:3358-3368.

Larsen CN, Price JS, Wilkinson KD (1996) Substrate binding and catalysis by ubiquitin C-terminal hydrolases: identification of two active site residues. Biochemistry 35:6735-6744.

Le Couteur DG, McLean AJ, Taylor MC, Woodham BL, Board PG (1999) Pesticides and Parkinson's disease. Biomed Pharmacother 53:122-130.

Lederer CW, Torrisi A, Pantelidou M, Santama N, Cavallaro S (2007) Pathways and genes differentially expressed in the motor cortex of patients with sporadic amyotrophic lateral sclerosis. BMC genomics 8:26.

Lee JT, Wheeler TC, Li L, Chin LS (2008) Ubiquitination of alpha-synuclein by Siah-1 promotes alpha-synuclein aggregation and apoptotic cell death. Human molecular genetics 17:906-917.

Lee SM, Chin LS, Li L (2012) Charcot-Marie-Tooth disease-linked protein SIMPLE functions with the ESCRT machinery in endosomal trafficking. The Journal of cell biology 199:799-816.

Lee SM, Sha D, Mohammed AA, Asress S, Glass JD, Chin LS, Li L (2013) Motor and sensory neuropathy due to myelin infolding and paranodal damage in a transgenic mouse model of Charcot-Marie-Tooth disease type 1C. Human molecular genetics 22:1755-1770.

Leroy E, Boyer R, Auburger G, Leube B, Ulm G, Mezey E, Harta G, Brownstein MJ, Jonnalagada S, Chernova T, Dehejia A, Lavedan C, Gasser T, Steinbach PJ, Wilkinson KD, Polymeropoulos MH (1998) The ubiquitin pathway in Parkinson's disease. Nature 395:451-452.

Lesage S, Brice A (2009) Parkinson's disease: from monogenic forms to genetic susceptibility factors. Human molecular genetics 18:R48-59.

Lewitt PA (2008) Levodopa for the treatment of Parkinson's disease. N Engl J Med 359:2468-2476.

Li L, Tao Q, Jin H, van Hasselt A, Poon FF, Wang X, Zeng MS, Jia WH, Zeng YX, Chan AT, Cao Y (2010) The tumor suppressor UCHL1 forms a complex with p53/MDM2/ARF to promote p53 signaling and is frequently silenced in nasopharyngeal carcinoma. Clinical cancer research : an official journal of the American Association for Cancer Research 16:2949-2958.

Li WW, Li J, Bao JK (2012) Microautophagy: lesser-known self-eating. Cellular and molecular life sciences : CMLS 69:1125-1136.

Li Y, Chin LS, Weigel C, Li L (2001) Spring, a novel RING finger protein that regulates synaptic vesicle exocytosis. J Biol Chem 276:40824-40833.

Liu X, Zeng B, Ma J, Wan C (2009a) Comparative proteomic analysis of osteosarcoma cell and human primary cultured osteoblastic cell. Cancer investigation 27:345-352.

Liu Y, Fallon L, Lashuel HA, Liu Z, Lansbury PT, Jr. (2002) The UCH-L1 gene encodes two opposing enzymatic activities that affect alpha-synuclein degradation and Parkinson's disease susceptibility. Cell 111:209-218.

Liu Y, Lashuel HA, Choi S, Xing X, Case A, Ni J, Yeh LA, Cuny GD, Stein RL, Lansbury PT, Jr. (2003) Discovery of inhibitors that elucidate the role of UCH-L1 activity in the H1299 lung cancer cell line. Chemistry & biology 10:837-846.

Liu Z, Meray RK, Grammatopoulos TN, Fredenburg RA, Cookson MR, Liu Y, Logan T, Lansbury PT, Jr. (2009b) Membrane-associated farnesylated UCH-L1 promotes alpha-synuclein neurotoxicity and is a therapeutic target for Parkinson's disease.

Proceedings of the National Academy of Sciences of the United States of America 106:4635-4640.

Love KR, Catic A, Schlieker C, Ploegh HL (2007) Mechanisms, biology and inhibitors of deubiquitinating enzymes. Nature chemical biology 3:697-705.

Lowe J, McDermott H, Landon M, Mayer RJ, Wilkinson KD (1990) Ubiquitin carboxyl-terminal hydrolase (PGP 9.5) is selectively present in ubiquitinated inclusion bodies characteristic of human neurodegenerative diseases. The Journal of pathology 161:153-160.

Lucking CB, Durr A, Bonifati V, Vaughan J, De Michele G, Gasser T, Harhangi BS, Meco G, Denefle P, Wood NW, Agid Y, Brice A (2000) Association between early-onset Parkinson's disease and mutations in the parkin gene. N Engl J Med 342:1560-1567.

Maraganore DM, Lesnick TG, Elbaz A, Chartier-Harlin MC, Gasser T, Kruger R, Hattori N, Mellick GD, Quattrone A, Satoh J, Toda T, Wang J, Ioannidis JP, de Andrade M, Rocca WA (2004) UCHL1 is a Parkinson's disease susceptibility gene. Ann Neurol 55:512-521.

Martyn CN, Hughes RA (1997) Epidemiology of peripheral neuropathy. Journal of neurology, neurosurgery, and psychiatry 62:310-318.

Mastoraki A, Ioannidis E, Apostolaki A, Patsouris E, Aroni K (2009) PGP 9.5 and cyclin D1 coexpression in cutaneous squamous cell carcinomas. International journal of surgical pathology 17:413-420.

Matsuda N, Sato S, Shiba K, Okatsu K, Saisho K, Gautier C, Sou Y-S, Saiki S, Kawajiri S, Sato F, Kimura M, Komatsu M, Hattori N, Tanaka K (2010) PINK1 stabilized by mitochondrial depolarization recruits Parkin to damaged mitochondria and activates latent Parkin for mitophagy. The Journal of cell biology 189:211-221.

Matsuda N, Tanaka K (2010) Does impairment of the ubiquitin-proteasome system or the autophagy-lysosome pathway predispose individuals to neurodegenerative disorders such as Parkinson's disease? Journal of Alzheimer's disease : JAD 19:1-9.

McCullough J, Clague MJ, Urbe S (2004) AMSH is an endosome-associated ubiquitin isopeptidase. The Journal of cell biology 166:487-492.

McKinnon C, Tabrizi SJ (2014) The Ubiquitin-Proteasome System in Neurodegeneration. Antioxidants & redox signaling.

Meray RK, Lansbury PT, Jr. (2007) Reversible monoubiquitination regulates the Parkinson disease-associated ubiquitin hydrolase UCH-L1. J Biol Chem 282:10567-10575.

Metzger MB, Hristova VA, Weissman AM (2012) HECT and RING finger families of E3 ubiquitin ligases at a glance. Journal of cell science 125:531-537.

Mijaljica D, Prescott M, Devenish RJ (2011) Microautophagy in mammalian cells: revisiting a 40-year-old conundrum. Autophagy 7:673-682.

Miocinovic S, Somayajula S, Chitnis S, Vitek JL (2013) History, applications, and mechanisms of deep brain stimulation. JAMA neurology 70:163-171.

Miura H, Oda K, Endo C, Yamazaki K, Shibasaki H, Kikuchi T (1993) Progressive degeneration of motor nerve terminals in GAD mutant mouse with hereditary sensory axonopathy. Neuropathology and applied neurobiology 19:41-51.

Miyoshi Y, Nakayama S, Torikoshi Y, Tanaka S, Ishihara H, Taguchi T, Tamaki Y, Noguchi S (2006) High expression of ubiquitin carboxy-terminal hydrolase-L1 and -L3 mRNA predicts early recurrence in patients with invasive breast cancer. Cancer science 97:523-529.

Mizushima N, Levine B, Cuervo AM, Klionsky DJ (2008) Autophagy fights disease through cellular self-digestion. Nature 451:1069-1075.

Morett E, Bork P (1999) A novel transactivation domain in parkin. Trends Biochem Sci 24:229-231.

Mori H, Kondo T, Yokochi M, Matsumine H, Nakagawa-Hattori Y, Miyake T, Suda K, Mizuno Y (1998) Pathologic and biochemical studies of juvenile parkinsonism linked to chromosome 6q. Neurology 51:890-892.

Mukoyama M, Yamazaki K, Kikuchi T, Tomita T (1989) Neuropathology of gracile axonal dystrophy (GAD) mouse. An animal model of central distal axonopathy in primary sensory neurons. Acta neuropathologica 79:294-299.

Murakami T, Shoji M, Imai Y, Inoue H, Kawarabayashi T, Matsubara E, Harigaya Y, Sasaki A, Takahashi R, Abe K (2004) Pael-R is accumulated in Lewy bodies of Parkinson's disease. Annals of neurology 55:439-442.

Nagamine S, Kabuta T, Furuta A, Yamamoto K, Takahashi A, Wada K (2010) Deficiency of ubiquitin carboxy-terminal hydrolase-L1 (UCH-L1) leads to vulnerability to lipid peroxidation. Neurochemistry international 57:102-110.

Nakada S, Tai I, Panier S, Al-Hakim A, Iemura S, Juang YC, O'Donnell L, Kumakubo A, Munro M, Sicheri F, Gingras AC, Natsume T, Suda T, Durocher D (2010) Non-canonical inhibition of DNA damage-dependent ubiquitination by OTUB1. Nature 466:941-946.

Narendra D, Tanaka A, Suen DF, Youle RJ (2008) Parkin is recruited selectively to impaired mitochondria and promotes their autophagy. J Cell Biol 183:795-803.

Nishikawa K, Li H, Kawamura R, Osaka H, Wang YL, Hara Y, Hirokawa T, Manago Y, Amano T, Noda M, Aoki S, Wada K (2003) Alterations of structure and hydrolase

activity of parkinsonism-associated human ubiquitin carboxyl-terminal hydrolase L1 variants. Biochem Biophys Res Commun 304:176-183.

Nixon RA (2013) The role of autophagy in neurodegenerative disease. Nature medicine 19:983-997.

Oda K, Yamazaki K, Miura H, Shibasaki H, Kikuchi T (1992) Dying back type axonal degeneration of sensory nerve terminals in muscle spindles of the gracile axonal dystrophy (GAD) mutant mouse. Neuropathology and applied neurobiology 18:265-281.

Okun MS (2012) Deep-brain stimulation for Parkinson's disease. N Engl J Med 367:1529-1538.

Olzmann JA, Brown K, Wilkinson KD, Rees HD, Huai Q, Ke H, Levey AI, Li L, Chin LS (2004) Familial Parkinson's disease-associated L166P mutation disrupts DJ-1 protein folding and function. J Biol Chem 279:8506-8515.

Olzmann JA, Chin LS (2008) Parkin-mediated K63-linked polyubiquitination: a signal for targeting misfolded proteins to the aggresome-autophagy pathway. Autophagy 4:85-87.

Olzmann JA, Li L, Chudaev MV, Chen J, Perez FA, Palmiter RD, Chin LS (2007) Parkin-mediated K63-linked polyubiquitination targets misfolded DJ-1 to aggresomes via binding to HDAC6. J Cell Biol 178:1025-1038.

Orenstein SJ, Kuo SH, Tasset I, Arias E, Koga H, Fernandez-Carasa I, Cortes E, Honig LS, Dauer W, Consiglio A, Raya A, Sulzer D, Cuervo AM (2013) Interplay of LRRK2 with chaperone-mediated autophagy. Nature neuroscience 16:394-406.

Osaka H, Wang YL, Takada K, Takizawa S, Setsuie R, Li H, Sato Y, Nishikawa K, Sun YJ, Sakurai M, Harada T, Hara Y, Kimura I, Chiba S, Namikawa K, Kiyama H, Noda M, Aoki S, Wada K (2003) Ubiquitin carboxy-terminal hydrolase L1 binds to

and stabilizes monoubiquitin in neuron. Human molecular genetics 12:1945-1958.

Pankiv S, Clausen TH, Lamark T, Brech A, Bruun JA, Outzen H, Overvatn A, Bjorkoy G, Johansen T (2007) p62/SQSTM1 binds directly to Atg8/LC3 to facilitate degradation of ubiquitinated protein aggregates by autophagy. J Biol Chem 282:24131-24145.

Patzko A, Shy ME (2011) Update on Charcot-Marie-Tooth disease. Current neurology and neuroscience reports 11:78-88.

Paulson HL, Das SS, Crino PB, Perez MK, Patel SC, Gotsdiner D, Fischbeck KH, Pittman RN (1997) Machado-Joseph disease gene product is a cytoplasmic protein widely expressed in brain. Ann Neurol 41:453-462.

Perez FA, Curtis WR, Palmiter RD (2005) Parkin-deficient mice are not more sensitive to 6-hydroxydopamine or methamphetamine neurotoxicity. BMC Neurosci 6:71.

Perez FA, Palmiter RD (2005) Parkin-deficient mice are not a robust model of parkinsonism. Proceedings of the National Academy of Sciences of the United States of America 102:2174-2179.

Periquet M, Corti O, Jacquier S, Brice A (2005) Proteomic analysis of parkin knockout mice: alterations in energy metabolism, protein handling and synaptic function. Journal of neurochemistry 95:1259-1276.

Picchio MC, Martin ES, Cesari R, Calin GA, Yendamuri S, Kuroki T, Pentimalli F, Sarti M, Yoder K, Kaiser LR, Fishel R, Croce CM (2004) Alterations of the tumor suppressor gene Parkin in non-small cell lung cancer. Clinical cancer research : an official journal of the American Association for Cancer Research 10:2720-2724.

Pickart CM, Eddins MJ (2004) Ubiquitin: structures, functions, mechanisms. Biochim Biophys Acta 1695:55-72.

Pickart CM, Fushman D (2004) Polyubiquitin chains: polymeric protein signals. Curr Opin Chem Biol 8:610-616.

Pickart CM, Rose IA (1985) Ubiquitin carboxyl-terminal hydrolase acts on ubiquitin carboxyl-terminal amides. J Biol Chem 260:7903-7910.

Piotrowski J, Beal R, Hoffman L, Wilkinson KD, Cohen RE, Pickart CM (1997) Inhibition of the 26 S proteasome by polyubiquitin chains synthesized to have defined lengths. J Biol Chem 272:23712-23721.

Polymeropoulos MH, Lavedan C, Leroy E, Ide SE, Dehejia A, Dutra A, Pike B, Root H, Rubenstein J, Boyer R, Stenroos ES, Chandrasekharappa S, Athanassiadou A, Papapetropoulos T, Johnson WG, Lazzarini AM, Duvoisin RC, Di Iorio G, Golbe LI, Nussbaum RL (1997) Mutation in the alpha-synuclein gene identified in families with Parkinson's disease. Science 276:2045-2047.

Poon HF, Hensley K, Thongboonkerd V, Merchant ML, Lynn BC, Pierce WM, Klein JB, Calabrese V, Butterfield DA (2005) Redox proteomics analysis of oxidatively modified proteins in G93A-SOD1 transgenic mice--a model of familial amyotrophic lateral sclerosis. Free radical biology & medicine 39:453-462.

Poon WW, Carlos AJ, Aguilar BL, Berchtold NC, Kawano CK, Zograbyan V, Yaopruke T, Shelanski M, Cotman CW (2013) beta-Amyloid (Abeta) oligomers impair brain-derived neurotrophic factor retrograde trafficking by down-regulating ubiquitin C-terminal hydrolase, UCH-L1. J Biol Chem 288:16937-16948.

Poulogiannis G, McIntyre RE, Dimitriadi M, Apps JR, Wilson CH, Ichimura K, Luo F, Cantley LC, Wyllie AH, Adams DJ, Arends MJ (2010) PARK2 deletions occur frequently in sporadic colorectal cancer and accelerate adenoma development in

Apc mutant mice. Proceedings of the National Academy of Sciences of the United States of America 107:15145-15150.

Priyadarshi A, Khuder SA, Schaub EA, Shrivastava S (2000) A meta-analysis of Parkinson's disease and exposure to pesticides. Neurotoxicology 21:435-440.

Rankin CA, Roy A, Zhang Y, Richter M (2011) Parkin, A Top Level Manager in the Cell's Sanitation Department. The open biochemistry journal 5:9-26.

Ravikumar B, Sarkar S, Davies JE, Futter M, Garcia-Arencibia M, Green-Thompson ZW, Jimenez-Sanchez M, Korolchuk VI, Lichtenberg M, Luo S, Massey DC, Menzies FM, Moreau K, Narayanan U, Renna M, Siddiqi FH, Underwood BR, Winslow AR, Rubinsztein DC (2010) Regulation of mammalian autophagy in physiology and pathophysiology. Physiological reviews 90:1383-1435.

Reyes-Turcu FE, Ventii KH, Wilkinson KD (2009) Regulation and cellular roles of ubiquitin-specific deubiquitinating enzymes. Annual review of biochemistry 78:363-397.

Rubinsztein DC (2006) The roles of intracellular protein-degradation pathways in neurodegeneration. Nature 443:780-786.

Sacco JJ, Coulson JM, Clague MJ, Urbe S (2010) Emerging roles of deubiquitinases in cancer-associated pathways. IUBMB life 62:140-157.

Sadowski M, Suryadinata R, Tan AR, Roesley SN, Sarcevic B (2012) Protein monoubiquitination and polyubiquitination generate structural diversity to control distinct biological processes. IUBMB life 64:136-142.

Safadi SS, Barber KR, Shaw GS (2011) Impact of autosomal recessive juvenile Parkinson's disease mutations on the structure and interactions of the parkin ubiquitin-like domain. Biochemistry 50:2603-2610.

Saigoh K, Wang YL, Suh JG, Yamanishi T, Sakai Y, Kiyosawa H, Harada T, Ichihara N, Wakana S, Kikuchi T, Wada K (1999) Intragenic deletion in the gene encoding ubiquitin carboxy-terminal hydrolase in gad mice. Nat Genet 23:47-51.

Sakurai M, Sekiguchi M, Zushida K, Yamada K, Nagamine S, Kabuta T, Wada K (2008) Reduction in memory in passive avoidance learning, exploratory behaviour and synaptic plasticity in mice with a spontaneous deletion in the ubiquitin C-terminal hydrolase L1 gene. Eur J Neurosci 27:691-701.

Satija YK, Bhardwaj A, Das S (2013) A portrayal of E3 ubiquitin ligases and deubiquitylases in cancer. International journal of cancer Journal international du cancer 133:2759-2768.

Satoh J, Kuroda Y (2001) A polymorphic variation of serine to tyrosine at codon 18 in the ubiquitin C-terminal hydrolase-L1 gene is associated with a reduced risk of sporadic Parkinson's disease in a Japanese population. J Neurol Sci 189:113-117.

Savitt JM, Dawson VL, Dawson TM (2006) Diagnosis and treatment of Parkinson disease: molecules to medicine. J Clin Invest 116:1744-1754.

Schlehe JS, Lutz AK, Pilsl A, Lammermann K, Grgur K, Henn IH, Tatzelt J, Winklhofer KF (2008) Aberrant folding of pathogenic Parkin mutants: aggregation versus degradation. J Biol Chem 283:13771-13779.

Schlossmacher M, Frosch M, Gai W, Medina M, Sharma N, Forno L, Ochiishi T, Shimura H, Sharon R, Hattori N, Langston J, Mizuno Y, Hyman B, Selkoe D, Kosik K (2002) Parkin localizes to the Lewy bodies of Parkinson disease and dementia with Lewy bodies. The American journal of pathology 160:1655-1667.

Seidel K, den Dunnen W, Schultz C, Paulson H, Frank S, de Vos R, Brunt E, Deller T, Kampinga H, Rüb U (2010) Axonal inclusions in spinocerebellar ataxia type 3. Acta neuropathologica 120:449-460.

Seidel K, Meister M, Dugbartey G, Zijlstra M, Vinet J, Brunt E, van Leeuwen F, Rüb U, Kampinga H, den Dunnen W (2012) Cellular protein quality control and the evolution of aggregates in spinocerebellar ataxia type 3 (SCA3). Neuropathology and applied neurobiology 38:548-558.

Semchuk KM, Love EJ, Lee RG (1991) Parkinson's disease and exposure to rural environmental factors: a population based case-control study. Can J Neurol Sci 18:279-286.

Semchuk KM, Love EJ, Lee RG (1992) Parkinson's disease and exposure to agricultural work and pesticide chemicals. Neurology 42:1328-1335.

Setsuie R, Wang YL, Mochizuki H, Osaka H, Hayakawa H, Ichihara N, Li H, Furuta A, Sano Y, Sun YJ, Kwon J, Kabuta T, Yoshimi K, Aoki S, Mizuno Y, Noda M, Wada K (2007) Dopaminergic neuronal loss in transgenic mice expressing the Parkinson's disease-associated UCH-L1 I93M mutant. Neurochemistry international 50:119-129.

Sha D, Chin LS, Li L (2010) Phosphorylation of parkin by Parkinson disease-linked kinase PINK1 activates parkin E3 ligase function and NF-kappaB signaling. Human molecular genetics 19:352-363.

Shiba-Fukushima K, Imai Y, Yoshida S, Ishihama Y, Kanao T, Sato S, Hattori N (2012) PINK1-mediated phosphorylation of the Parkin ubiquitin-like domain primes mitochondrial translocation of Parkin and regulates mitophagy. Scientific reports 2:1002.

Shimura H, Hattori N, Kubo S, Mizuno Y, Asakawa S, Minoshima S, Shimizu N, Iwai K, Chiba T, Tanaka K, Suzuki T (2000) Familial Parkinson disease gene product, parkin, is a ubiquitin-protein ligase. Nat Genet 25:302-305.

Shulman JM, De Jager PL, Feany MB (2011) Parkinson's disease: genetics and pathogenesis. Annu Rev Pathol 6:193-222.

Shy ME, Patzko A (2011) Axonal Charcot-Marie-Tooth disease. Current opinion in neurology 24:475-483.

Sierra MI, Wright MH, Nash PD (2010) AMSH interacts with ESCRT-0 to regulate the stability and trafficking of CXCR4. J Biol Chem 285:13990-14004.

Sigismund S, Polo S, Di Fiore PP (2004) Signaling through monoubiquitination. Current topics in microbiology and immunology 286:149-185.

Singhal S, Taylor MC, Baker RT (2008) Deubiquitylating enzymes and disease. BMC biochemistry 9 Suppl 1:S3.

Singleton AB, Farrer M, Johnson J, Singleton A, Hague S, Kachergus J, Hulihan M, Peuralinna T, Dutra A, Nussbaum R, Lincoln S, Crawley A, Hanson M, Maraganore D, Adler C, Cookson MR, Muenter M, Baptista M, Miller D, Blancato J, Hardy J, Gwinn-Hardy K (2003) alpha-Synuclein locus triplication causes Parkinson's disease. Science 302:841.

Spillantini MG, Schmidt ML, Lee VM, Trojanowski JQ, Jakes R, Goedert M (1997) Alpha-synuclein in Lewy bodies. Nature 388:839-840.

Spratt DE, Martinez-Torres RJ, Noh YJ, Mercier P, Manczyk N, Barber KR, Aguirre JD, Burchell L, Purkiss A, Walden H, Shaw GS (2013) A molecular explanation for the recessive nature of parkin-linked Parkinson's disease. Nature communications 4:1983.

Sriram SR, Li X, Ko HS, Chung KK, Wong E, Lim KL, Dawson VL, Dawson TM (2005) Familial-associated mutations differentially disrupt the solubility, localization, binding and ubiquitination properties of parkin. Human molecular genetics 14:2571-2586.

Sun F, Kanthasamy A, Anantharam V, Kanthasamy AG (2007) Environmental neurotoxic chemicals-induced ubiquitin proteasome system dysfunction in the pathogenesis and progression of Parkinson's disease. Pharmacol Ther 114:327-344.

Sun X, Liu M, Hao J, Li D, Luo Y, Wang X, Yang Y, Li F, Shui W, Chen Q, Zhou J (2013) Parkin deficiency contributes to pancreatic tumorigenesis by inducing spindle multipolarity and misorientation. Cell cycle 12:1133-1141.

Takahashi H, Ohama E, Suzuki S, Horikawa Y, Ishikawa A, Morita T, Tsuji S, Ikuta F (1994) Familial juvenile parkinsonism: clinical and pathologic study in a family. Neurology 44:437-441.

Tanida I, Ueno T, Kominami E (2004) LC3 conjugation system in mammalian autophagy. The international journal of biochemistry & cell biology 36:2503-2518.

Tay SP, Yeo CW, Chai C, Chua PJ, Tan HM, Ang AX, Yip DL, Sung JX, Tan PH, Bay BH, Wong SH, Tang C, Tan JM, Lim KL (2010) Parkin enhances the expression of cyclin-dependent kinase 6 and negatively regulates the proliferation of breast cancer cells. J Biol Chem 285:29231-29238.

Tezel E, Hibi K, Nagasaka T, Nakao A (2000) PGP9.5 as a prognostic factor in pancreatic cancer. Clinical cancer research : an official journal of the American Association for Cancer Research 6:4764-4767.

Thao DT, An PN, Yamaguchi M, LinhThuoc T (2012) Overexpression of ubiquitin carboxyl terminal hydrolase impairs multiple pathways during eye development in Drosophila melanogaster. Cell and tissue research 348:453-463.

Thrower JS, Hoffman L, Rechsteiner M, Pickart CM (2000) Recognition of the polyubiquitin proteolytic signal. EMBO J 19:94-102.

Trempe JF, Sauve V, Grenier K, Seirafi M, Tang MY, Menade M, Al-Abdul-Wahid S, Krett J, Wong K, Kozlov G, Nagar B, Fon EA, Gehring K (2013) Structure of parkin reveals mechanisms for ubiquitin ligase activation. Science 340:1451-1455.

Ummanni R, Jost E, Braig M, Lohmann F, Mundt F, Barett C, Schlomm T, Sauter G, Senff T, Bokemeyer C, Sultmann H, Meyer-Schwesinger C, Brummendorf TH, Balabanov S (2011) Ubiquitin carboxyl-terminal hydrolase 1 (UCHL1) is a potential tumour suppressor in prostate cancer and is frequently silenced by promoter methylation. Molecular cancer 10:129.

Valdmanis PN, Dupre N, Lachance M, Stochmanski SJ, Belzil VV, Dion PA, Thiffault I, Brais B, Weston L, Saint-Amant L, Samuels ME, Rouleau GA (2011) A mutation in the RNF170 gene causes autosomal dominant sensory ataxia. Brain : a journal of neurology 134:602-607.

Valente EM, Bentivoglio AR, Dixon PH, Ferraris A, Ialongo T, Frontali M, Albanese A, Wood NW (2001) Localization of a novel locus for autosomal recessive early-onset parkinsonism, PARK6, on human chromosome 1p35-p36. Am J Hum Genet 68:895-900.

Valente EM, Salvi S, Ialongo T, Marongiu R, Elia AE, Caputo V, Romito L, Albanese A, Dallapiccola B, Bentivoglio AR (2004) PINK1 mutations are associated with sporadic early-onset parkinsonism. Ann Neurol 56:336-341.

van Tijn P, Hol EM, van Leeuwen FW, Fischer DF (2008) The neuronal ubiquitin-proteasome system: murine models and their neurological phenotype. Prog Neurobiol 85:176-193.

Veeriah S, Taylor BS, Meng S, Fang F, Yilmaz E, Vivanco I, Janakiraman M, Schultz N, Hanrahan AJ, Pao W, Ladanyi M, Sander C, Heguy A, Holland EC, Paty PB, Mischel PS, Liau L, Cloughesy TF, Mellinghoff IK, Solit DB, Chan TA (2010) Somatic mutations of the Parkinson's disease-associated gene PARK2 in glioblastoma and other human malignancies. Nat Genet 42:77-82.

Vigo T, Nobbio L, Hummelen PV, Abbruzzese M, Mancardi G, Verpoorten N, Verhoeven K, Sereda MW, Nave KA, Timmerman V, Schenone A (2005) Experimental Charcot-Marie-Tooth type 1A: a cDNA microarrays analysis. Mol Cell Neurosci 28:703-714.

Vital A, Meissner W, Canron M-H, Martin-Negrier M-L, Bezard E, Tison F, Vital C (2014) Intra-axonal protein aggregation in the peripheral nervous system. Journal of the peripheral nervous system : JPNS 19:44-49.

Wada H, Kito K, Caskey LS, Yeh ET, Kamitani T (1998) Cleavage of the C-terminus of NEDD8 by UCH-L3. Biochemical and biophysical research communications 251:688-692.

Walters BJ, Campbell SL, Chen PC, Taylor AP, Schroeder DG, Dobrunz LE, Artavanis-Tsakonas K, Ploegh HL, Wilson JA, Cox GA, Wilson SM (2008) Differential effects of Usp14 and Uch-L1 on the ubiquitin proteasome system and synaptic activity. Mol Cell Neurosci 39:539-548.

Wang WJ, Li QQ, Xu JD, Cao XX, Li HX, Tang F, Chen Q, Yang JM, Xu ZD, Liu XP (2008) Over-expression of ubiquitin carboxy terminal hydrolase-L1 induces apoptosis in breast cancer cells. International journal of oncology 33:1037-1045.

Wang X, Winter D, Ashrafi G, Schlehe J, Wong YL, Selkoe D, Rice S, Steen J, LaVoie MJ, Schwarz TL (2011) PINK1 and Parkin target Miro for phosphorylation and degradation to arrest mitochondrial motility. Cell 147:893-906.

Wang YL, Takeda A, Osaka H, Hara Y, Furuta A, Setsuie R, Sun YJ, Kwon J, Sato Y, Sakurai M, Noda M, Yoshikawa Y, Wada K (2004) Accumulation of beta- and gamma-synucleins in the ubiquitin carboxyl-terminal hydrolase L1-deficient gad mouse. Brain Res 1019:1-9.

Wauer T, Komander D (2013) Structure of the human Parkin ligase domain in an autoinhibited state. EMBO J 32:2099-2112.

Webber E, Li L, Chin LS (2008) Hypertonia-associated protein Trak1 is a novel regulator of endosome-to-lysosome trafficking. Journal of molecular biology 382:638-651.

Weeks SD, Grasty KC, Hernandez-Cuebas L, Loll PJ (2011) Crystal structure of a Josephin-ubiquitin complex: evolutionary restraints on ataxin-3 deubiquitinating activity. J Biol Chem 286:4555-4565.

Wenzel DM, Lissounov A, Brzovic PS, Klevit RE (2011) UBCH7 reactivity profile reveals parkin and HHARI to be RING/HECT hybrids. Nature 474:105-108.

Wertz IE, O'Rourke KM, Zhou H, Eby M, Aravind L, Seshagiri S, Wu P, Wiesmann C, Baker R, Boone DL, Ma A, Koonin EV, Dixit VM (2004) De-ubiquitination and ubiquitin ligase domains of A20 downregulate NF-kappaB signalling. Nature 430:694-699.

West AB, Maidment NT (2004) Genetics of parkin-linked disease. Hum Genet 114:327-336.

Wheeler TC, Chin LS, Li Y, Roudabush FL, Li L (2002) Regulation of synaptophysin degradation by Mammalian homologues of seven in absentia. J Biol Chem 277:10273-10282.

Wiborg O, Pedersen MS, Wind A, Berglund LE, Marcker KA, Vuust J (1985) The human ubiquitin multigene family: some genes contain multiple directly repeated ubiquitin coding sequences. EMBO J 4:755-759.

Wilkinson KD, Lee KM, Deshpande S, Duerksen-Hughes P, Boss JM, Pohl J (1989) The neuron-specific protein PGP 9.5 is a ubiquitin carboxyl-terminal hydrolase. Science 246:670-673.

Wilkinson KD, Tashayev VL, O'Connor LB, Larsen CN, Kasperek E, Pickart CM (1995) Metabolism of the polyubiquitin degradation signal: structure, mechanism, and role of isopeptidase T. Biochemistry 34:14535-14546.

Wilson SM, Bhattacharyya B, Rachel RA, Coppola V, Tessarollo L, Householder DB, Fletcher CF, Miller RJ, Copeland NG, Jenkins NA (2002) Synaptic defects in ataxia mice result from a mutation in Usp14, encoding a ubiquitin-specific protease. Nat Genet 32:420-425.

Wolters E (2009) Non-motor extranigral signs and symptoms in Parkinson's disease. Parkinsonism Relat Disord 15 Suppl 3:S6-12.

Wooten MW, Geetha T, Babu JR, Seibenhener ML, Peng J, Cox N, Diaz-Meco MT, Moscat J (2008) Essential role of sequestosome 1/p62 in regulating accumulation of Lys63-ubiquitinated proteins. J Biol Chem 283:6783-6789.

Wu J, Ichihara N, Chui DH, Yamazaki K, Kikuchi T (1995) [Ubiquitin immunoreactivity in the central nervous system of gracile axonal dystrophy (GAD) mouse]. No to shinkei = Brain and nerve 47:881-885.

Xiang T, Li L, Yin X, Yuan C, Tan C, Su X, Xiong L, Putti TC, Oberst M, Kelly K, Ren G, Tao Q (2012) The ubiquitin peptidase UCHL1 induces G0/G1 cell cycle arrest and apoptosis through stabilizing p53 and is frequently silenced in breast cancer. PloS one 7:e29783.

Xilouri M, Kyratzi E, Pitychoutis PM, Papadopoulou-Daifoti Z, Perier C, Vila M, Maniati M, Ulusoy A, Kirik D, Park DS, Wada K, Stefanis L (2012) Selective

neuroprotective effects of the S18Y polymorphic variant of UCH-L1 in the dopaminergic system. Human molecular genetics 21:874-889.

Xu L, Lin DC, Yin D, Koeffler HP (2014) An emerging role of PARK2 in cancer. Journal of molecular medicine 92:31-42.

Yamazaki K, Moriya H, Ichihara N, Mitsushio H, Inagaki S, Kikuchi T (1993) Substance P-immunoreactive astrocytes in gracile sensory nervous tract of spinal cord in gracile axonal dystrophy mutant mouse. Molecular and chemical neuropathology / sponsored by the International Society for Neurochemistry and the World Federation of Neurology and research groups on neurochemistry and cerebrospinal fluid 20:1-20.

Yamazaki K, Wakasugi N, Tomita T, Kikuchi T, Mukoyama M, Ando K (1988) Gracile axonal dystrophy (GAD), a new neurological mutant in the mouse. Proceedings of the Society for Experimental Biology and Medicine Society for Experimental Biology and Medicine 187:209-215.

Yao D, Gu Z, Nakamura T, Shi ZQ, Ma Y, Gaston B, Palmer LA, Rockenstein EM, Zhang Z, Masliah E, Uehara T, Lipton SA (2004) Nitrosative stress linked to sporadic Parkinson's disease: S-nitrosylation of parkin regulates its E3 ubiquitin ligase activity. Proceedings of the National Academy of Sciences of the United States of America 101:10810-10814.

Yao T, Cohen RE (2002) A cryptic protease couples deubiquitination and degradation by the proteasome. Nature 419:403-407.

Ye Y, Scheel H, Hofmann K, Komander D (2009) Dissection of USP catalytic domains reveals five common insertion points. Molecular bioSystems 5:1797-1808.

Yeo CW, Ng FS, Chai C, Tan JM, Koh GR, Chong YK, Koh LW, Foong CS, Sandanaraj E, Holbrook JD, Ang BT, Takahashi R, Tang C, Lim KL (2012) Parkin pathway

activation mitigates glioma cell proliferation and predicts patient survival. Cancer research 72:2543-2553.

Ylikallio E, Poyhonen R, Zimon M, De Vriendt E, Hilander T, Paetau A, Jordanova A, Lonnqvist T, Tyynismaa H (2013) Deficiency of the E3 ubiquitin ligase TRIM2 in early-onset axonal neuropathy. Human molecular genetics 22:2975-2983.

Young AB (2009) Four decades of neurodegenerative disease research: how far we have come! J Neurosci 29:12722-12728.

Yuan A, Rao MV, Veeranna, Nixon RA (2012) Neurofilaments at a glance. Journal of cell science 125:3257-3263.

Zhang C, Lin M, Wu R, Wang X, Yang B, Levine AJ, Hu W, Feng Z (2011) Parkin, a p53 target gene, mediates the role of p53 in glucose metabolism and the Warburg effect. Proceedings of the National Academy of Sciences of the United States of America 108:16259-16264.

Zhang ZJ, Burgunder JM, An XK, Wu Y, Chen WJ, Zhang JH, Wang YC, Xu YM, Gou YR, Yuan GG, Mao XY, Peng R (2008) Lack of evidence for association of a UCH-L1 S18Y polymorphism with Parkinson's disease in a Han-Chinese population. Neurosci Lett 442:200-202.

Zhou ZR, Zhang YH, Liu S, Song AX, Hu HY (2012) Length of the active-site crossover loop defines the substrate specificity of ubiquitin C-terminal hydrolases for ubiquitin chains. Biochem J 441:143-149.